REPUBLIC OF TÜRKİYE
HASAN KALYONCU UNIVERSITY
GRADUATE EDUCATION INSTITUTE
DEPARTMENT OF CIVIL ENGINEERING

USE OF GIS FOR GEOTECHNICAL DATA PROCESSING AND MAPPING IN ANTAKYA, TÜRKİYE

Ali Servet ATEŞ

M.Sc. THESIS

IN

CIVIL ENGINEERING

GAZİANTEP - 2023

Use of GIS for Geotechnical Data Processing and Mapping in Antakya, Türkiye

M.Sc. Thesis

in

Civil Engineering Department

Hasan Kalyoncu University

Supervisor

Assist. Prof. Dr. Nurullah AKBULUT

by

Ali Servet ATEŞ

November 2023

GRADUATE EDUCATION INSTITUTE
MASTER'S THESIS ACCEPTANCE AND APPROVAL FORM

Civil Engineering Department, student of the Master of Civil Engineering program Ali Servet ATEŞ prepared and submitted the thesis titled "Use of GIS for Geotechnical Data Processing and Mapping in Antakya, Türkiye" and defended successfully at the date of 08/11/2023 and accepted by the jury as a M.Sc. thesis.

Position	Title, Name and Surname	Department/University	Signature
Supervisor	Assist. Prof. Dr. Nurullah AKBULUT	Hasan Kalyoncu University	
Jury Member	Prof. Dr. Hanifi ÇANAKCI	Hasan Kalyoncu University	
Jury Member	Assoc. Prof. Dr. M. Eren GÜLŞAN	University of Gaziantep	

This thesis is accepted by the jury members selected by institute management board and approved by institute management board.

Prof. Dr. M. Serhat YENİCE
Director

TEZ BİLDİRİMİ

Bu tezdeki bütün bilgilerin etik davranış ve akademik kurallar çerçevesinde elde edildiğini ve tez yazım kurallarına uygun olarak hazırlanan bu çalışmada bana ait olmayan her türlü ifade ve bilginin kaynağına eksiksiz atıf yapıldığını bildiririm.

DECLARATION PAGE

I hereby declare that all information in this document has been obtained and presented in accordance with academic rules and ethical conduct. I also declare that, as required by these rules and conduct, I have fully cited and referenced all material and results that are not original to this work.

Ali Servet ATEŞ
08.11.2023

HASAN KALYONCU UNIVERSITY
GRADUATE EDUCATION INSTITUTE
DEPARTMENT OF CIVIL ENGINEERING

USE OF GIS FOR GEOTECHNICAL DATA PROCESSING AND MAPPING IN ANTAKYA, TÜRKİYE

Ali Servet ATEŞ

MASTER THESIS

Supervisor
Assist. Prof. Dr. Nurullah AKBULUT

ABSTRACT

Geographic Information Systems (GIS) is a data collection tool that offers various features, including the analysis, querying, visualization, statistical analysis, and spatial analysis of geographical data. In the context of construction areas and urban planning, GIS is used for digital mapping studies, allowing for a more effective examination, interpretation, conclusion, and planning of data. The aim of this study was to mitigate risks associated with geotechnical issues, specifically seismic site effects and weak soil properties. To conduct the study, geotechnical survey reports and field and laboratory test results from the archives of the Provincial Directorate of Environment and Urbanisation of Antakya were utilized. In an area of approximately 110 km² within the Central District of Antakya Province, geological, geophysical, and geotechnical data from 221 borehole logs were analyzed using the GIS Inverse Distance Weighting (IDW) method. Engineering properties of the soils were examined at various depths (1.5, 3.0, 6.0, 7.5, and 9.0) within the study area. The analyses conducted included the standard penetration test, bearing capacity, groundwater level, consistency limits (LL, PL and PI), shear wave velocity, and soil classification based on NEHRP, EUROCODE-8, and TDBY2018 earthquake regulations. The standard penetration test (SPT-N) indicated blow numbers ranging from 2 to 50. A total of 1680 soil samples were classified into five different groups (CH, CL, MH, SC, and SM), with clayey soil samples dominating 91% of the study area. Shear wave velocity analysis at a depth of 30 meters categorized the soil classes as B and C according to the EUROCODE-8 classification, or C and D according to NEHRP and TDBY2018, indicating their importance in evaluating the seismic characteristics of the soil. The bearing capacity ranged from 0.2 to 6.6 kg/cm^2 for the first 1.5-meter depth, increasing as depth increased and ranging from 0.4 to 11 kg/cm^2. The study area also included flood-prone areas surrounding Amik Lake and river flood-prone areas, with groundwater levels fluctuating between 1 and 10 meters. The predominant geological composition in the Antakya region consists of Quaternary alluvial fill, comprising clay, silt, and sand. These alluvial materials tend to amplify ground motions during earthquakes, emphasizing the importance of identifying and mapping such areas for further studies.

Keywords: Antakya, GIS, geotechnics, geophysics, mapping.

HASAN KALYONCU ÜNİVERSİTESİ
LİSANSÜSTÜ EĞİTİM ENSTİTÜSÜ
İNŞAAT MÜHENDİSLİĞİ BÖLÜMÜ

GEOTEKNİK VERİ İŞLEME VE HARITALANDIRMADA CBS KULLANIMI: ANTAKYA ÖRNEĞİ

Ali Servet ATEŞ

YÜKSEK LİSANS TEZİ

Danışman
Dr. Öğr. Üyesi Nurullah AKBULUT

ÖZET

Coğrafi Bilgi Sistemleri (CBS), coğrafi verilerin analizi, sorgulanması, görselleştirmesi, istatistiksel analizi ve mekânsal analizini içeren bir veri toplama aracıdır. İnşaat alanları ve kentsel planlama bağlamında CBS, dijital harita çalışmaları için kullanılır, bu da verilerin daha etkili bir şekilde incelenmesine, yorumlanmasına, sonuçlandırılmasına ve planlanmasına olanak tanımaktadır. Bu çalışmanın amacı, özellikle deprem etkileri ve zayıf zemin özellikleri ile ilişkili olan geoteknik sorunlara yönelik riskleri azaltmaktı. Çalışma kapsamında, Antakya Çevre ve Şehircilik İl Müdürlüğü arşivlerinde yer alan geoteknik zemin etüt raporları ile saha ve laboratuvar deney sonuçları kullanıldı. Antakya merkez sınırları içindeki yaklaşık 110 km²'lik bir alanda, 221 sondaj kuyusundan elde edilen jeolojik, jeofizik ve geoteknik veriler, CBS Ters Mesafe Ağırlıklı (TMA) yöntemi kullanılarak analiz edildi. Zeminlerin mühendislik özellikleri çalışma alanı içinde çeşitli derinliklere (1.5, 3.0, 6.0, 7.5 ve 9.0) göre incelendi. Çalışma kapsamında standart penetrasyon testi, taşıma kapasitesi, yeraltı su seviyesi, zemin indeks özellikler (LL, PL ve PI), kayma dalgası hızı ve NEHRP, EUROCODE-8 ve TDBY2018 deprem yönetmeliklerine göre zemin sınıflandırması analizleri yapıldı. Standart penetrasyon testine göre, 2 ila 50 arasında değişen vuruş sayılarını gözlemlenmiştir. Toplam 1680 numune analizi sonucunda, kil ağırlıklı numunelerinin çalışma alanının %91'ini oluşturduğunu ve bunların beş farklı gruba (CH, CL, MH, SC ve SM) ayrıldığını göstermiştir. 30 metre derinlikte yapılan kayma dalgası hızı analizi, zemin sınıflarını EUROCODE-8 sınıflandırmasına göre B ve C zemin sınıfı iken, NEHRP ve TDBY2018'e göre C ve D olarak kategorize edilmiştir. Taşıma kapasitesi, ilk 1.5 metre derinlik için 0.2 ila 6.6 kg/cm² arasında değişirken, derinlik arttıkça 0.4 ila 11 kg/cm² arasında değişmiştir. Çalışma alanı aynı zamanda Amik Gölü çevresindeki taşkın bölgeleri ve Asi nehri taşkın bölgelerini içermekte olup, yeraltı su seviyeleri 1 ila 10 metre arasında değişmektedir. Antakya bölgesindeki baskın jeolojik oluşum, kil, silt ve kum içeren Kuvaterner alüvyon dolgusudur. Bu alüvyon malzemeleri depremlerde zemin büyütmesi eğilimindedir ve bölgelerin gelecekteki çalışmalar için çalışılması ve haritalandırılması gerekmektedir.

Anahtar Kelimeler: Antakya, CBS, geoteknik, jeofizik, haritalandırma.

My precious family ....

ACKNOWLEDGMENT

First of all, I would like to express my heartfelt gratitude to my esteemed thesis advisor and mentor, Assist. Prof. Dr. Nurullah AKBULUT, for generously sharing his knowledge and experiences with me during the process of determining my thesis topic. I am immensely thankful for his unwavering support and contributions throughout every stage of the thesis. His guidance and assistance in my profession and master's thesis have been invaluable, and I am truly grateful for that.

To my esteemed colleagues Abdulsamed AKGUL and Emirhan SAYIK, who guided me with their constructive and guiding ideas in the preparation of my master's thesis, and who contributed greatly to the formation of my thesis with their suggestions and guidance.

To my close friend, Erhan BEKEN, who did not spare his moral support and did not allow me to give up during this period when I was going through psychologically difficult times, and to all my friends whose names I cannot mention here one by one,

To my precious brother Hursit Ziya ATES, who has always been my best friend throughout my life, whom I trusted with his presence,

And most importantly, I would like to express my gratitude to my dear family, who have made great efforts to get me to where I am today, and for their moral support during my thesis work as well as throughout my life.

I hope this thesis will serve as a valuable resource for engineers, geotechnical experts and project stakeholders involved in similar projects and help them make informed decisions about soil improvement strategies.

I offer my endless respect, love and gratitude.

Ali Servet ATEŞ

Gaziantep- 2023

TABLE OF CONTENTS

Page No

LIST OF TABLES

Page No

LIST OF FIGURES

ABBREVIATIONS OR SYMBOLS LIST

AASHTO	American Association of State Highway and Transportation Officials
ASTM	American Society for Testing and Materials
BSSC	Building Seismic Safety Council
E	Modulus of Elasticity
FEMA	Federal Emergency Management Agency
G	Shear Modulus
g	Gravitational acceleration (cm/s^2)
GIS	Geographic Information System
IDW	Inverse Distance Weighting
JRC	Joint Research Centre
Md	Dry mass of sample
Mw	Wet mass of sample
NEHRP	National Earthquake Hazard Reduction Program
P_I	Plasticity index
q_a	Bearing capacity for allowable bearing capacity (kN/m^2)
q_u	Ultimate Bearing capacity (kN/m^2)
SPT	Standard Penetration Test
To	Soil dominant vibration period (sec)
USCS	Unified Soil Classification System
Vp	Compression wave velocity (m/sec)
Vs	Shear wave velocity (m/sec)
V_{S30}	Average shear wave velocity at 30 m depth
w	Water content value
W_L	Liquid limit
W_P	Plastic limit
W_S	Shrinkage limit
w_w	Water mass value
γ	Unit weight (kN/m^3)
μ	Poisson Ratio
σ	Stress (kN/m^2)

1. INTRODUCTION

1.1. General

Geotechnical Engineering underscores the importance of accurately identifying and evaluating soil parameters due to the direct interaction between engineering structures and soil. These parameters significantly influence the reliability and cost-effectiveness of such structures. Despite our limited understanding of soil behavior, it is vital to precisely evaluate soil properties to ensure the successful construction and design of engineering projects. (Shaik, 2007).

The increase in the global population has directly impacted the expansion of construction activities. This growth has created an urgent need for constructing more infrastructure such as tall buildings, dams, ports, and bridges. This emphasizes the importance of identifying soil properties and studying its behavior, as it is a crucial step in any construction project.

Soil properties are determined through field tests, laboratory tests, and geophysical methods. Each method has its own advantages and limitations in assessing soil properties. Therefore, there are both pros and cons associated with using field and laboratory test methods for this purpose. Consequently, the most suitable approach to determining soil parameters is to analyze the results from all three test methods collectively. (İyisan, 1994).

Geotechnical engineering utilizes a variety of techniques to evaluate soil properties in the field. These techniques involve collecting both disturbed and undisturbed soil samples. Undisturbed samples are directly obtained from the field. However, even with undisturbed soil sampling and subsequent laboratory testing, there may still be some degree of disturbance. These samples are subjected to various laboratory tests to acquire information about soil properties. Sampling in cohesive soils is relatively straightforward, while sampling in non-cohesive soils can be more expensive due to the need for specialized techniques and equipment. As a result, geophysical methods are also employed when obtaining desired samples for every soil type is not always feasible. (İyisan, 1994).

Geophysical methods are employed to collect information on the internal structure of soils by measuring their electrical and magnetic properties using field instruments. These methods present a cost-effective and eco-friendly option as they deliver rapid results without the need for soil sampling. However, their sensitivity is lower compared

to field and laboratory testing methods and can be influenced by field conditions. It is crucial to acknowledge that the accuracy of results derived from geophysical methods is also inferior to those obtained from soil samples tested in the laboratory (İyisan, 1994).

The objective of this investigation is to demonstrate the more efficient utilization of soil properties obtained through laboratory tests, field tests, and geotechnical engineering in soil engineering. Geographic Information System (GIS) is employed to visualize and manage the data collected on soil properties in maps, improving understanding. This enables the rapid assessment of soil properties, ensuring their optimal use and effectiveness in construction projects.

Consequently, GIS technology offers a significant advantage in maximizing the effectiveness and efficiency of soil engineering. It allows for easy assessment of soil properties at any location within our workspace, seamlessly integrating additional data into the created maps. This results in time, labor, and cost savings during construction projects. The purpose of this research is to create a database by compiling soil property parameters using GIS technology.

1.2. Aim of the Study

This study utilizes geotechnical survey data obtained from the Antakya Provincial Directorate of Environment and Urbanization to evaluate various aspects of soil properties. The dataset includes general information about the study area, including its geographical location, geological characteristics, and seismic activity.

The aim of this thesis was to mitigate risks associated with geotechnical issues, specifically seismic site effects and weak soil properties. To conduct the study, geotechnical survey reports and field and laboratory test results from the archives of the Provincial Directorate of Environment and Urbanisation of Antakya were utilized. In an area of approximately 110 km² within the Central District of Antakya Province, geological, geophysical, and geotechnical data from 221 borehole logs were analyzed using the GIS Inverse Distance Weighting (IDW) method. Engineering properties of the soils were examined at various depths (1.5, 3.0, 6.0, 7.5, and 9.0) within the study area. The analyses conducted included the standard penetration test, bearing capacity, groundwater level, consistency limits (LL, PL and PI), shear wave velocity, and soil classification based on NEHRP, EUROCODE-8, and TDBY2018 earthquake regulations.

The implementation of GIS software has greatly facilitated the application of geographic information systems in geotechnical engineering. The objective is to optimize the effectiveness and efficiency of using geotechnical data in GIS applications.

1.3. Outline of the Thesis

Chapter 1 – Introduction: In this chapter, the research questions and hypotheses are presented, along with an explanation of the research goals and the significance of contributing to the topic. The chapter also discusses the various techniques used to assess soil properties, emphasizing both the differences and commonalities among these methods. Additionally, the chapter provides an overview of the results obtained from the Geographic Information System (GIS) in relation to the employed techniques for evaluating soil properties.

Chapter 2 - Literature review: This chapter provides an overview of GIS and presents previous studies that have explored the use of GIS in relation to geotechnical features.

Chapter 3 – Materials and Method: This chapter provides a thorough description of the methods employed in the study, including the standard penetration test, bearing capacity, groundwater level, consistency limits (LL, PL and PI), shear wave velocity, and soil classification based on NEHRP, EUROCODE-8, and TDBY2018 earthquake regulations.

Chapter 4 - Results and Discussion: In this chapter, the evaluation and discussion of the maps and graphs created as part of the research are conducted.

Chapter 5 - Conclusions and Recommendations: Conclusions and recommendations are presented in this chapter.

2. LITERATURE REVIEW

2.1. General

In this chapter, an overview of GIS is given, along with an exploration of previous studies that have examined the application of GIS in relation to geotechnical features. The literature review includes an overview of the previous studies that utilized GIS, and specific mapping studies related to geotechnics are emphasized.

2.2. Geographical Information Systems

2.2.1. Definition of geographical information systems

Advancements in technology have facilitated the storage of data in digital formats, leading to the creation of data and information management systems commonly referred to as "information systems." These systems are designed to systematically collect, process, and transform data into valuable information. Their ultimate goal is to riverline and simplify the decision-making process (Yomralıoğlu, 2000).

GIS is a computer-based information system that has the capability to handle digital data based on location (Singh & Fiorentino, 2013).

Various fields may have varying applications and interpretations of GIS. However, in general, GIS refers to software that enables the collection, analysis, modeling, and visualization of data with a geographic component. These systems are specifically designed to address complex planning and management issues and have gained significant attention in various industries in recent years (Töreyen et al., 2010).

2.2.2. Historical development of the geographical information system

The inception of GIS can be attributed to the recognition of the need for visual tools such as thematic maps and graphics. In the 18th and 19th centuries, pioneering efforts were made in different geographical areas to tackle specific challenges. These initiatives are considered the early explorations in the field of GIS.

The earliest instance of linking the relationship between 'what' and 'where' can be traced back to 1854 during a cholera outbreak. While it was commonly believed at that time that the disease was being transmitted through the air, Dr. Jon Snow, an innovative English Doctor, had doubts. To investigate further, he created a map that depicted the outbreak locations, roads, property boundaries, and water pumps. This mapping exercise led to a remarkable revelation - a clear pattern emerged. This pattern disproved the theory

of airborne transmission and instead indicated that the disease was being spread through contaminated water, specifically one infected water pump. John Snow's cholera map was a groundbreaking event that connected the characteristics of the disease with its geographical distribution.

This event not only marked the beginning of spatial analysis but also initiated a whole new field of study: Epidemiology, which focuses on the spread of diseases. Snow's work exemplified the problem-solving capabilities of GIS as he effectively displayed the 'what' on a map to reveal the corresponding 'where', leading to a life-saving discovery. (Vinten-Johansen et al.,2003; Uyguçgil, 2011; Çabuk, 2015).

From 1958 to 1961, the foundation for GIS was laid with a research program conducted in the Department of Geography at the University of Washington. The aim of this program was to enhance data retrieval through computer-based methods. In 1963, Roger Tomlinson established the Canadian Geographic Information System with two main objectives. The first goal was to collect and analyze a comprehensive inventory of land-based data in Canada. The second objective was to generate statistical data that could be utilized in land management planning (Çabuk 2015).

The first mapping program, called Synagraphic Mapping System (SYMAP), was developed at Harvard University in 1965. SYMAP became very popular worldwide and was widely used until the 1990s. Currently, there are several GIS software programs available, with ArcGIS being the most used. ArcGIS was created by Environmental Systems Research Institute, a nonprofit organization founded in Redlands, California in 1969 (Coppock & Rhind, 1991).

The widespread use of GIS became increasingly popular from 1990 to 2010. This was made possible by various advancements in IT: computers became more affordable, faster, and more capable, and there was a greater variety of GIS software options available. Additionally, there was a greater availability of digitized mapping data. These advancements, along with the introduction of new earth observation satellites and the integration of remote sensing technology with GIS, resulted in the development of a growing number of applications. As a result, GIS began being used in classrooms, businesses, and governments worldwide.

As a result of the growing popularity of GIS in the past two decades, open-source GIS emerged. The use of GIS data has become increasingly widespread, with examples such as Landsat satellite imagery now being accessible to everyone. GIS has now expanded to be available online, in the cloud, and on mobile devices.

2.2.3. Advantages of GIS

As computing technology has advanced, GIS tools have been improved. Tasks that used to take a long time, such as layer overlay methods and map production, are now faster and more efficient thanks to computer software. GIS is used in various sectors and plays a crucial role in decision-making processes. It is a valuable tool for problem-solving and has applications in diverse fields such as environmental protection, agriculture, cultural heritage, mapping engineering, geology, earth sciences, sociology, and logistics (Özcan et al., 2021).

GIS offers a multitude of advantages to users in different sectors. These advantages include the following key characteristics:

1. GIS simplifies the process of collecting, storing, analyzing, and visualizing data, making data-related tasks more efficient.
2. GIS supports decision-making by aiding in the analysis and visualization of data, serving as a valuable tool in decision support systems.
3. GIS allows for quick and easy access to data, enabling easy updates and improving overall accessibility.
4. By electronically storing and analyzing data, GIS speeds up workflows and increases time and cost efficiency.
5. GIS can be customized to fit specific requirements in various fields, enhancing its flexibility.
6. Through data sharing and collaboration, GIS promotes cooperation among different departments and organizations.
7. It enables the integration of diverse data sources and analysis of multi-source data.
8. GIS ensures the use of accurate and up-to-date geographical data.
9. It enables the creation of visually appealing and easy-to-understand reports using mapping and visualization features.
10. GIS can adapt to changes and advancements in geographical data over time.
11. It offers support for multiple users and the option for remote access.
12. GIS allows for the comparison and analysis of data at different scales and in different geographical regions.

2.2.4. Working methods and components of a GIS

GIS is an information system that is designed to analyze, store, update, and query spatial positions of vector and literary data. When combined with geographical data, GIS

data allows for visualization and integration with other data types, providing an analytical overview. GIS data refers to locations that are defined by a specific coordinate system and are stored as either areas, lines, or points. The GIS framework includes personnel, software, data, and hardware, which helps protect and archive spatial data. Refer to Figure 2.1 for a visual representation of GIS components (Küpçü et al., 2015).

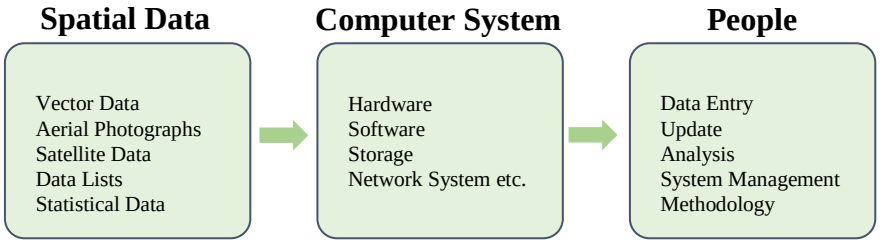

Figure 2.1. A view of GIS components (Küpçü et al., 2015).

2.2.5. Usage areas of GIS

GIS is a system that is used to gather, store, analyze, display, and manage geographical data. It is applied in various fields, and below are a few examples of its application areas:

1. **City Planning:** Within urban planning, GIS helps analyze geographical data to improve planning efforts. It utilizes various data sources such as transportation, population statistics, infrastructure, green spaces, and social activities. For example, GIS allows for the examination of factors like population density, traffic patterns, and availability of green spaces, which inform decision-making processes in urban planning.
2. **Agriculture**: In the agriculture sector, GIS is a valuable tool for collecting, analyzing, and managing data. It incorporates data sources such as land usage, water resources, vegetation coverage, soil analysis, and weather predictions.
3. **Disaster Management:** GIS plays a crucial role in mitigating damage and facilitating emergency response during natural disasters. It enables risk analysis, emergency planning, and damage assessment through the use of geographical data. For instance, GIS allows for the analysis of factors like disaster risks, positioning of emergency teams, and locations of healthcare facilities, aiding in the preparation and formulation of emergency plans.

4. **Health:** GIS is employed in gathering, analyzing, and managing data within the healthcare industry. It incorporates data related to epidemic outbreaks, public health, and disease mapping. GIS facilitates the analysis of variables like disease transmission, hospital placements, population density, and the development of health policies. This analysis supports informed decision-making and policy formulation in healthcare.
5. **Geology:** GIS is utilized for collecting, analyzing, and managing geological data. It encompasses data related to subterranean resources, volcanic occurrences, seismic activity, and categorization of rock types.

In addition to these particular application domains, GIS has utility in various other fields. Forestry, tourism, the energy sector, the military, and archaeological research are just a few examples of the diverse areas where GIS plays a crucial role.

2.3. Geotechnical Studies Related with GIS

Many studies have been conducted in a variety of fields that are related to GIS. Here are a few examples of these studies.

Dai and Lee (2001) developed a method using GIS to determine the probability of landslides happening on Lantau Island. The research involved assessing various factors of the terrain, such as rock composition, slope direction, height, land vegetation, and distance to waterways in order to determine the vulnerability to landslides. To enhance accuracy, they combined this information with actual records of landslide occurrences to conduct suitability analyses.

Haşimoğlu and Murat (2004) conducted research in the Yoncalı Thermal Springs settlement area, which is under the authority of the Kütahya Municipality. The study utilized satellite images and Geographic Information System methods to create digital maps of residential areas, road networks, rivers, and culverts. These maps consisted of different layers of geographic data, including zoning plans, geological formations, fault lines, and soil surveys. The main aim of this study was to create a comprehensive "Soil Survey Information System" by utilizing all the gathered data.

Kunapo et al. (2005) proposed a novel approach that integrates Web-GIS with a relational database management system to give the construction sector the ability to access geotechnical data online. The research introduces user-friendly tools that enable users to easily find information about specific boreholes on a map through search

functions and geotechnical spatial queries. This system provides users with digital data that is crucial for planning construction projects.

In the study conducted by Orhan (2005), the objective was to examine the geotechnical traits of the southern area of Eskisehir Urban Region. To achieve this, geological, geomorphological, and tectonic data were collected by executing boreholes in the region and entered into a computer system. With the use of this information, a database and geotechnical engineering map were developed in the GIS system for a certain area inside the study limits, to discover the geotechnical attributes of the fundamental units.

Şişman (2006) performed an evaluation of the risk of soil liquefaction in the Fethiye settlement area by utilizing SPT (standard penetration test) and shear wave velocity data. The research aimed to assess the likelihood of liquefaction happening in the event of a hypothetical earthquake in the Fethiye district of Muğla city. The analysis involved studying SPT-N blows and measuring shear wave velocity to conduct liquefaction analyses. Additionally, potential liquefaction maps were created for the study area using the liquefaction strength risk index as a basis.

Karaca (2007) examined the engineering attributes of the soils in the vicinity of Fethiye and generated geotechnical maps that depict these characteristics. These maps offer details on slope, liquefaction likelihood, groundwater depth from the surface, groundwater levels, vibration period, soil seismic amplification, and elastic wave velocities across various soil layers. With the help of these comprehensive maps, the author assessed the appropriateness of the study area for settlement purposes.

Kolat (2010) carried out a study to develop a geotechnical microzonation model for evaluating the suitability of the Yenişehir settlement center in Bursa for habitation. The research involved analyzing the soil properties and dynamic behavior of the area. Borehole data and microtremor measurements were used to assess soil classification, soil amplification, dominant soil period, resonance phenomenon, and liquefaction potential. The study evaluated the potential for liquefaction in both a two-dimensional planar and a three-dimensional volumetric manner. Based on the findings, geotechnical microzonation maps were created for the study area to determine the feasibility of the settlement center for habitation.

In their study, Avin (2011) utilized the ArcGIS software program to identify critical geological and geotechnical data. These data included soil classifications according to EUROCODE-8 standards, groundwater levels and formation conditions,

bearing capacity, soil safety stresses, and previous settlement values obtained from Balkesir Municipality. To locate and visualize the distribution of this information on cadastral maps provided by the municipality, the researcher utilized the capabilities of the ArcGIS program.

The research conducted by Wan-Mohamad and Abdul-Ghani (2011) aimed to provide crucial information for planners, architects, and engineers involved in designing structurally sound and cost-effective buildings in Seri Iskandar, District of Perak Tengah, Perak, Malaysia. To accomplish this goal, the authors investigated different soil types and performed field and laboratory tests to determine the Standard Penetration Test (SPT) values at various depths. The findings were then presented as maps, which can serve as a valuable resource for evaluating soil conditions in the area. These maps can guide decision-making during the design and construction phases of a project.

In Özcan's (2012) study, the researcher aimed to investigate the geological and geotechnical characteristics of the soil in the Selçuklu district of Konya city. To reach this goal, a combination of field observations, previous studies, and borehole data were utilized to create a comprehensive geological map of the study area. Furthermore, soil samples were collected and subjected to various laboratory tests, such as sieve analysis, specific gravity, unit weight, and water content tests to determine the physical properties of the soil. The test results were used to gain knowledge about the properties and characteristics of the soil, which could assist planners and designers in engineering projects. The study also conducted consolidation, triaxial compression, and uniaxial compression tests to determine mechanical properties. Based on these tests, the soil classifications in the study area and the geotechnical structure of the soil were examined by analyzing representative soil samples.

Demir (2013) conducted a study where a database was established using geological, geophysical, and geotechnical data from 131 geotechnical survey reports in the Gürsu settlement area of Bursa. By utilizing GIS software, geotechnical maps were created to illustrate the variations in essential soil properties. This facilitated quick, cost-effective, reliable, and practical decision-making for land use in the region. The research generated maps that contained various types of information about the study area, including slope, vegetation depth, groundwater level, elevation, soil classification based on the Unified Soil Classification System, standard penetration test data, shear wave velocity, compression wave velocity, and seismic velocity ratio. These maps provide a comprehensive understanding of the physical and geotechnical characteristics of the study

area, making them valuable for land use planning, engineering design, and disaster mitigation planning.

A study conducted by Cabalar et al. in 2019 focused on investigating the potential for liquefaction in Kahramanmaraş, a city located in southern-central Turkey along the East Anatolian and Dead Sea fault lines. The research involved extensive geotechnical investigations carried out in both the field and laboratory settings. A total of 238 boreholes were drilled throughout the city, and soil samples collected from these locations underwent various tests, including standard penetration tests to determine physical properties such as sieve analysis, Atterberg limits, and soil classification.

The liquefaction potential of the soil was evaluated based on the results of the standard penetration tests, assuming a hypothetical earthquake scenario with a magnitude of 7.5. The findings revealed that the southern regions of the city had a significant risk of liquefaction, while the northern areas generally had a lower probability. To visually represent these results, the researchers utilized GIS-based computer software to generate informative maps. These GIS maps can serve as valuable resources for researchers and engineers involved in land use planning and urban development, facilitating more in-depth studies in these areas.

In their 2019 study, Karabaş analyzed data from geotechnical survey reports conducted at 192 borehole locations in the designated study area. The author employed geographic information system (GIS) analysis to conduct various assessments. These included calculations for SPT-N (standard penetration test) analysis, bearing capacity analysis, analysis of groundwater levels and water content, liquefaction potential analysis, soil classification analysis, and earthquake hazard level analysis based on soil amplification calculations.

The findings from these analyses were presented and interpreted using GIS software, ultimately resulting in the creation of maps. These maps offer detailed information on the physical and geotechnical characteristics of the study area, encompassing factors such as soil properties, earthquake hazard levels, and potential for liquefaction. Engineers and planners can utilize these maps to make well-informed decisions regarding land use planning and urban development projects within the area (Karabas, 2019).

Demirtaş (2022) focused on Elazığ, where they collected data from 210 borehole logs to conduct an analysis of soil index properties, soil classification, and bearing capacity calculations. To further examine this data, the researcher utilized ArcGIS

software and the IDW method to create several types of maps. These included maps for soil classification, groundwater levels, water content, shear wave velocity, compression wave velocity, and soil amplification.

According to Demirtaş, these maps provide valuable insights for preliminary studies, feasibility assessments, land use policies, urban planning, and design. By accurately illustrating the distribution of various soil properties, these maps offer a convenient and informative tool for decision-making processes related to construction or development projects in the area.

Göksular (2022), geotechnical data obtained from 178 boreholes in Siirt city was utilized. The data was then employed to generate maps using a geographic information system, focusing on soil classification, bearing capacity, shear wave velocity, soil amplification, and dominant vibration period. Furthermore, the study employed four different methods based on geophysical and geotechnical approaches to calculate the bearing capacity. Additionally, the study estimated and compared shear wave velocity values, taking into consideration different approaches and formations described in previous literature.

3. MATERIALS AND METHODS

3.1. Introduction

This chapter provides a detailed description of the methods used. General information such as the geographical location, geological characteristics, and seismicity of the study area is also given. To conduct the study, geotechnical survey reports and field and laboratory test results from the archives of the Provincial Directorate of Environment and Urbanisation of Antakya were utilized. In an area of approximately 110 km² within the Central District of Antakya Province, geological, geophysical, and geotechnical data from 221 borehole logs were analyzed using the GIS Inverse Distance Weighting (IDW) method. Engineering properties of the soils were examined at various depths (1.5, 3.0, 6.0, 7.5, and 9.0) within the study area. The analyses conducted included the standard penetration test, bearing capacity, groundwater level, consistency limits (LL, PL and PI), shear wave velocity, and soil classification based on NEHRP, EUROCODE-8, and TDBY2018 earthquake regulations.

3.2. Location of the Study Area

Antakya is located at the easternmost part of the Adana Section of the Mediterranean Region, serving as the central hub of Hatay, the southernmost province in Turkey. The city stretches east and west of a valley that continues southward after crossing the Amik Plain of the Asi River. Positioned between 36°-10' north latitude and 36°-06' east longitude, Antakya has specific geographical characteristics. It was the provincial center of Hatay before becoming a metropolitan city and is situated 22 kilometers from the coast. The city is established in the valley between Amanos Mountains (Nur Mountains) and Habib Neccar Mountain (Silpius). With the Asi River passing through its middle, the city has a landscape that has developed since the 19th century. New neighborhoods have been built on the plains on the northwest side of the river, creating a distinction between "New Antakya" and "Old Antakya". (Demir, 1996).

Figure 3.1. Physical map of Antakya (Ozsahin, 2013).

3.3. General Characteristics of the Study Area

The research area chosen for the study is Antakya, which is situated in the central district of Hatay province at the southernmost part of Turkey, in the Mediterranean Region. It is located approximately 25 km away from the Mediterranean coast and at an elevation of about 80m above sea level. Although the city center of Antakya is mostly flat, it is surrounded by tall mountains with some passages in between. Amanos (Nur) Mountains are situated in the north, while Kel Mountain can be found in the south. The city was established at the base of Habib-i Neccar Mountain, which is located in the east and rises to 440m. The northeast region, where Amik Lake once existed, has been dried up and transformed into the wide and fertile Amik Plain (Bouchier, 1921; Rifaioğlu, 2012; Çekmecelioğlu, 2016).

Antakya is geographically adjacent to and integrated with the Defne district in the southwest. Previously, Defne district was within the boundaries of Antakya but was separated in 2012.

Considering the urban development and settlement patterns in and around Antakya, the city center, originally established at the foothills of Habib-i Neccar Mountains, has expanded approximately 5 km to the northwest, 5 km to the southwest, and 6.5 km to the north. The city stretches from its core to the coast where Samandağ district is located, approximately 20 km southwest, and to the Belen pass, where Belen district is located, approximately 20 km north. The Belen pass continues westward for about 15 km until it reaches the coast of Iskenderun district. This route is not only significant for trade but also for urbanization and settlement. The location of Antakya can be viewed in Figure 3.2 and Figure 3.3 shows the borehole distribution of the study area.

Figure 3.2. Location map showing the study area.

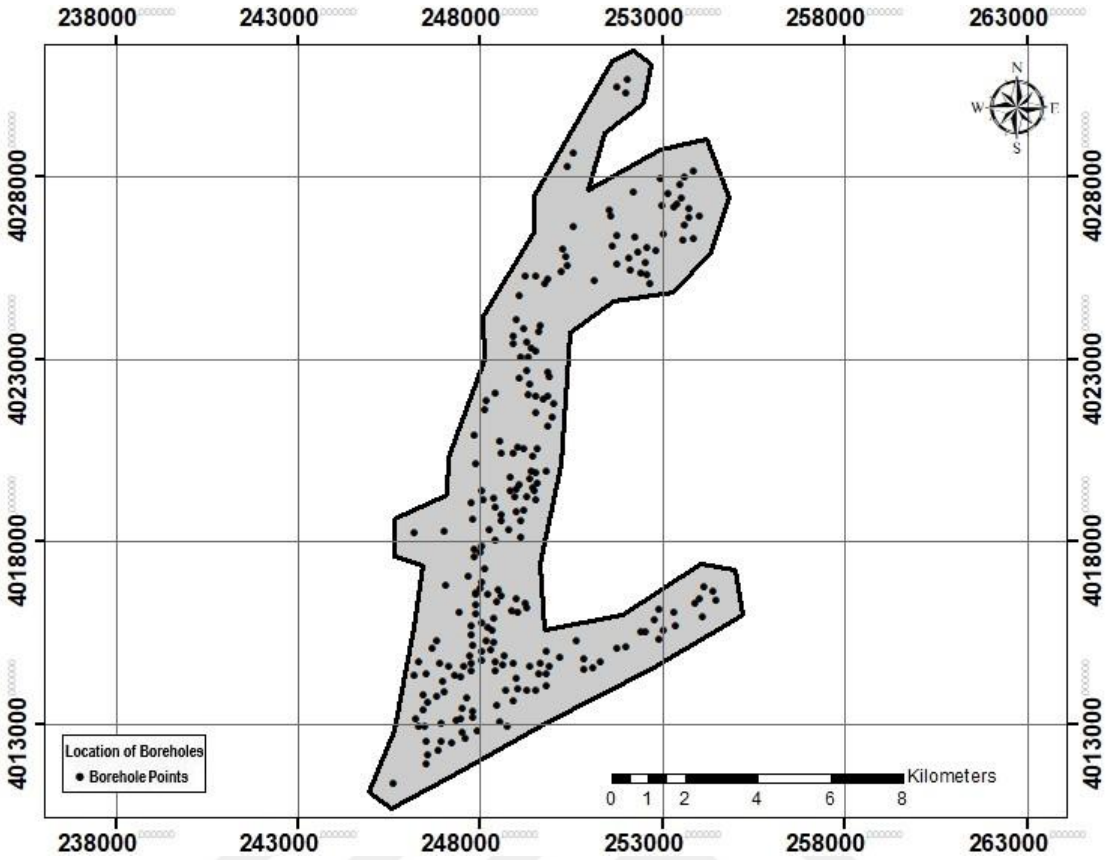

Figure 3.3. Location map showing boreholes of the study area.

3.4. Geological Situation

Antakya is located at the base of Mount Habib-i Neccar to the north, with the Asi River flowing through the city. The plain where Antakya is built consists largely of alluvium deposited by the Asi River. Geologically, the boundary between the mountainous areas to the north, which consist of rocks from different ages, and the plain is marked by fault lines.

The youngest land in the study area consists of alluvial deposits from the Quaternary period, which also have the weakest soils. Most of the urban development in Antakya and its surroundings has taken place on these lands. This development extends towards the Amik Plain and along the Asi Valley (Selçuk, 1985; Ateş et al., 2004).

The area where Antakya is situated, known as the graben area, experienced slow collapse with faulting at the end of the Cretaceous and Eocene periods. Initially, the area was affected by the Miocene sea, followed by the Pliocene sea (Öztemir et al., 2000). Over time, the effective stress regime in the area changed from strike-slip to extensional from the Plio-Quaternary period to the present (Över et al., 2001). The graben area,

including Antakya, gradually subsided due to faulting in the Cretaceous and Eocene periods, and this subsidence continued. The Miocene and later Pliocene seas entered the subsided areas (Öztemir et al., 2000:88). From the Plio-Quaternary period onwards, an active extensional regime evolved, resulting in the formation of the northeast-southwest oriented Amik Plain. This tectonic regime also activated old fault systems in the region and contributed to the formation of new fault systems (Över et al., 2001:12). These faults fragmented and offset alluvial cones and cut through Quaternary deposits.

The main geological fill in the Antakya Graben consists of a thick succession of Pliocene sedimentary layers known as the Samandağ formation, along with fluvial and marine terrace deposits (Figure 3.4).

The Samandağ formation, as described by Selçuk (1985), is composed of alternating layers of marl, sandstone, siltstone, shale, and conglomerate. Marl and sandstones are predominant in the sequence, while conglomerates are more commonly found in the lower and upper parts of the sequence. In the Antakya Graben, the lower contact of the Samandağ formation is rarely exposed.

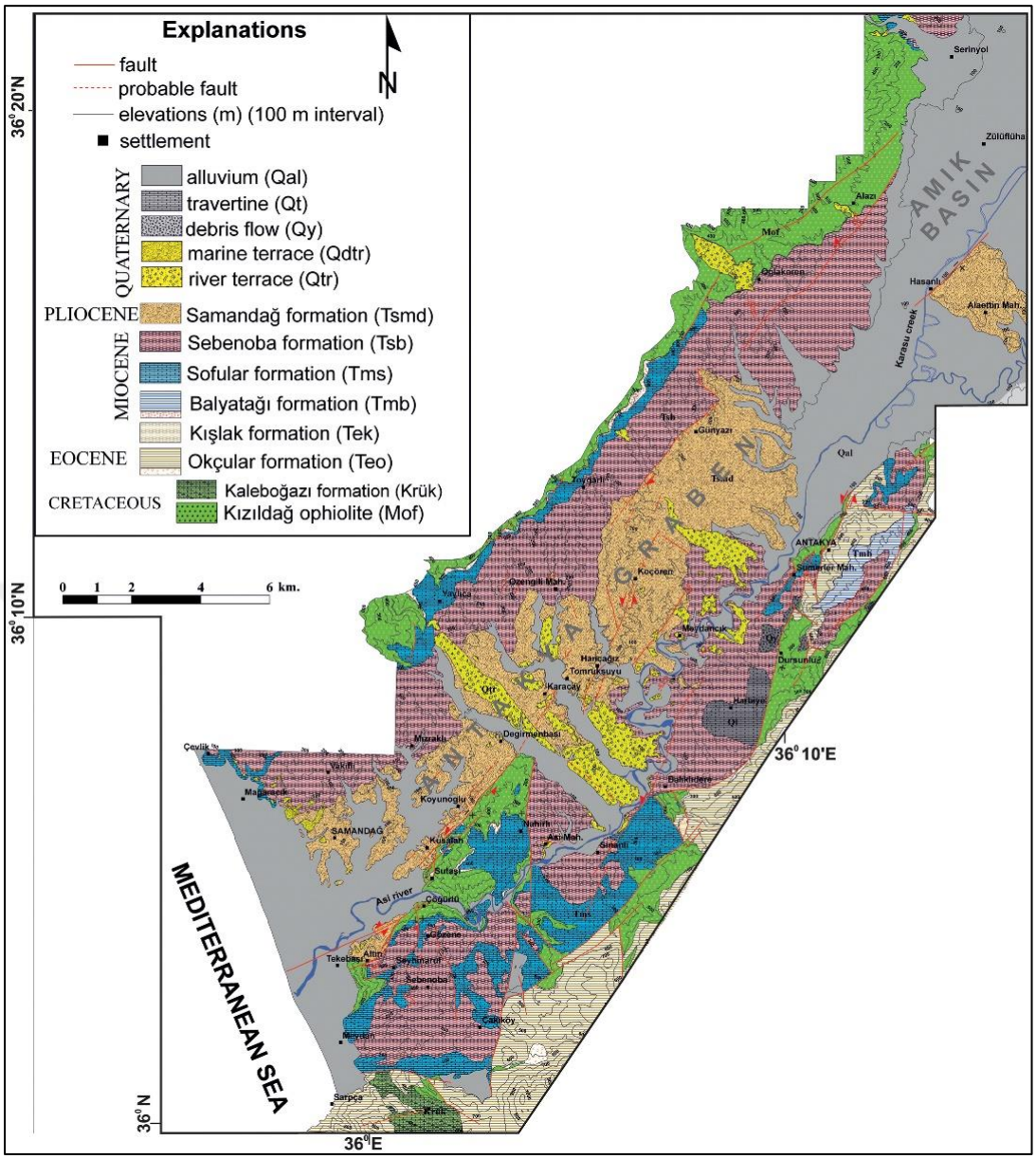

Figure 3.4. The geologic map of the Antakya Graben (Tarı et al., 2013).

North and northeast trending faults are the main structural elements of the Antakya Graben. The faults in the northwestern margin and center of the graben are mainly obliquely or purely sinistral, while most of the faults on the southeastern margin are normal or obliquely sinistral (Figures 3.4 and 3.5).

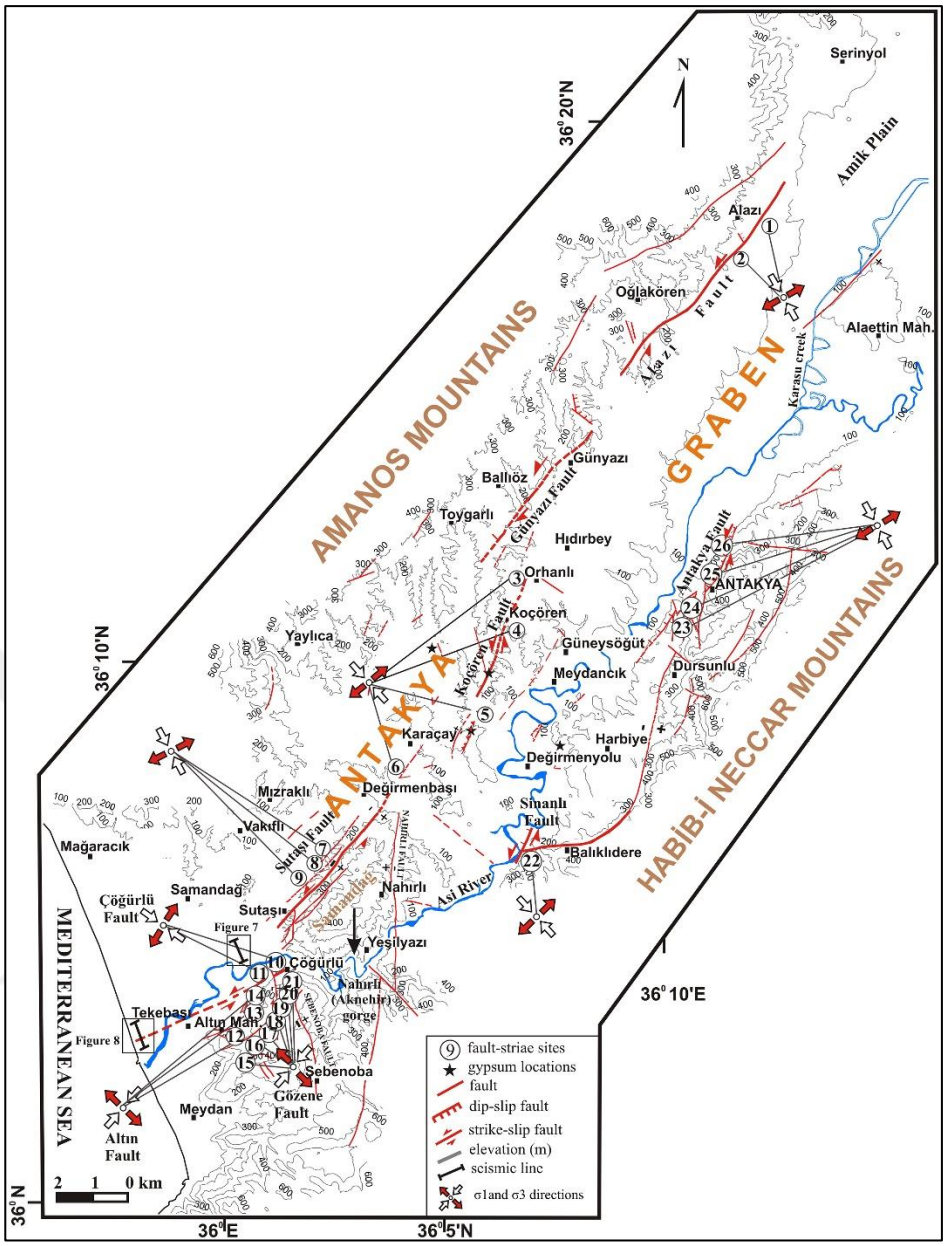

Figure 3.5. The fault map for the Antakya Graben (Tarı et al., 2013).

3.5. Stratigraphy

The development of the Antakya Graben and its surroundings can be divided into two distinct phases: the palaeotectonic phase and the neotectonic phase. The palaeotectonic phase, which occurred during the Late Cretaceous to Miocene period, was mainly associated with the closure of the Bitlis-Zagros Ocean. During this time, Mesozoic ophiolites were moved onto the Arabian margin during the Campanian, and sediment was deposited on both the ophiolite nappes and the Arabian Platform from the Maastrichtian to the Miocene period. Since the rock units developed during this period evolved before

the Antakya Graben opened, they are collectively referred to as "basement rocks." A brief overview of these rocks is included below. On the other hand, the rock units deposited during the neotectonic phase (The Plio-Quaternary units) are referred to as "Graben fill," and they will be described in greater detail (see Figure 3.6).

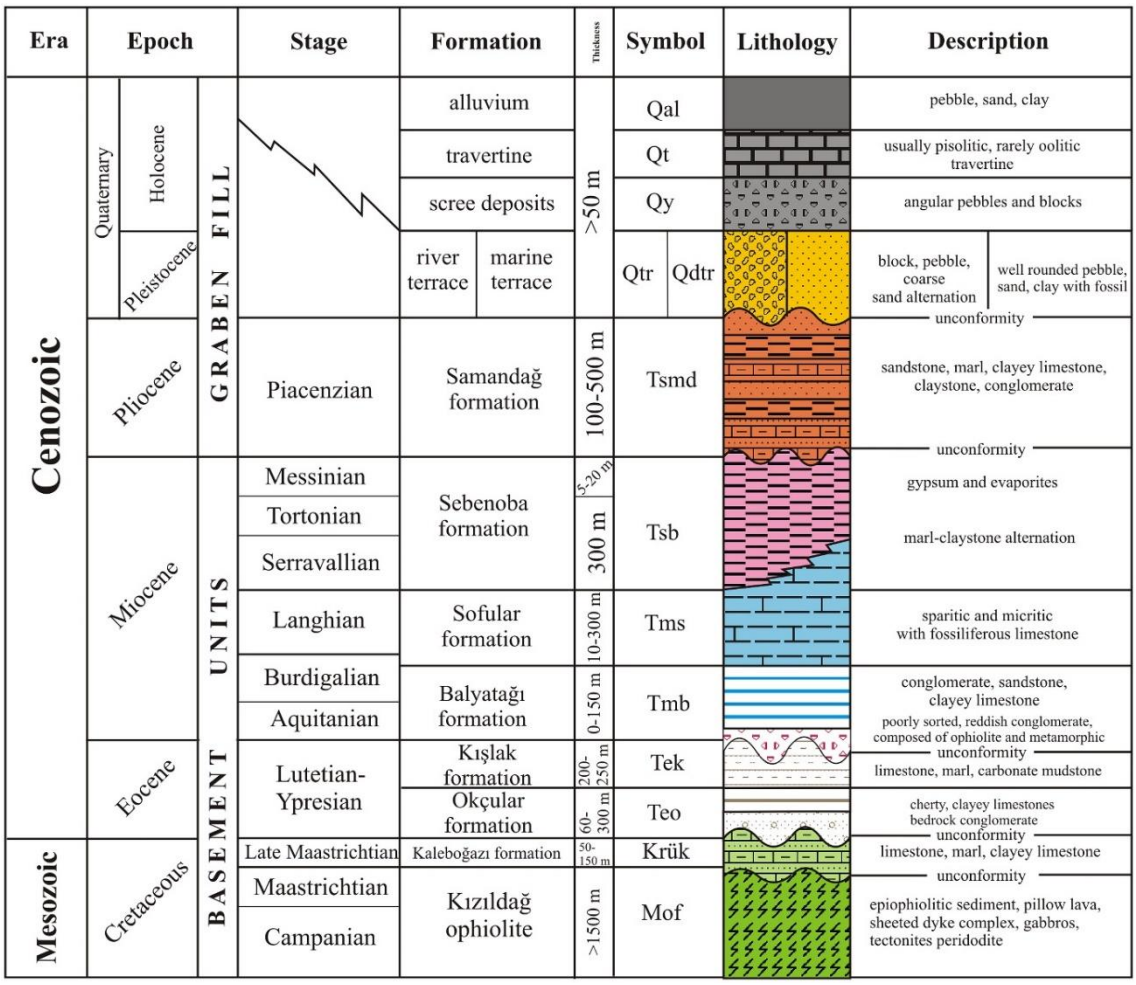

Figure 3.6. A generalized columnar stratigraphic section through the Antakya Graben (Tarı et al., 2013).

The Kızıldağ Ophiolite, located at the base of the region, is a well-studied ophiolitic complex consisting of various rock types such as ultramafic tectonites, mafic and ultramafic cumulates, gabbros, sheeted dyke complexes, plagiogranites, pillow lava, and epi-ophiolitic sediment like cherts and pelagic limestones. The age of the plagiogranites in the Kızıldağ Ophiolite has been determined to be approximately 90.3 ± 2.4 million years ago. Due to its age and geological setting, it can be correlated with the Bear-Bassit and Troodos ophiolites. The Kızıldağ Ophiolite was emplaced over the

preexisting Cambrian to Campanian sediment on the Arabian Platform before the Late Maastrichtian.

Above the Kızıldağ Ophiolite, there is a nonconformable layer of Upper Maastrichtian carbonate-dominated sediment, which is 50-150 meters thick. This is followed by a layer of cherty and sandy limestones from the lower to middle Eocene, which includes some in situ reefs at the base. The Eocene sequence is approximately 200-300 meters thick and is found mainly along the southeastern margin of the Antakya Graben. The Oligocene period was marked by erosion, followed by the deposition of a thick Miocene sedimentary sequence, which is unconformably layered on top of the Eocene and older units.

In the study area, the Miocene deposits are similar to those found in the well-studied Adana Basin. The basal deposits of the Aquitanian-Burdigalian age consist of red beds, siliciclastics, and carbonates, known as the Balyatağı formation. These were deposited in a continental to marginal marine environment. Above the Balyatağı formation are the Latest Burdigalian-Langhian limestones, called the Sofular formation, indicating a transgression that led to deeper deposition. The limestones then transition into Langhian-Tortonian clayey limestones and marls, known as the Sebenoba formation. The age assessments for these formations were based on foraminifera and ostracoda paleontology, as well as isotopic ratios. During the Messinian, gypsum horizons alternate with marls and conglomerates. These horizons have not been separated in this study and are collectively referred to as the Sebenoba formation, which covers the Langhian to Messinian sequence. Coeval gypsum deposits found in the Eastern Mediterranean were formed during a salinity crisis when the Mediterranean was isolated from the Atlantic Ocean.

3.6. Seismicity of the Region

Türkiye is located in the Alpine-Himalayan earthquake belt and is prone to significant earthquakes due to the compression between the Eurasian plate in the north and the African and Arabian plates. The Anatolian plate in Türkiye moves in a westward direction along the North and East Anatolian fault zones. In the eastern part of the country, the Bitlis-Zagros Rim Belt, also known as the Bitlis Thrust Zone, acts as the boundary between the Arabian Plate and eastern Anatolia. The compression resulting from the past

northward movement of the Arabian Plate along this belt has led to the formation of the Southeastern Taurus Mountains.

On January 1, 2019, the Türkiye Earthquake Hazard Map was implemented as part of the National Earthquake Strategy and Action Plan (NESEP-2023) and the National Earthquake Research Programme of the Presidency for Disaster and Emergency Management. The map, shown in Figure 3.7, provides information about the earthquake hazards in Türkiye.

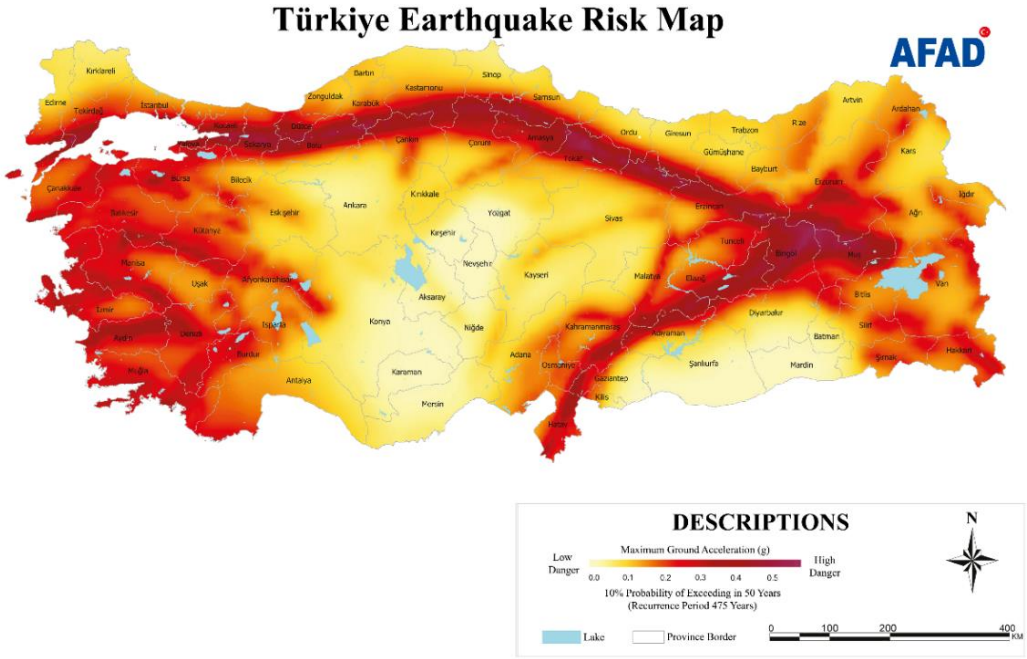

Figure 3.7. Map of earthquake zones of Türkiye (AFAD, 2022).

After analysing earthquakes that have taken place during both historical and instrumental periods, nearly 90,000 earthquakes have happened in and around the Antakya district of Hatay province. This region is in a first-degree earthquake zone, so it is crucial to strictly adhere to the regulations regarding "Structures to be Built in Disaster Areas" before undertaking any development projects (refer to Figure 3.8).

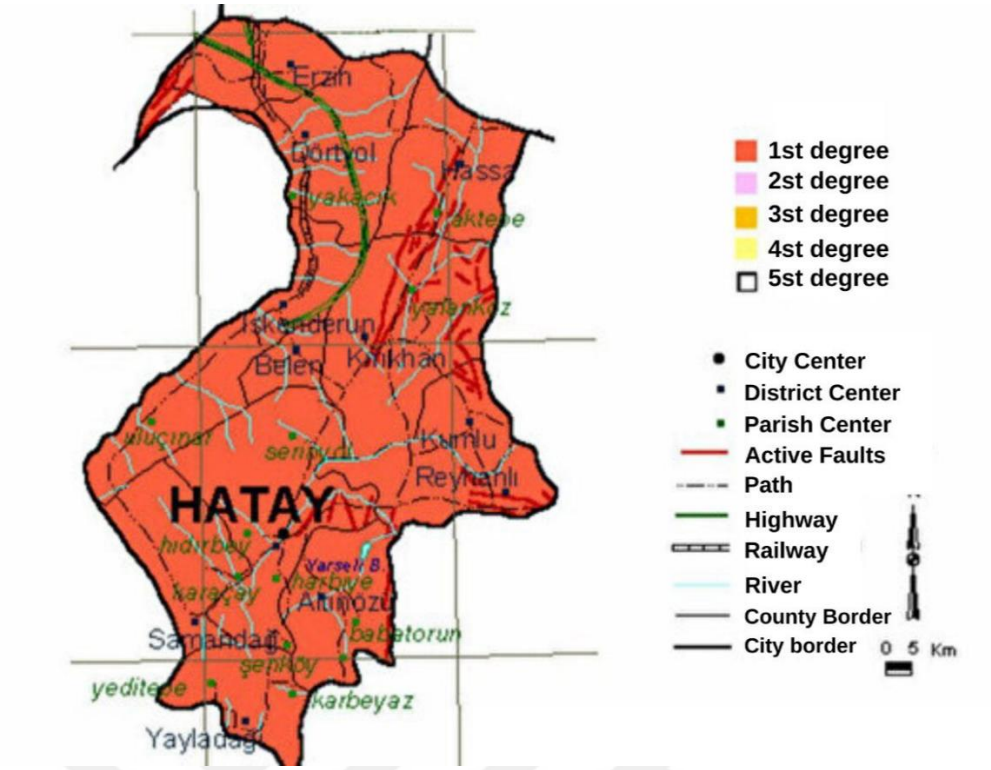

Figure 3.8. Earthquake hazard levels of Antakya AFAD, 2022).

In terms of engineering, the determination of seismicity relies on a probability-statistics calculation. As part of the geotechnical study within the scope of the urban development plan for Hatay Province, Antakya District, seismicity, and Poisson probability distribution, earthquake hazard analysis has been conducted. For this purpose, earthquakes with a surface wave magnitude of 4.5 (Mw > 4.5) and above, occurring between the latitudes 36.20 (N) and 36.22 (N), and longitudes 36.22 (E) in the region with a radius of 100 km around the center of Antakya, during the period 1900-2023, were obtained from Bogazici University Kandilli Observatory earthquake research center's data, accessible at www.koeri.boun.edu.tr. The date, latitude (N), longitude (E), source, focal depth, and magnitude values for the earthquakes used in the calculations are provided in Table 3.1

Table 3.1. Earthquakes occurred within a 100 km radius of the study area between 1900-2023.

No	Date	Time	Latitude	Longitude	Depth (km)	Mw	Location
1	09.11.2023	02:32:14	36.5478	36.4147	12.6	4.7	Kodalli-Kirikhan (Hatay)
2	07.02.2023	05:26:31	36.3017	36.1045	9.4	4.6	Gulderen- (Hatay)
3	18.12.2022	18:13:09	36.3978	36.4455	8.4	4.7	Akkuyu-Kumlu (Hatay)
4	10.2.2015	04:01:54	36.0278	359750	11.6	4.6	Meydan-Samandag (Hatay)
5	9.6.2014	03:38:35	36.7702	360077	22	4.6	Iskenderun Korfezi (Akdeniz)
6	14.11.2010	23:08:25	36.5950	359983	5.9	5	Iskenderun Korfezi (Akdeniz)
7	17.6.2009	04:29:12	36.0625	360140	8.6	5	Gozene-Samandag (Hatay)
8	17.1.2009	07:45:25	370867	363592	13.9	4.6	Ceyhan (Adana)
9	9.10.2006	05:01:31	357600	355900	17	4.5	Akdeniz
10	18.10.2001	15:50:29	367800	353700	19	4.8	Cagsiru-Karatas (Adana)
11	25.6.2001	13:28:48	371200	362800	27	5.5	Arslanli- (Osmaniye)
12	17.1.2001	12:09:54	370100	362700	8	4.7	Karacalar- (Osmaniye)
13	15.1.1999	02:04:30	370400	358100	18	4.5	Ceyhan (Adana
14	4.7.1998	09:24:22	368500	355100	20	4.5	Beloren-Yuregir (Adana)
15	4.7.1998	02:15:47	368500	354700	35	5.1	Beloren-Yuregir (Adana)
16	28.6.1998	03:59:24	370000	356800	6	4.9	Cakaldere-Ceyhan (Adana)
17	22.1.1997	18:24:51	361300	360800	23	5	Ozbek-Samandag (Hatay)
18	22.1.1997	17:57:19	361400	361200	23	5.5	Yesilpinar- (Hatay)
19	19.6.1996	00:18:01	359900	360500	6	4.6	Yesiltepe-Yayladagi (Hatay)
20	18.6.1996	23:44:10	359900	361400	11	4.5	Ayisigi-Yayladagi (Hatay)
21	5.6.1996	13:13:15	356100	358100	12	4.8	Akdeniz
22	10.2.1994	06:15:18	369700	358300	17	4.9	Korkuyu-Ceyhan (Adana)
23	3.1.1994	21:00:30	370000	358400	26	5	Ciftlikler-Ceyhan (Adana)
24	24.6.1989	03:09:58	367100	359300	46	4.9	Iskenderun Körfezi (Akdeniz)
25	3.8.1988	20:42:34	358800	356500	56	4.6	Akdeniz
26	24.11.1983	00:14:08	370500	361200	37	4.7	Sazlik-Toprakkale (Osmaniye)
27	19.1.1982	18:38:52	359300	356100	46	4.5	Akdeniz
28	30.6.1981	07:59:08	361700	358900	63	4.7	Kapisuyu-Samandag (Hatay)
29	2.1.1980	12:52:27	365600	363800	32	4.6	Ceylanli-Kirikhan (Hatay)
30	1.1.1975	00:30:01	366700	364900	35	5.2	Narlihopur-Kirikhan (Hatay)
31	26.6.1966	13:17:01	368400	359200	58	4.8	Golovasi-Yumurtalik (Adana)
32	10.9.1961	16:17:28	370200	361100	100	4.9	Buyuktuysuz-Toprakkale (Osmaniye)
33	16.7.1956	00:21:46	357200	360100	100	4.7	Türkiye-Suriye Sinir Bölgesi
34	8.4.1951	21:38:13	365800	358500	50	5.8	Iskenderun Körfezi (Akdeniz)
35	14.1.1950	22:19:40	365000	358000	30	4.7	Iskenderun Körfezi (Akdeniz)
36	14.6.1936	17:01:37	366400	358500	70	5.6	Iskenderun Körfezi (Akdeniz)
37	4.8.1929	15:12:03	365000	360000	5	4.7	Asagikepirce-Iskenderun (Hatay)
38	5.10.1921	19:09:46	364000	352000	30	5.6	Karatas Aciklari-Adana (Akdeniz)
39	25.12.1915	06:06:09	364700	361400	10	5.4	Guzelyayla-Belen (Hatay)

Considering the destructive earthquake threshold as M=5.0 for our country's building stock, it is observed that the number of moderate-sized earthquakes is relatively high in the construction area and its surroundings. Additionally, within the study area, between 1900-2023, there were 31 earthquakes with $4.5 < Mw < 5.0$, 7 earthquakes with $5.0 < Mw < 5.5$, 5 earthquakes with $5.5 < Mw < 6.0$, and 1 earthquake with $6.0 < Mw < 6.5$.

The relative movements of the Eurasian, Arabian, and African plates are reflected in the morphotectonics of Antakya and its surrounding areas. The Arabian and African plates, which possess a weak resistance upper asthenosphere, move northward as a result of convective currents in the mantle. Seismic activities in the region, including earthquake faults and global kinematic models based on oceanic spreading, illustrate that the Arabian plate moves at an average speed of about 25 mm per year towards Eurasia in a north-northwest direction, while the African plate moves northward at about 10 mm per year in association with Eurasia.

As a result, there is compression in the north-south direction of the Anatolian plate. This compression was initially accommodated by east-west trending folds and thrusts, but this became unsustainable by the Upper Miocene, giving rise to lateral strike-slip faults such as the right-lateral North Anatolian Fault and the left-lateral East Anatolian and Dead Sea Faults. The northward movement of the African plate resulted in subduction beneath the Anatolian plate along the Helen-Cyprus Arc.

Antakya and its surrounding areas are located to the south of the Antakya-Kahraman Maraş graben, which evolves under the influence of the Dead Sea and East Anatolian Faults and the Cyprus Arc. The southern part of the graben is shaped by the Dead Sea Fault, which extends northward until it intersects with the East Anatolian Fault at Türkoğlu. This fault has a general north-south direction and is represented in the country by the Gharb and Karasu segments. The Karasu Segment begins at Samandağ and continues north to Türkoğlu, while the pull-apart basin is located between the Karasu and Gharb segments in the Amik Plain.

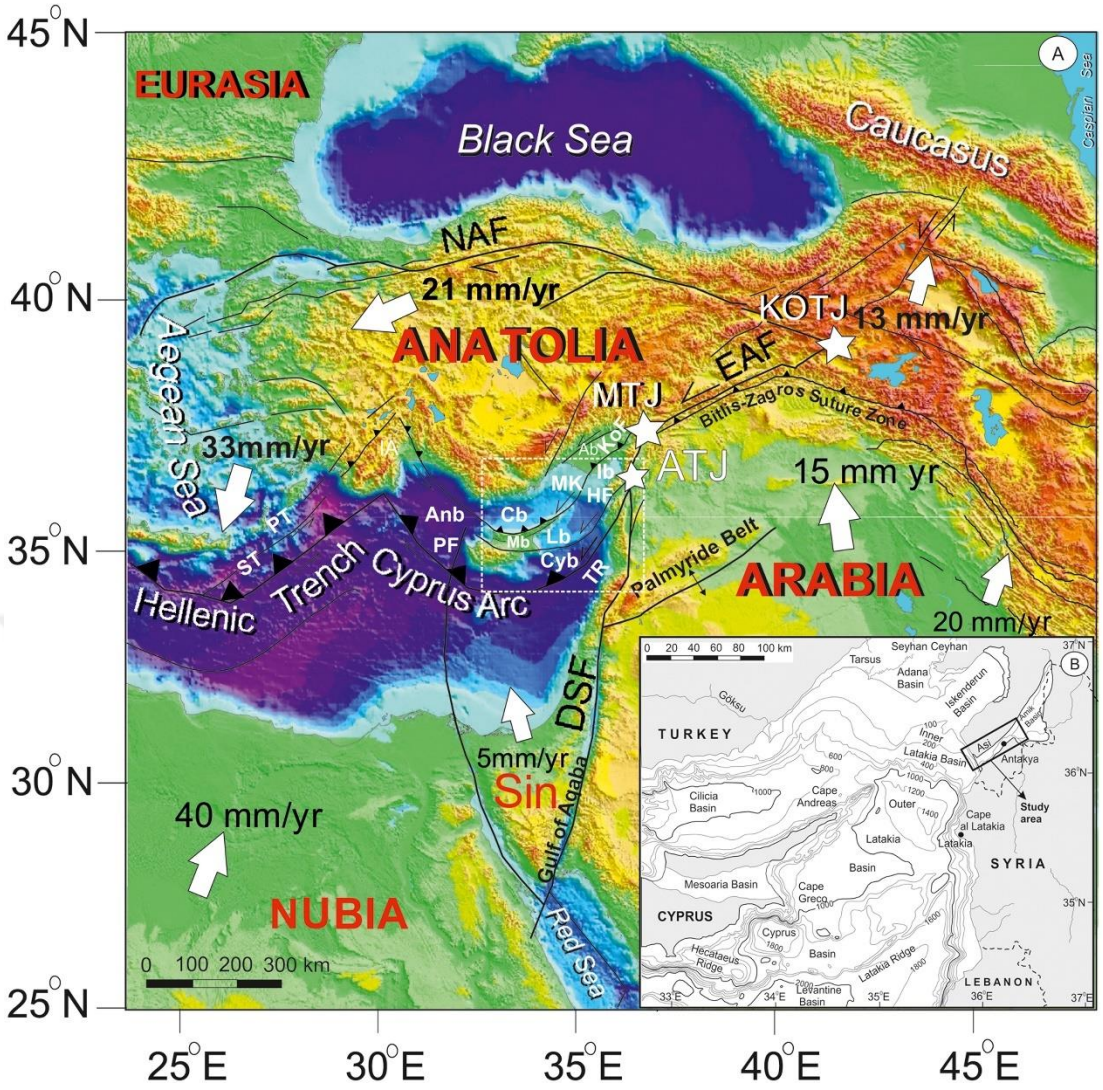

Figure 3.9. Simplified tectonic setting of the eastern Mediterranean and surroundings, complied from Hall et al. (2005) and Reilinger et al. (2006).

The movement of the Arabian plate towards the north results in an increase in cumulative stresses on the Dead Sea Fault. When the geological units' resistance power is exceeded by this stress, energy is suddenly released in the form of earthquakes, creating a highly risky potential for earthquakes in Antakya and its surrounding areas. This has been further supported by earthquakes that have taken place in historical and instrumental periods. Due to this high risk, Antakya and its immediate surroundings are classified as areas with a first-degree earthquake risk on the "Turkey Earthquake Regions" map.

The principal fault passing through the Antakya region is the Amanos Fault. It extends in a line from the Amanos Mountains in Türkoğlu to Antakya and is approximately 145 km long, with a strike-slip type of faulting. In the Antakya region,

both the Eastern Anatolian Fault Zone and the Dead Sea Fault Zone have an impact. The Amik basin, which is about 30 km wide and situated between these two belts, has been affected by earthquakes for around 2000 years.

Figure 3.10. A digital elevation model for the study area and its surroundings, showing the major active faults and the morphotectonic units. *MTJ: Kahramanmaraş or Türkoğlu Triple Junction, ATJ: Amik Triple Junction.*

3.7. Climate Features of the Region

According to the Köppen-Geiger Climate Classification, Antakya falls under class C (Subclass: CSA). This classification indicates a Mediterranean climate for the region. The Thornthwaite climate classification results show that Antakya has d, b3, s, and b4 climate types. The winters in this area are warm and rainy, while the summers are hot and dry. Although the number of rainy days per year is not very high, the amount of precipitation received is significant. The region experiences winds, particularly during

the summer, thanks to its geographic location in a corridor. Additional climatic graphs can be found in Figures 3.11 and 3.12.

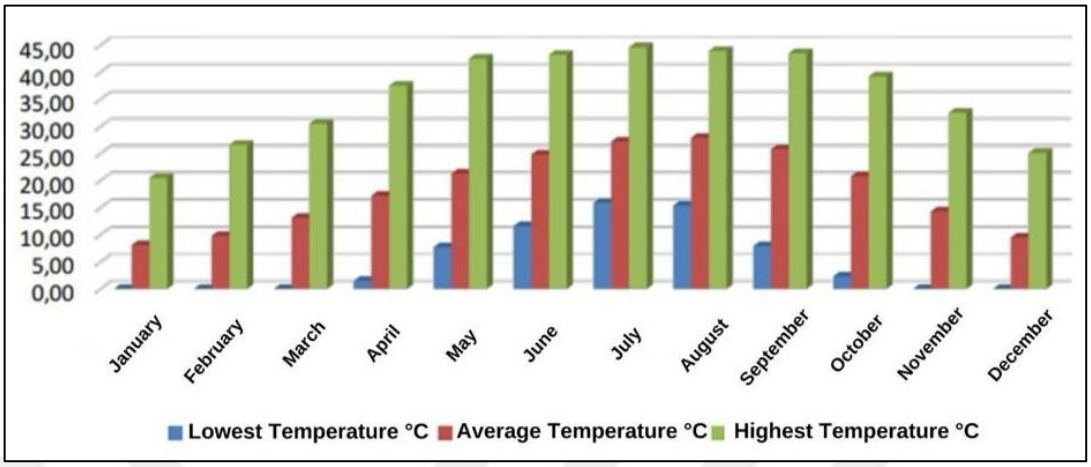

Figure 3.11. Highest, lowest and average temperature (T.R. General Directorate of Meteorology, 2022).

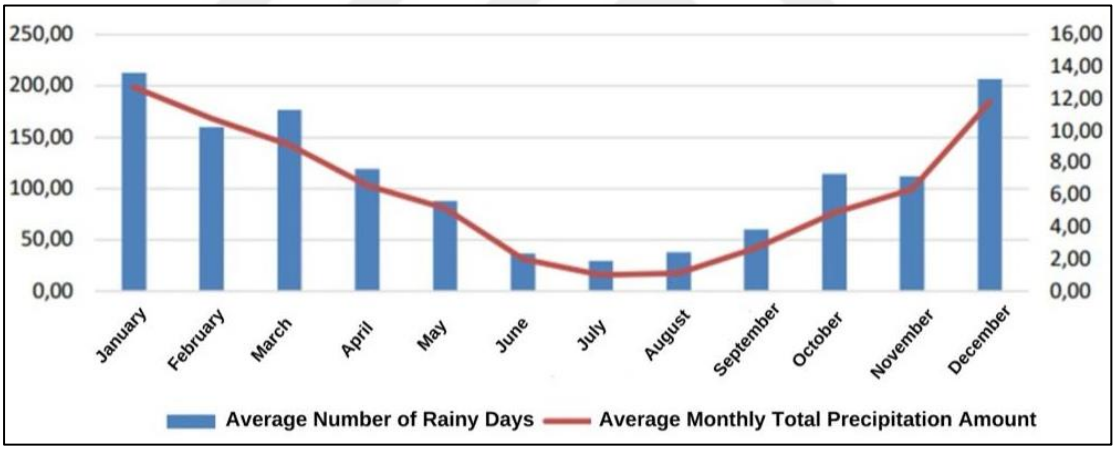

Figure 3.12. Precipitation and number of rainy days (T.R. General Directorate of Meteorology, 2022).

Based on the climatic graphs, it can be inferred that temperature plays a crucial role in shaping the living conditions in Antakya. This leads to the emergence of various natural and cultural characteristics. While the average temperature and rainfall contribute to enhanced productivity in terms of agricultural output, they have a negative impact on living environments.

3.8. Hydrographic Features of the Region

The main river in our study area is the Asi (Orontes) River, originating from Lebanon and flowing through the Syrian borders into Hatay. Other important rivers in the region include Altınçay, Kavaslı, Hanna, and Hacı Kuriş, which are tributaries of the Asi River (Erol, 1963:8,59). Before completely entering Turkish territory, the Asi River serves as the Turkey-Syria border for approximately 30 km. Once inside Turkey, it turns towards the southwest in the Amik Plain and continues its course through meandering in the flat areas. Geographically dividing Antakya into two parts, the old and new, the Asi River passes through the city until it reaches the sea following the Antakya-Samandağ trough in the northeast-southwest direction (DSİ, 2007) (Figure 3.13).

The Asi River delta, located within the borders of Hatay province, forms the southernmost delta plain in Turkey. The plain is surrounded by Mount Musa on the north, which is the southernmost tip of the Amanos mountain range, Mount Saman and Mount Ziyaret on the east, and Keldag (Mount Kilic) on the south. It is bordered by the Mediterranean Sea on the west (see Figure 3.13). Originating from the Lebanon mountains, the Asi River follows a graben area formed by the Dead Sea fault line as it passes through Syrian lands. The river enters the Turkish border near the village of Esrefli. After flowing northward through the Amik plain, it changes its direction to the south-southwest in an arch-like manner. In Antakya-Samandag Graben, it follows a distinctive valley and then passes through Ziriye Gorge between Mount Saman and Mount Ziyaret before flowing into the Mediterranean Sea southwest of Samandag. At the point of its outflow, the river forms a triangular delta due to its sediment content, with the long edge of the triangle resting along the coastline. The length of this delta, from northwest to southeast, is approximately 15 km, and the width from east to west is approximately 6 km (see Figure 3.13).

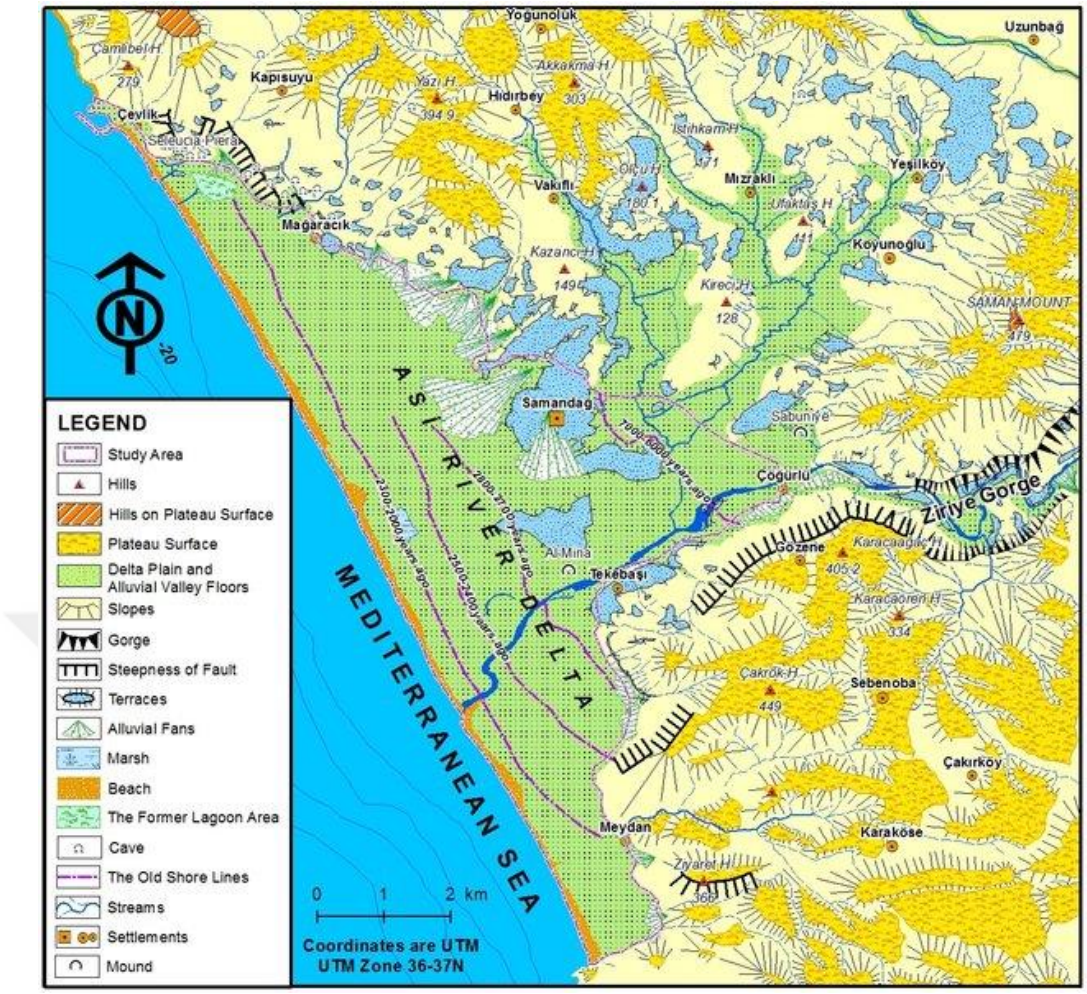

Figure 3.13. Location map of Asi river delta (Korkmaz et al., 2012)

Hacı Kuriş river is among the major rivers that supply water to the Asi River, which forms the boundary between Turkey and Syria. The river starts from Habib-i Neccar Mountain and flows towards Narlıca, where it joins the Asi River. Hacı Kuriş River is characterized by an inconsistent flow pattern, with water flowing during the winter months and drying up during the summer season. Altınçay River is another significant source of water for the Asi River, but it results in significant pollution as it passes through the Armutlu and Esentepe neighborhoods. The water in this river also tends to dry up in the summer. Kavaslı River emerges from the Amanos Mountains and cuts across the city center, flowing through the Antakya-İskenderun ring road before merging with Asi. The rivers in our study area significantly impact the city of Antakya, with their respective basin areas shaping its surroundings (DSI, 2007) (Table 3.2).

Table 3.2. Length of rivers in Antakya and surroundings (DSI, 2007).

River Name	Length (km)
Asi (Orontes) River	90
Kavaslı Stream	19.5
Altınçay Stream	12.5
Hanna Stream	21.25
Hacı Kuriş	8.5

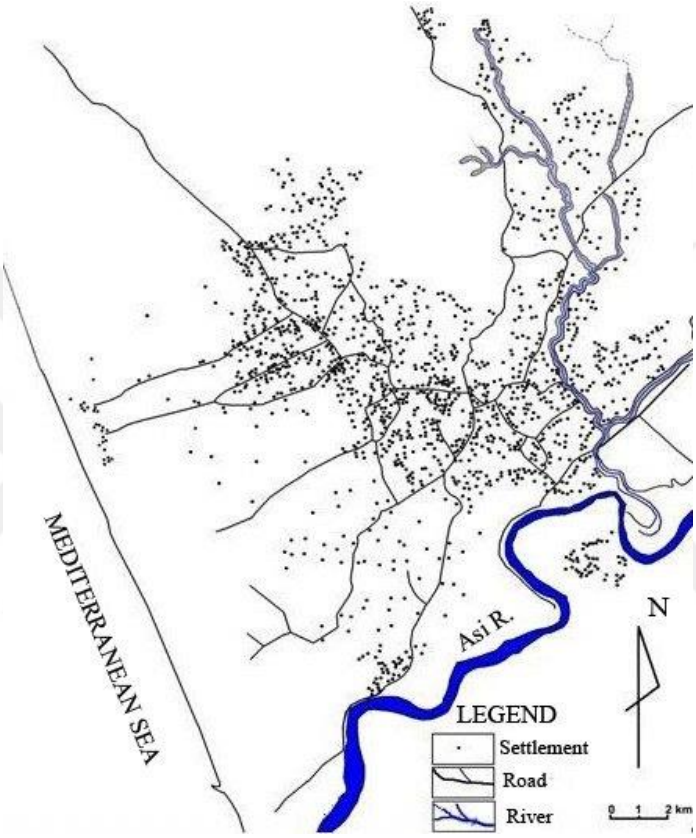

Figure 3.14. Settlement pattern of Antakya and Asi River (Korkmaz et al., 2012).

3.9. Population and Settlement

Hatay province covers an area of 5,525 km^2, while Antakya district occupies 703 km^2. According to the 2020 census, the total population of Hatay province is 1,659,320, with Antakya having a population of 389,377 and Defne having a population of 160,066. However, due to the irregular migrations caused by the events in Syria in recent years, it is believed that the population is significantly higher than the registered population based on addresses. In Antakya district, there are a total of 95 neighbourhoods', and in Defne district, there are 37 neighbourhoods.

3.10. Standard Penetration Test

The Standard Penetration Test has become a standard field test for determining soil properties. Since its development in the late 1920s, this test has been widely used in several countries. This test method, generally for sand and sandy silt and fine gravels, was developed to obtain some soil parameters in cohesionless sandy soils and there is extensive experimental experience in its use (M. Orhan, 2022a).

This test, which is used to determine the density, strength, consistency and liquefaction status of cohesive and non-cohesive soils, as well as the bearing capacity and estimated settlement of the foundation soil, was first defined by Terzaghi in 1974 as the "Standard Penetration Test" and is defined as driving the sampling tube into the ground (Clayton, 1995).

The SPT is widely used because of its short test duration, simplicity of construction, the fact that it is the most widely used field test internationally, the ability to sample while measuring penetration resistance, its lower cost than other tests, and its applicability to cohesive and non-cohesive soils as well as solid, fine gravel and fill. It is also highly sensitive, subject to operator error and dependent on many variables ranging from drilling equipment to application method (M. Orhan, 2022a).

The test is very practical and gives very good results if the necessary precision is applied. The standard penetration test is the measurement of how many blows are required to drive a sampler 45 cm deep into the ground. This is done by repeatedly dropping a 63.5 kg heavy hammer or driving it down to the bottom. The number of blows (N) obtained by driving the sampler 15 cm to penetrate the spalled soil at the bottom of the manhole is not considered. The soil penetration resistance is defined by the number of impacts that correspond to the first 15 cm of penetration, followed by the 30 cm of penetration (SPT-N).

If more than 50 blows are required for each 15 cm of penetration, or more than 100 blows for two 30 cm penetrations in total, the driving shall be stopped. In addition, if no progress is made during the 10-pulse application. It is recorded as REFU (M. Orhan, 2022a). The sampler in the tube is removed and the sample placed in it is sent to a laboratory for testing.

The test is carried out at intervals of 1.75m to 1.5m along the borehole. According to the practice in Türkiye, the test is carried out every 1.5 m. If the soil is gravelly, the

lug at the end of the tube is removed and a conical tip with 60 bevelled edges is inserted (Aydın, 2010).

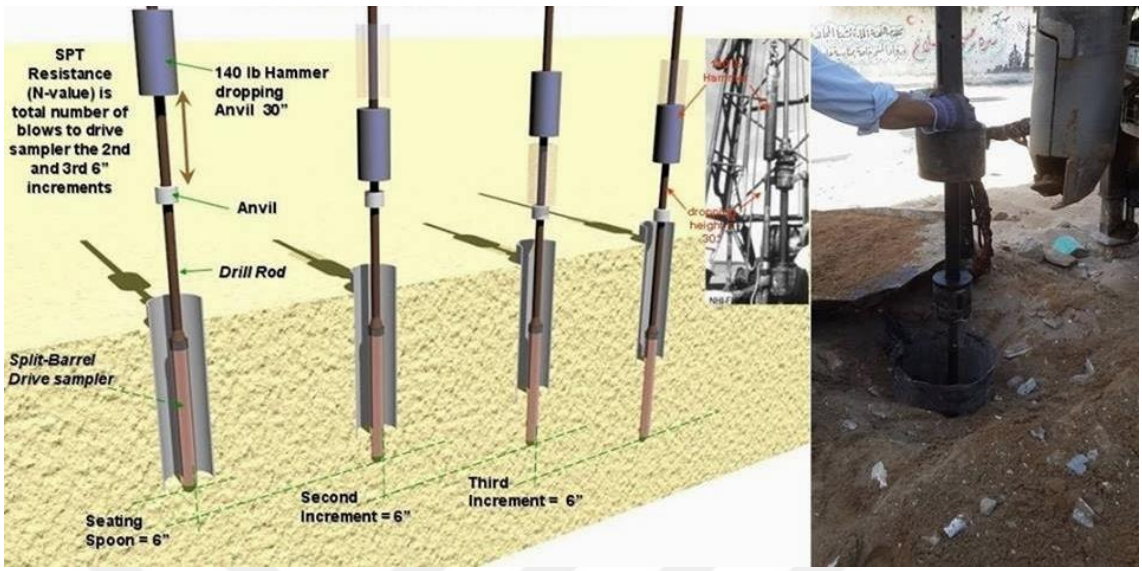

Figure 3.15. Standard penetration test stages (Mayne et al., 2002).

3.11. Bearing Capacity Calculations

The elements that transfer the building loads to the ground by converting them into stresses that the ground can withstand, depending on their shape, size and burial depth, are called foundations, and the medium that carries the loads directly or through the foundations is called the foundation soil (Genç, 2008).

The bearing capacity can be defined as maximum bearing pressure a soil can support while not exceeding its shear strengths and without settling in different areas. SPT-N data are widely used to determine the bearing capacity of soils. The first studies on this subject were carried out by Meyerhof (1956).

The equations developed by Meyerhof are used in this approach to determine the allowable bearing capacity values for single foundations which have a dimension 2 m width and 2 m depth. These values correspond to a maximum settlement of 25 mm of the foundation and are calculated (Çinicioğlu 2005).

$$q_a = 12 \times N \times K_d \quad \text{for } B \leq 1.22 \text{ m} \quad (3.1)$$

$$q_a = 8N \times \left(\frac{B+0.305}{B} \right)^2 \times K_d \quad \text{for } B > 1.22 \text{ m} \quad (3.2)$$

$$K_d = 1 + 0.33 \frac{D}{B} \leq 1.33 \quad (3.3)$$

Definitions:

q_a : 25 mm. safe bearing capacity for settlement (kN/m²)

N : SPT blow count

D : Foundation depth (m)

B : Foundation width (m)

Meyerhof considered the depth of the affected zone and the increased settlement in wide raft foundations when developing the formula for allowable bearing capacity. According to Bowles (1996), the formula for safe bearing capacity of raft foundations is as follows.

$$q_a = 12,5 \times N \times K_d \quad (3.4)$$

3.12. Groundwater

Groundwater can lead to various issues in different soil types. In silty-sandy soils, it can cause liquefaction, while in clay soils, it can result in swelling or changes in the viscosity limit. Hollow soils can experience collapse due to increased water content. The interaction between water and structures is also crucial. When part of a structure's foundation is below the water table, there is a risk of corrosion occurring between the water and the structural elements or materials. This corrosion can weaken the structure. Hence, during the design phase of engineering projects, the presence of groundwater must be carefully considered, and appropriate protective measures must be implemented to safeguard the structures (Uyan, 2018).

When boreholes are fitted with firm perforated tubes, they serve as excellent tools for measuring groundwater levels. By emptying the borehole and monitoring the static water level for a minimum of three consecutive days, the static water level can be determined. If groundwater is encountered and found to be near the foundation, water samples are extracted and subjected to laboratory tests. These tests aim to assess the potential impact of the water on concrete or other building materials. Parameters like sulphate content and pH are analyzed to understand the water properties. This process is crucial in safeguarding the structural elements and maintaining control over the water level (IMO, 2016).

3.13. Water Content

The soil water content is expressed as the ratio of water in the intergranular spaces to the dry mass of the soil, represented as a percentage of the soil's dry weight. This calculation involves subtracting the remaining water weight from the dry weight of the soil, as outlined by Uzuner (2007).

At specific thresholds, the soil exhibits different behaviors based on its water content. When the water content exceeds a certain value (wn ≥ wLL), the soil becomes liquid and behaves like a viscous liquid. Conversely, when the water content falls below the plastic limit (wn ≤ wPL), the soil becomes semi-solid. The moisture level at which the soil becomes solid is known as the shrinkage limit (wSL). When the soil water content is between the liquid and plastic limits (wPL < wn < wLL), it exhibits plastic behavior, as described by Tüzen (2019).

These water limits have an impact on various soil properties, including consistency, bearing capacity, and dynamic and mechanical properties. These properties play a vital role in geotechnical engineering design, directly influencing the behavior of the soil structure. Consequently, the determination of soil water content and water limits holds significant importance.

$$w = \frac{M_w}{M_d} = \frac{w_w}{w_s} \tag{3.5}$$

In this equation;

w: Water content value

M_d: Dry mass value

M_w: Wet mass value

w_w: Water mass value

w_s: It gives the value of the grain mass value.

Water content is a unitless measurement that is typically conveyed as a decimal or percentage. Occasionally, it may exceed 1. The water content of soil fluctuates based on its water mass, while the dry weight remains consistent. Consequently, the dry mass is utilized as the denominator in the formula for calculating water content. When referring to water content in natural soils, it is commonly referred to as the "natural water content" (wn) (Uzuner, 2007).

3.14. Grain Size Distribution

Soil consists of grains of various sizes, and the analysis of soil particle size involves the utilization of a set of standard sieves with different aperture sizes. These sieves are employed to separate and collect particles, and the weight percentage of particles within each size range is subsequently determined. Table 3.4 provides a list of commonly used standard sieves (Özaydın, 2015).

Table 3.3. Standard sieve openings to measure the grain size distribution of soils (ASTM D422).

Sieve No	Sieve Opening (mm)
4	4.75
10	2.00
20	0.85
40	0.425
60	0.25
100	0.15
140	0.106
200	0.075

The process of sieve analysis involves arranging sieves in a stack with decreasing aperture, with the smallest aperture sieve placed at the bottom. The samples are then placed on the top sieve and subjected to sieving using a sieve analyzer at 15-minute intervals. The remaining samples on each sieve are weighed and analyzed. These tests adhere to the guidelines outlined in TS EN 933-1 (Danışman, 2022). Figure 3.16 depict typical curves illustrating the distribution of grain diameters.

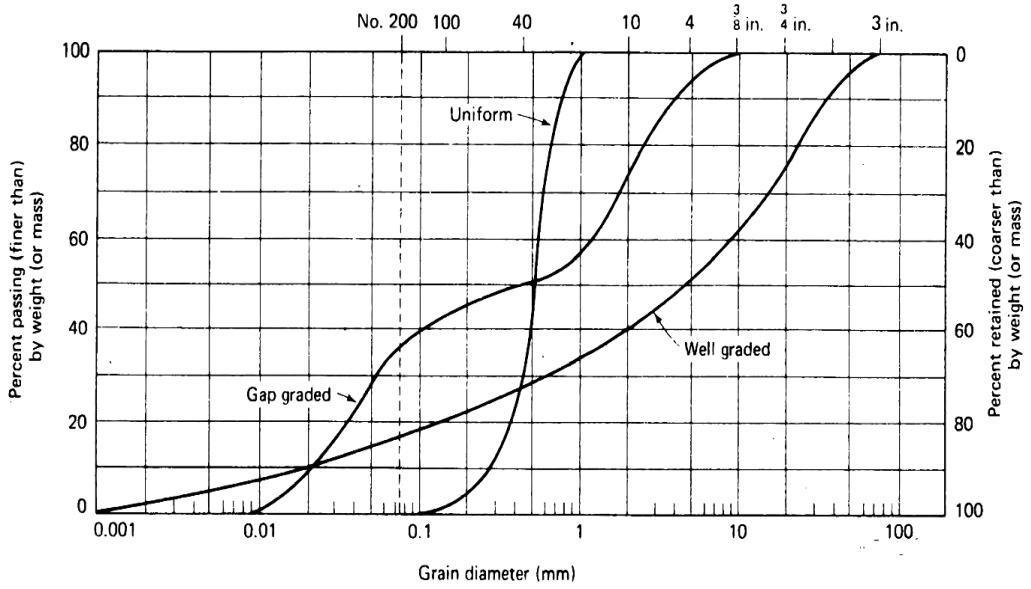

Figure 3.1. Typical grain size distribution curves (Holtz et al., 1981).

3.15. Consistency Limits

Cohesion force, also referred to as gravitational forces between soil grains, binds them together if the grains are below a specific size. Soils in which grains are held together by this force are classified as cohesive soils (Okman, 1998).

Fine-grained soils can exist in different states depending on their water content. As water is added incrementally to a dry soil and mixed, the soil transitions from being solid to semi-solid, plastic, and eventually liquid, with a slight increase in volume. The states and associated water contents that separate them were defined by Swedish scientist Albert Atterberg in 1911. These limits are known as Atterberg limits or consistency limits (Uzuner, 2016).

The engineering behavior of soils, particularly fine-grained soils, is influenced by the amount of water present in their pores. Understanding the water content alone is insufficient; it must be compared to standard values with specific engineering behavior. This is where the Atterberg limits (consistency limits) become significant. By knowing the water content according to the Atterberg limits, predictions can be made about the engineering behavior of the soil (Holtz et al., 1981).

In geotechnical practice, the liquid limit (WL or LL) and plastic limit (WP or PL) are commonly used, while the shrinkage limit (WS or SL) is less frequently applied. Albert Atterberg also defined the plasticity index as the range of water content at which soils exhibit plasticity, and this property is utilized in soil classification. Consistency limits were standardized by Terzaghi and Casagrande (Holtz et al., 1981).

Liquid Limit (W_L or L_L) is the minimum water content at which the soil can flow under its own weight. Essentially, it is the water content that marks the transition of the soil from a plastic state to a liquid state (Genç, 2008; Uzuner, 2016).

Plastic Limit (W_P or P_L) refers to the water content at which the soil undergoes a change from the plastic state to the semi-solid state due to a reduction in water content. It is at this point that cracks start to develop on the soil surface (Whyte, 1982).

Shrinkage Limit (W_S or S_L) is the minimum water content required for soils to be completely saturated with water. This specific water content indicates that the soil volume no longer undergoes any further reduction (Sekercioglu, 1993; Uzuner, 2016).

Plasticity Index (P_I or I_P), is defined as the range of water content values at which the soil demonstrates its plastic behavior. In simpler terms, it is the numerical difference between the liquid limit and the plastic limit (Sekercioglu, 1993).

Figure 3.17 illustrates the stress-strain characteristics of the soil at various water contents and consistency limits, as defined by Atterberg.

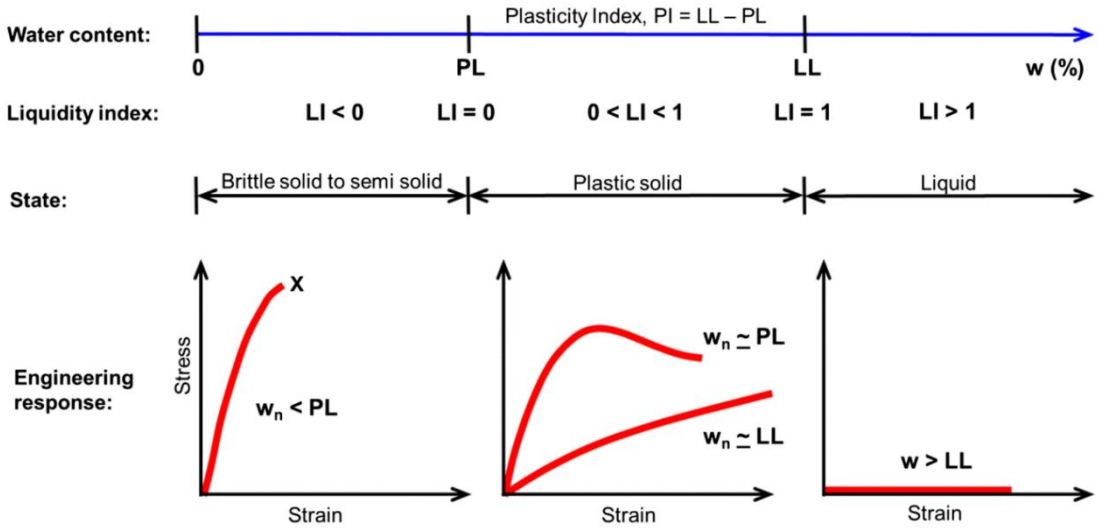

Figure 3.2. Consistency limits and stress-strain of soils at different water contents (adapted from Holtz et al., 2011).

3.16. Shear Wave Velocity

Earthquakes are significant events that can result in immense devastation and loss of life among the natural disasters occurring on Earth. Vibrations, known as earthquake waves, occur as a result of the energy released by the earthquake source and propagate in various waves on and within the Earth's surface. Among these earthquake waves, there are two types called P-waves and S-waves. Figure 3.18 illustrates the propagation of both P and S waves.

Analyzing the velocities of P-waves and S-waves can help determine the mechanical properties of soil. P-waves travel in the same direction as their vibrations, while S-waves travel perpendicular to their vibration direction. These two wave types are crucial factors for understanding the behavior of soil under stress and can provide valuable information for applications in geotechnical engineering (for instance, the direction perpendicular to the displacement of particles in the soil).

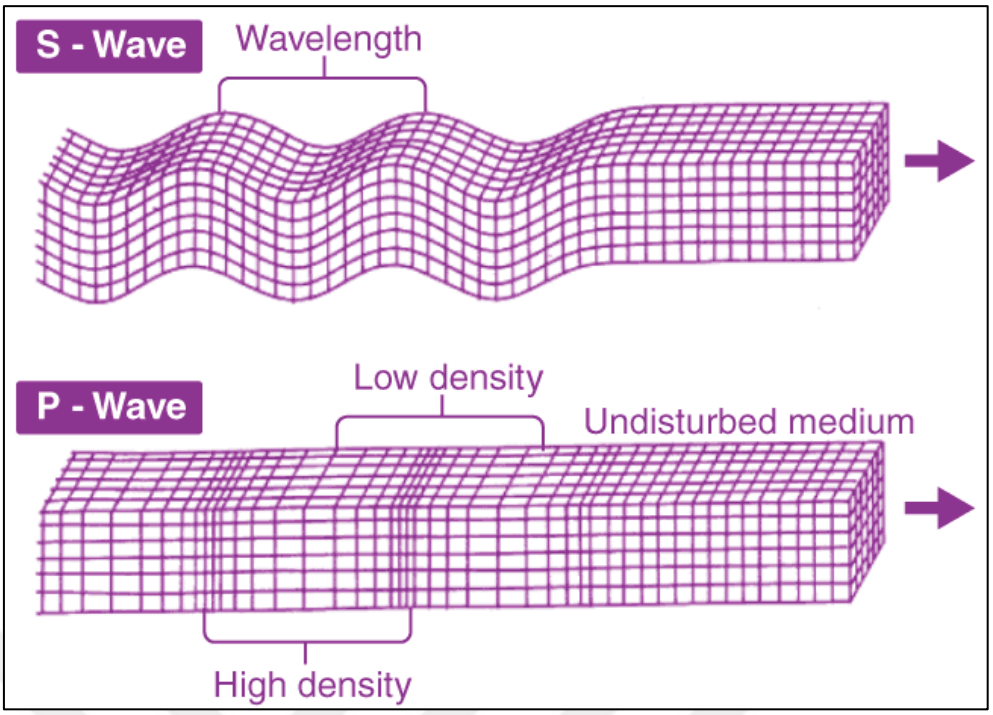

Figure 3.3. Propagation of P and S waves (Thitimakorn, 2003).

P-waves are the quickest waves within a medium, and as a result, they are the first to be detected in earthquake recordings. The equation for calculating the velocity of the P-wave is as follows;

$$V_P = \sqrt{\frac{\lambda+2\mu}{\rho}} = \sqrt{\frac{E(1-\sigma)}{\rho(1+\mu)(1-2\mu)}} \quad (3.6)$$

$\boldsymbol{\lambda}$ = Amplitude

σ = Stress

G = Shear Modulus

D = Density

μ = Poisson Ratio

E = Modulus of Elasticity

To determine the velocity of the S-wave (VS), the following formula is utilized;

$$Vs = \sqrt{\frac{G}{P}} = \sqrt{\frac{E}{2\rho(1+\mu)}} \quad (3.7)$$

Shear waves are a seismic wave type that generally follows primary earthquake waves. Unlike primary waves that move along particle movement, shear waves move perpendicular to it. They do not travel through liquids or gases. Shear wave velocities are a significant parameter representing soil strength, and soil classifications are based on these velocities. Vs(30) is the average shear wave velocity obtained from in-situ seismic

studies up to a depth of 30 meters (Uyanık, 2015).

Shear wave velocity is utilized in current earthquake codes such as NEHRP, EUROCODE-8, TBDY 2018 for determining soil classes, calculating shear modulus and modulus of elasticity at low levels of deformation, liquefaction, loss of bearing capacity, and soil amplification analyses. Therefore, soil shear wave velocity plays a crucial role in geotechnical earthquake engineering (Akdeniz, 2015). Vs_{30} can be expressed mathematically as follows:

$$Vs_{30} = \frac{30}{t_d + \frac{30-d}{Vs_1}} \tag{3.8}$$

In simpler terms, Vs_1 represents the velocity of the layer located between a depth, d, and 30 meters. In its most basic form, it is equivalent to the velocity at the deepest point of the subsurface model. t_d refers to the amount of time it takes for the wave to propagate through the layers up to the given depth, d. To provide a clearer understanding of the equation mentioned above, let's consider a three-layer medium.

$$Vs_{30} = \frac{30}{\frac{h_1}{Vs_1} + \frac{h_2}{Vs_2} + \frac{30-(h_1+h_2)}{Vs_1}} \tag{3.9}$$

3.17. Soil Classification according to NEHRP

NEHRP is a code developed by the BSSC for the FEMA that outlines the requirements for seismic design and construction of new structures in the United States. The main purpose of earthquake codes is to reduce the potential hazards posed by new and existing buildings, particularly in high-risk seismic regions. By setting standards for construction materials, design criteria, and practices, earthquake codes aim to ensure that infrastructure and buildings can withstand seismic activity and protect human life and property during and after an earthquake event (Baştürk, 2003).

Soil classification is an essential component of engineering structure construction according to the NEHRP. Based on the shear wave velocity (Vs_{30}), soils are categorized into six groups: A, B, C, D, E, and F. Class A soils have the hardest bedrock and Vs_{30} values of 1500 m/s or higher, whereas Class E soils, which are the lowest quality soils, have Vs_{30} values of 180 m/s or less. In determining soil classification, Vs_{30} velocity within a depth of up to 30 meters from the surface in the area where the structure will be built is applicable. Additionally, if the Vs_{30} value is 180 m/s or less, soils that are 36 meters or

deeper in depth are classified as Class F soil. Table 3.4 illustrates the NEHRP soil classification system (Ayday et al., 2001).

Table 3.4. Soil classification criterias according to NEHRP (Romero & Rix, 2001).

Soil Type	General Description	Average S wave speed (up to 30 m) Vs,30
A	Hard Rock	> 1500 m/s
B	Rock	760 - 1500 m/s
C	Hard and/or stiff/very stiff soils; most gravels	360 - 760 m/s
D	Sand, silts and/or stiff/very stiff clays, some gravels. Having average blow counts of $15 \leq N \leq 50$ or average shear strength of 50 kPa $\leq S \leq$ 100 kPa	180 - 360 m/s
E	Having thickness lower than 3 meters and PI > 20, w > 40% and s_u < 25 kPa soft clay	< 180 m/s
F	(1) Soils susceptible to failure or collapse under seismic loading such as liquefiable soils, quick and highly sensitive clays, collapsible weakly cemented soils (2) Peats/highly organic clays with a thickness greater than 3 m. (3) Very high plasticity clays with a thickness greater than 8 m and PI > 75 (4) Very thick soft/medium stiff clays with a thickness greater than 36 m	

3.18. Soil Classification according to EUROCODE-8

EUROCODE 8 is a regulatory code published by the European Committee for Standardisation that establishes standards for the design and evaluation of structures in European Union countries. Its purpose is to provide guidelines for assessing the seismic vulnerability of structures and designing new buildings or retrofitting existing ones to withstand seismic activity. The aim is to ensure safety in regions with increased risks of earthquakes by implementing uniform standards for earthquake-resistant design.

The regulation includes application rules that allow for calculations to be tailored to specific conditions in different countries, such as climate, seismic risk, and traditional building practices. As a result, EUROCODE approaches are also utilized in many countries outside the European Union. The map shown in Figure 3.19 has been created by the Joint Research Centre (JRC) and will be regularly updated with new information collected from the other countries (Joint Research Centre, 2023). Table 3.5 provides the soil classes and their corresponding properties as defined in EUROCODE- 8.

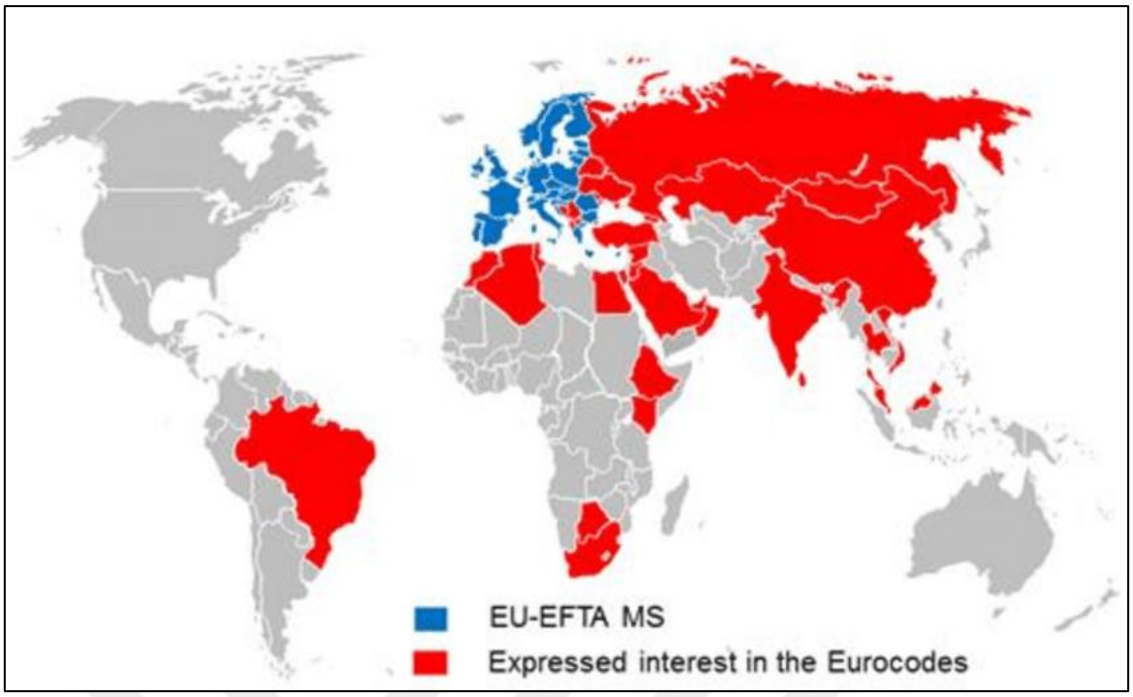

Figure 3.4. A world map showing the interest in EUROCODE regulations (European Commission, 2014).

Table 3.5. Soil classification criterias according to EUROCODE-8.

Ground Type	Description of stratigraphic profile	Parameters		
		$Vs_{,30}$ (m/s)	N_{SPT} (blows/ 30 cm)	Cu (kPa)
A	Rock or other rock-like geological formation, including at most 5 m of weaker material at the surface.	>800	-	-
B	Deposits of very dense sand, gravel or very stiff clay, at least several tens of metres in thickness, characterised by a gradual increase of mechanical properties with depth.	360-800	>50	>250
C	Depth deposits of dense or medium-dense sand, gravel or stiff clay with thickness from several tens to many hundreds of metres.	180-360	15- 50	70-250
D	Deposits of loose-to-medium cohesionless soil (with or without some soft cohesive layers), or of predominantly soft-to-firm cohesive soil.	<180	<15	<70
E	A soil profile consisting of a surface al1uvium layer with Vs values of type C or D and thickness varying between about 5 m and 20 m, underlain by stiffer material with Vs>800 m/s.			
S_1	Deposits consisting, or containing a layer at least 10 m thick, of soft clays/silts with a high plasticity index (PI > 40) and high-water content	< 100 (indicative)	-	10-20
S_2	Deposits of liquefiable soils, of sensitive clays, or any other soil profile not included in types A – E or S_1			

3.19. Soil Classification according to TBDY 2018

The Turkey Building Earthquake Code (TBDY), which entered on force on January 1, 2019, was published in the Official Gazette on March 18, 2018, with the Council of Ministers' decision numbered 2018/11275.

Section 16 of the TBDY, entitled "Special Rules for the Design of Foundation Soil and Foundations under Earthquake Effects," determines local soil classes based on the average shear wave velocity Vs_{30} values in the upper 30 meters, as outlined in Table 3.6. For this study, a database was created u sing Vs_{30} values derived from geological-geotechnical survey reports, and GIS was utilized to generate soil class maps of the study area.

$$V_{s30} = \frac{30}{\sum_{i=1}^{N} \frac{hi}{Vs,i}} \tag{3.10}$$

Table 3.6. Soil classification criterias according to TBDY 2018 (TBDY, 2018).

Ground Type	Description of stratigraphic profile	$Vs_{,30}$ (m/s)
ZA	Solid, hard rocks	> 1500
ZB	Lightly weathered, moderately intact rocks	760-1500
ZC	Very compact layers of sand, gravel and hard clay or weathered, weak rocks with many cracks	360-760
ZD	Moderately compact to compact sand, gravel or very stiff clay layers	180-360
ZE	Profiles containing loose sand, gravel or soft-solid clay layers or soft clay layers (c_u < 25 kPa)more than 3 metres thick in total, meeting the conditions *PI* >20 or *w* > 40%.	< 180
ZF	Grounds requiring site-specific investigation and evaluation, 1) Soils with the risk of collapse and potential collapse under earthquake impact (liquefiable soils, highly vulnerable clays, collapsible weak cement soils, etc.); 2) Peat and/or clays with high organic content with a total thickness of more than 3 meters, 3) High plasticity (*PI* >50) clays with a total thickness of more than 8 meters, 4) Very thick (>35 m) soft or medium-stiff clays	

4. RESULTS AND DISCUSSION

4.1. Introduction

This chapter focuses on evaluating and discussing the maps and graphs created during the research. The objective is to assess the suitability of an area spanning approximately 110 km² within the boundaries of Antakya Province for settlement. The research incorporates geotechnical survey reports based on 221 geological-geotechnical borehole data.

Various parameters were investigated, including the standard penetration test, natural water content, consistency limits, sieve analysis, and groundwater level at different depths (1.5m, 3m, 7.5m, 9m). Additional factors assessed included soil classification based on the USCS system, bearing capacity, and shear wave velocity.

The study also covers topics such as shear wave velocity (Vs30), soil classification according to NEHRP, EUROCODE-8, and TBDY 2018 standards, seismic hazard level based on soil amplification, and local soil class considering the prevailing vibration period.

To conduct the evaluations, GIS maps were generated using ArcGIS software and the IDW (Inverse Distance Weighting) method. ArcGIS is a widely utilized software for geographic data analysis, mapping, and geographic information systems. The IDW method is an interpolation technique employed to estimate values across a non-point surface using the relationships between point data. The IDW method calculates the estimated value of a point based on the values of nearby points. Points in proximity carry more weight in the estimation process, while distant points have less influence.

4.2. Analysis of SPT-N Maps

The Standard Penetration Test (SPT) is a significant field test used in soil investigations to ascertain the engineering properties of the soil. It is indispensable as it enables the determination of crucial parameters like bearing capacity and liquefaction potential. In this particular research, the focus is on examining the engineering behavior and soil characteristics using SPT maps derived from 221 boreholes. Table 4.1 illustrates the correlations between the standard penetration test results and the soil conditions as per various scientific experts. Throughout this study, the SPT-N numbers were evaluated following the methodology developed by Terzaghi & Peck.

Table 4.1. Relationships between standard penetration test and relative density (Demir, 2013).

Description (Soil State)	[1]Neo* [2]N1/60* (Terzaghi & Peck 1967)	Relative Density D_r (%)			
		Meyerhof (1956)[1]	Bowles (1968)[1]	Duncan ve Buchinani (1976)[2]	Mitchell ve Katti (1981)[2]
Very loose	< 4	< 20	< 15	< 15	< 15
Loose	4-10	20-40	15-30	13-35	15-35
Medium	10-30	40-60	35-65	35-65	35-65
Dense	30-50	60-80	65-85	65-85	65-85
Very dense	> 50	> 80	85-100	85-100	85-100

The study incorporates maps that visually represent the distribution of SPT values across different depths, ranging from the surface down to 10 meters. These maps effectively demonstrate how SPT values change as depth increases. Specifically, variations in SPT values at depths of 1.5m, 3.0m, 4.5m, and 9.0m are presented through maps such as Figure 4.1 to Figure 4.5. As depth increases, the SPT-N numbers also increase. In the study area, there is a consistent linear progression of SPT-N values with depth, a trend that is clearly evident in the maps where deeper depths are indicated by a stronger presence of blue color and a decrease in the red color. The initial 3 meters of depth in the northern region of the study area, which encompasses neighborhoods like Serinyol, Ovakent, Atatürk, University, Bahçelievler, and Kuzeytepe, are characterized by higher SPT-N values. The generated maps based on the SPT-N analyses illustrate that the soil in different sections of the study area possesses distinct properties. For example, the northern part generally consists of dense soil, whereas the southern and central regions predominantly have loose soil.

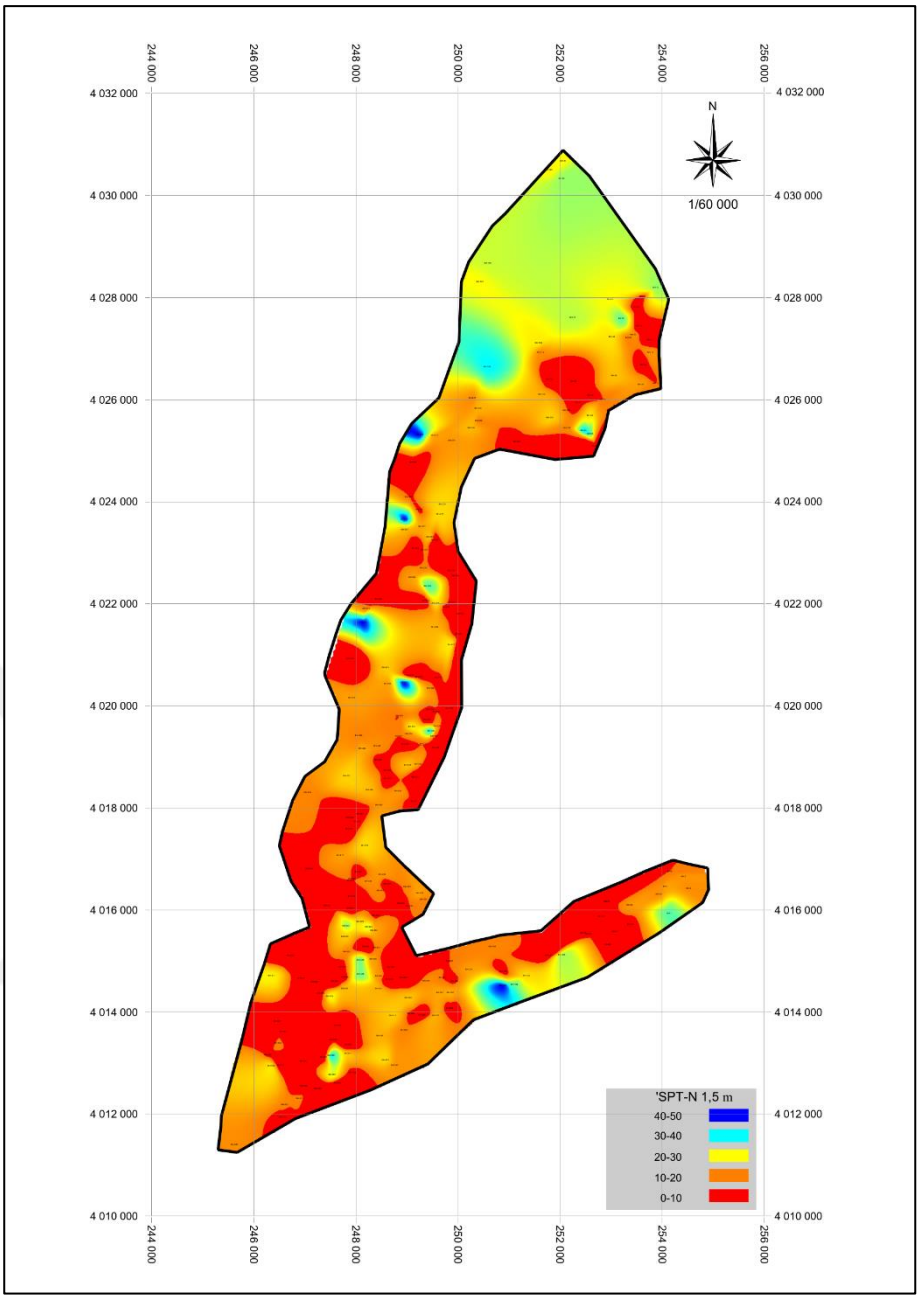

Figure 4.1. Distribution of SPT-N values according to 1.5 m depth.

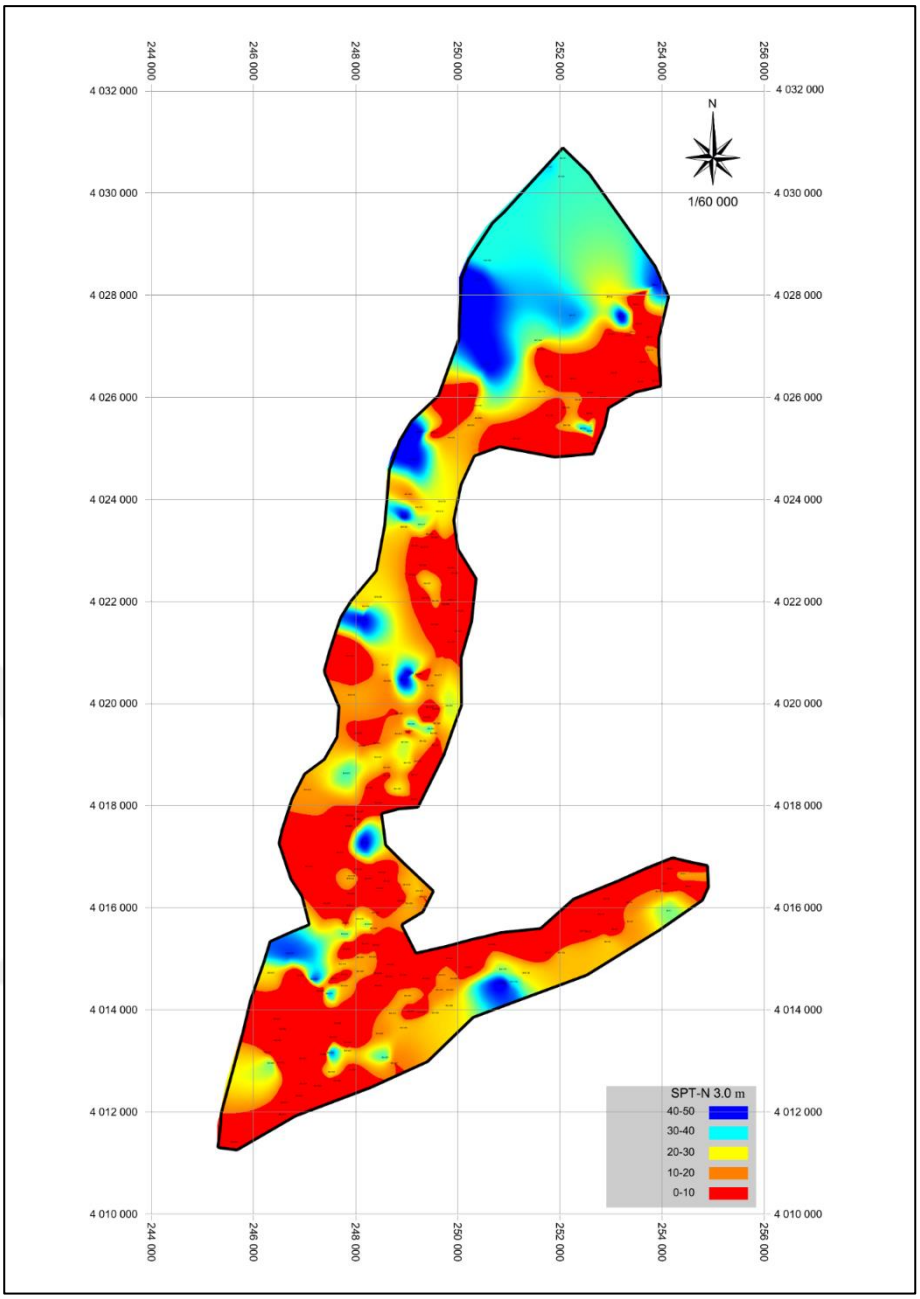

Figure 4.2. Distribution of SPT-N values according to 3.0 m depth.

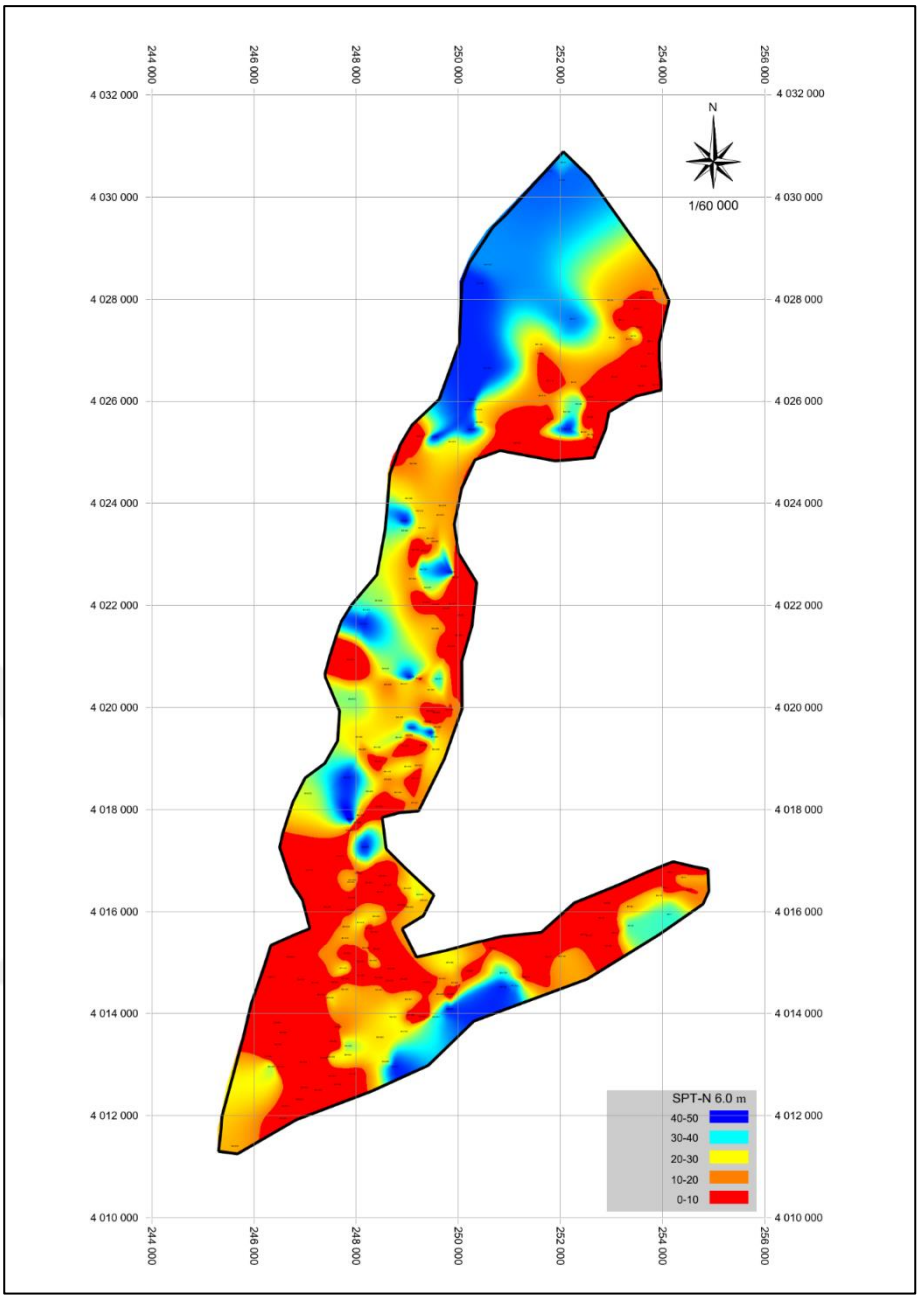

Figure 4.3. Distribution of SPT-N values according to 6.0 m depth.

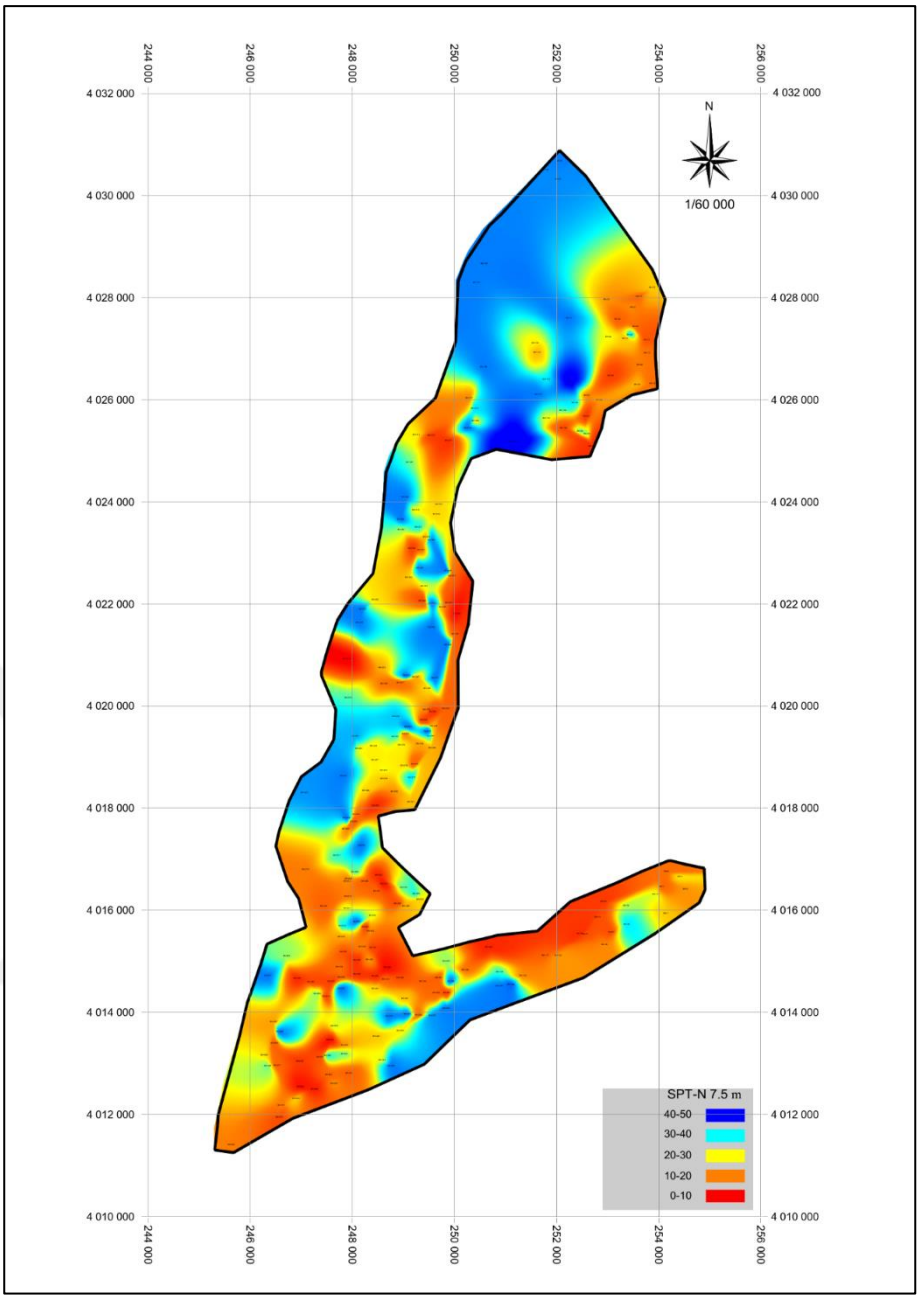

Figure 4.4. Distribution of SPT-N values according to 7.5 m depth.

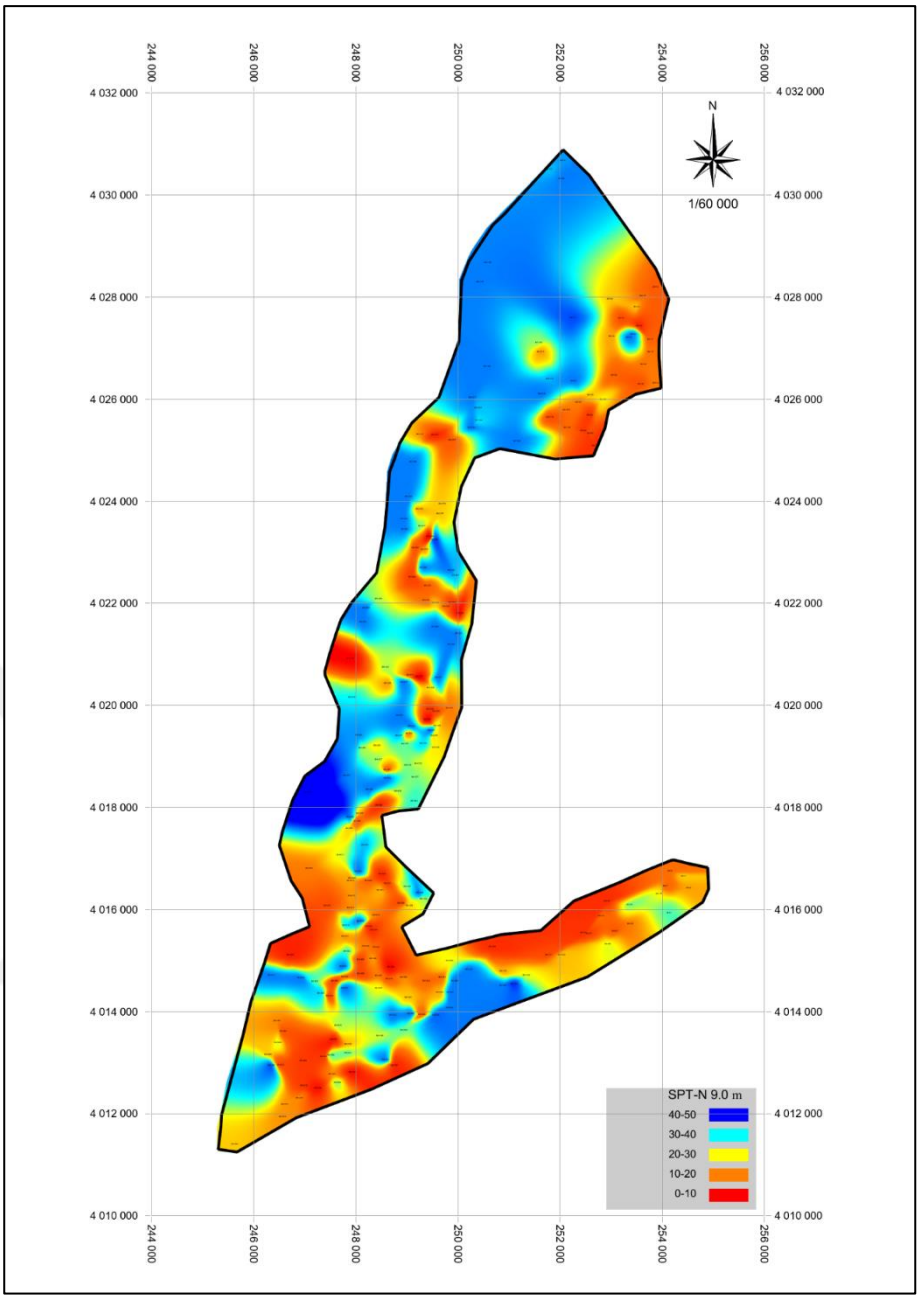

Figure 4.5. Distribution of SPT-N values according to 9.0 m depth.

4.3. Analysis of Bearing Capacity Maps

The Meyerhof method was utilized for the calculation procedures. This method is widely employed for estimating bearing capacity by utilizing SPT-N values and soil parameters. The calculations were conducted based on a foundation width of 2 meters, using data from boreholes that ranged in depth from the surface down to 10 meters. Bearing capacity maps were generated at various depths, including 1.5 meters, 3 meters, 6.0 meters, 7.5 meters, and 9 meters. These maps were created using the IDW (Inverse Distance Weighting) method on a 10-meter square grid, with the assistance of GIS software.

The calculations were performed using data collected from 221 boreholes, specifically related to SPT-N values. Figures 4.6 to 4.10 showcase the bearing capacity maps calculated using the Meyerhof method for different depths. Similar to the SPT-N maps, the bearing capacity maps also displayed a consistent trend, with bearing capacity increasing as the depth increased. Upon analyzing the maps depicting the spatial distribution of bearing capacity based on Meyerhof's criteria, it is evident that bearing capacity tends to rise as depth increases. The map at a depth of 1.5 meters indicates a range of bearing capacity between 0.3 kg/cm^2 and 6.3 kg/cm^2. As the depth increases to 9 meters, the bearing capacity also increases, ranging from 0.6 kg/cm^2 to 7.5 kg/cm^2.

The discussion on the spatial distribution of bearing capacity based on Meyerhof's criteria further contributes to the understanding of the geotechnical characteristics of the study area. The observed increase in bearing capacity as depth increases is a crucial finding for foundation design and construction planning. The detailed maps illustrating the bearing capacity variations provide engineers and planners with valuable information for making informed decisions regarding site suitability and structural design.

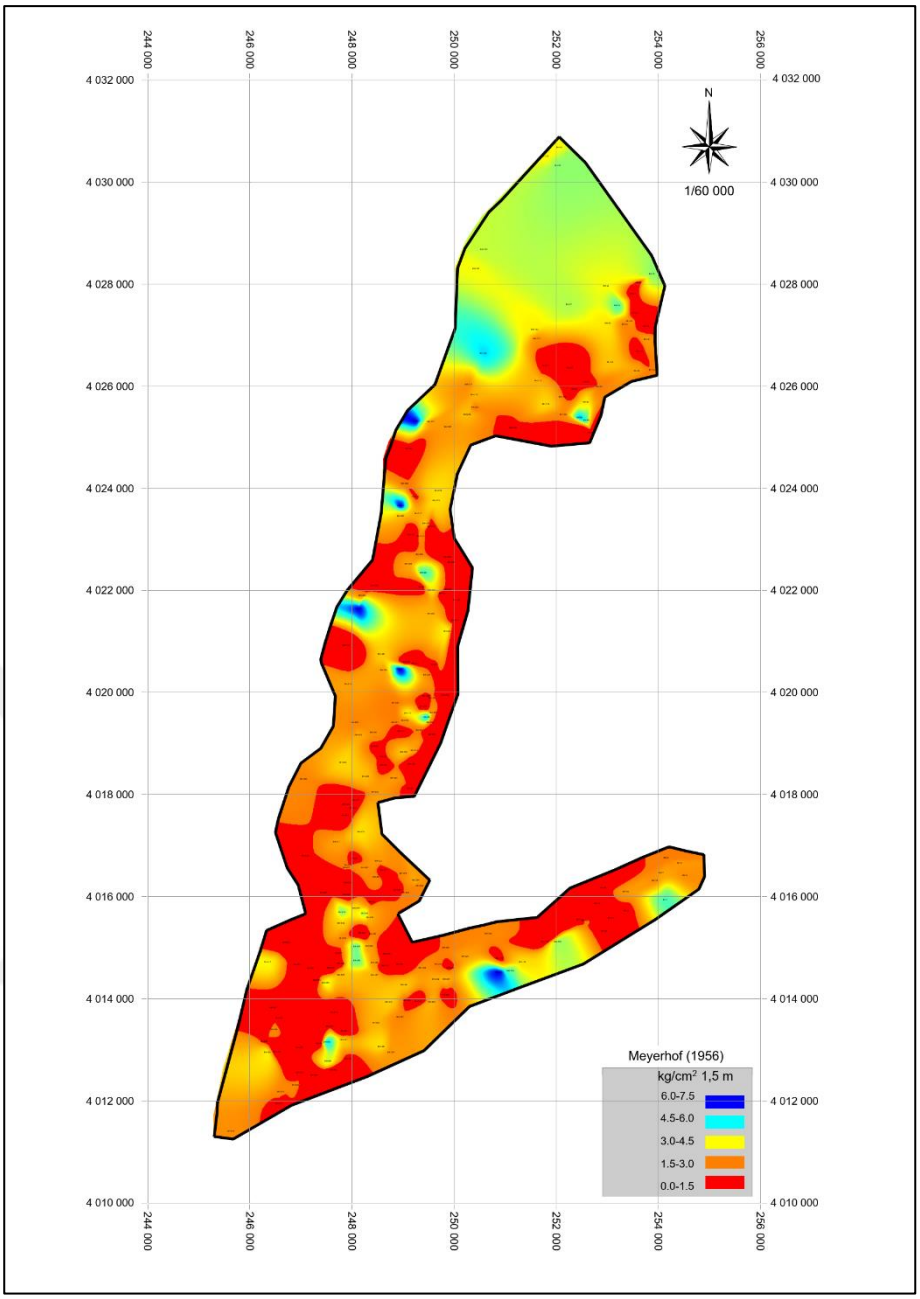

Figure 4.6. Bearing capacity map according to Meyerhof for 1.5 m depth.

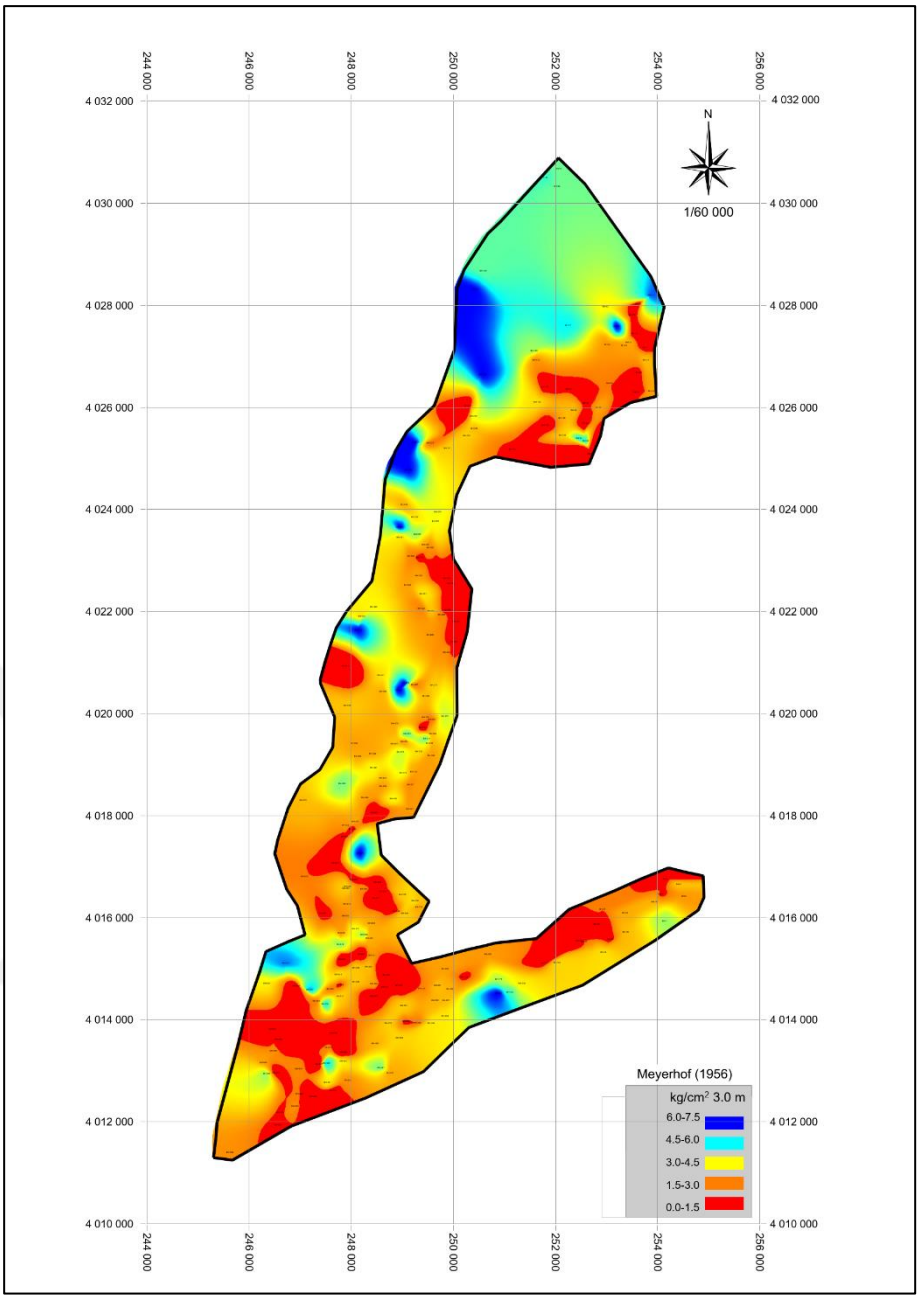

Figure 4.7. Bearing capacity map according to Meyerhof for 3.0 m depth.

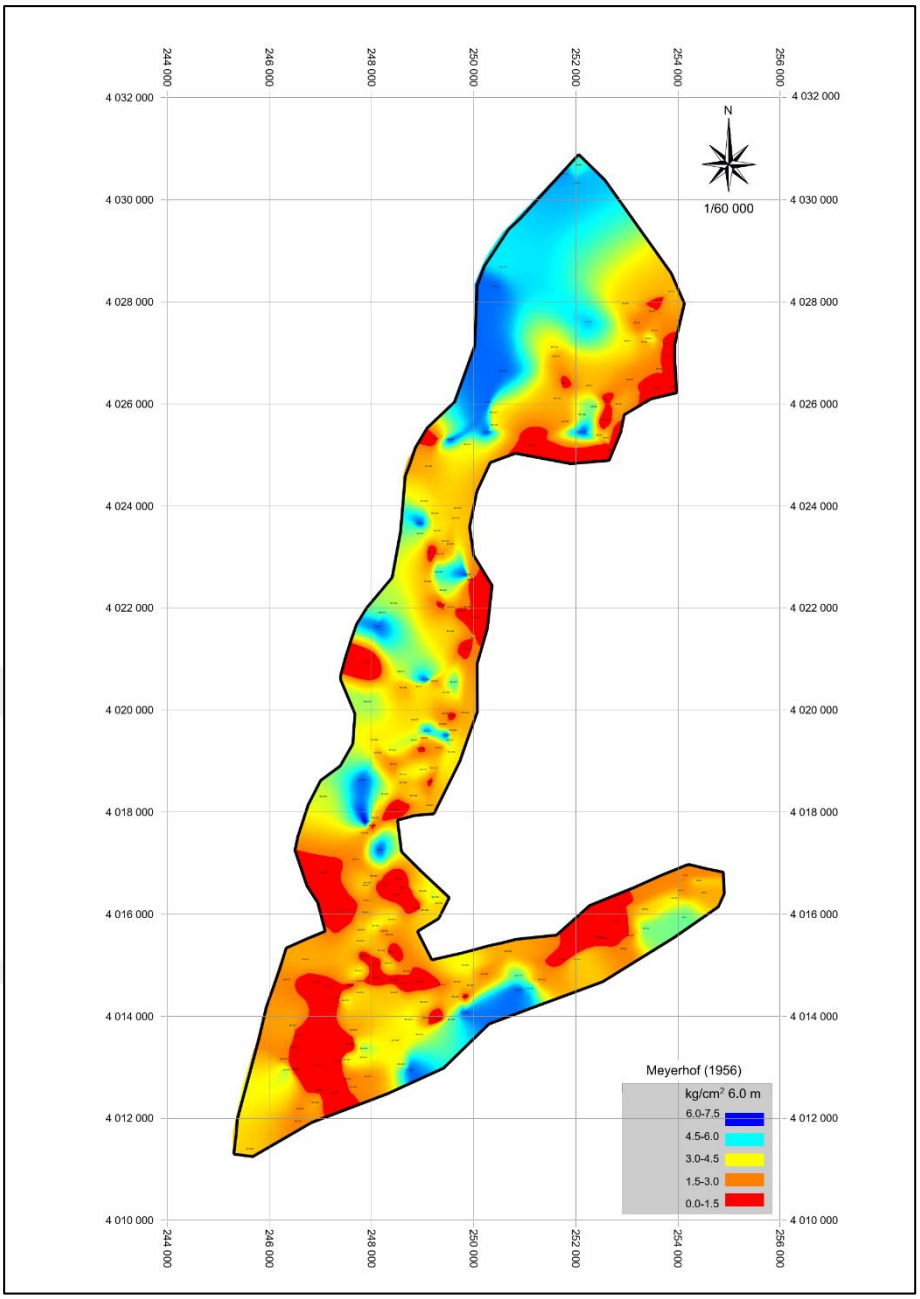

Figure 4.2. Bearing capacity map according to Meyerhof for 6.0 m depth.

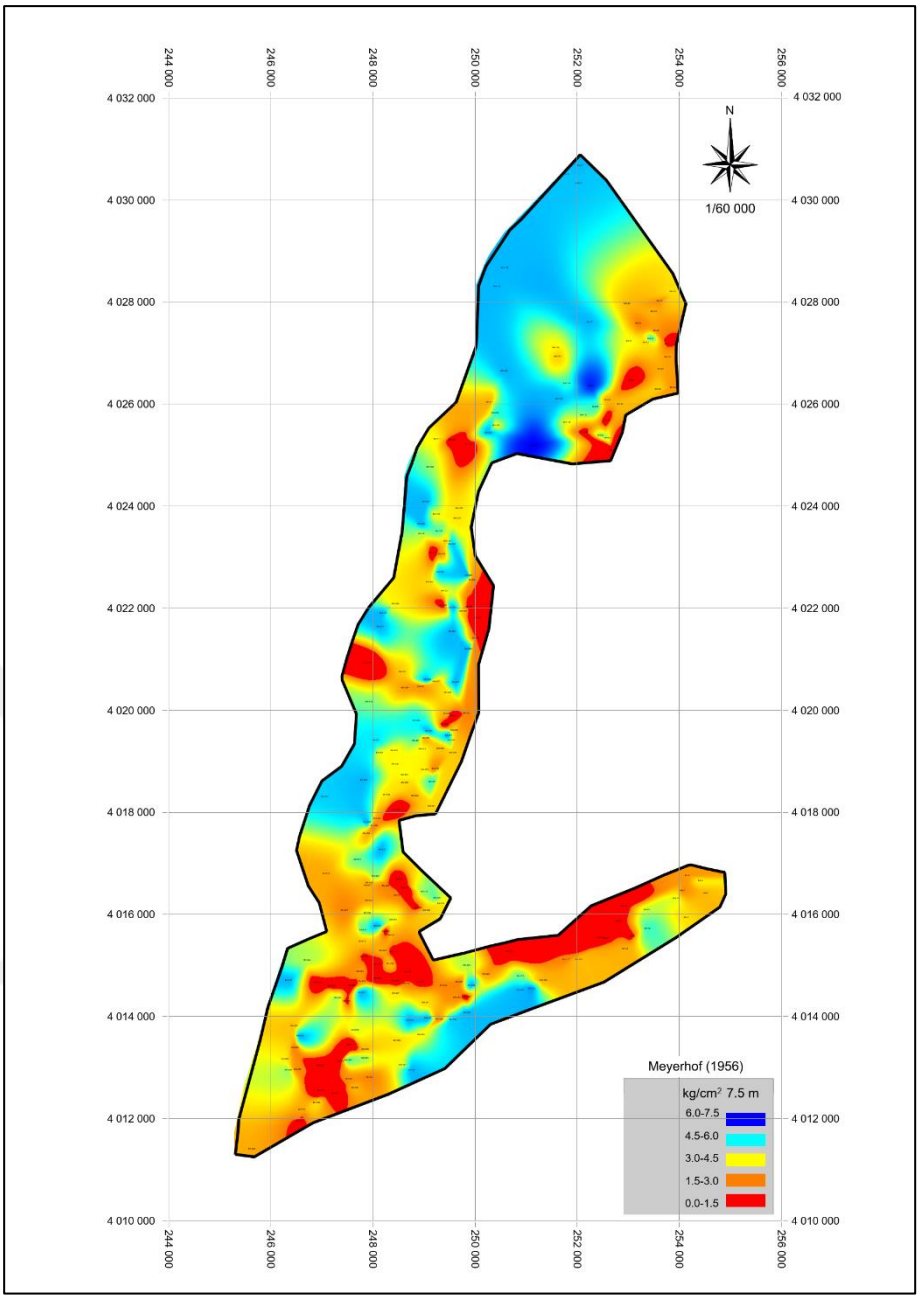

Figure 4.9. Bearing capacity map according to Meyerhof for 7.5 m depth.

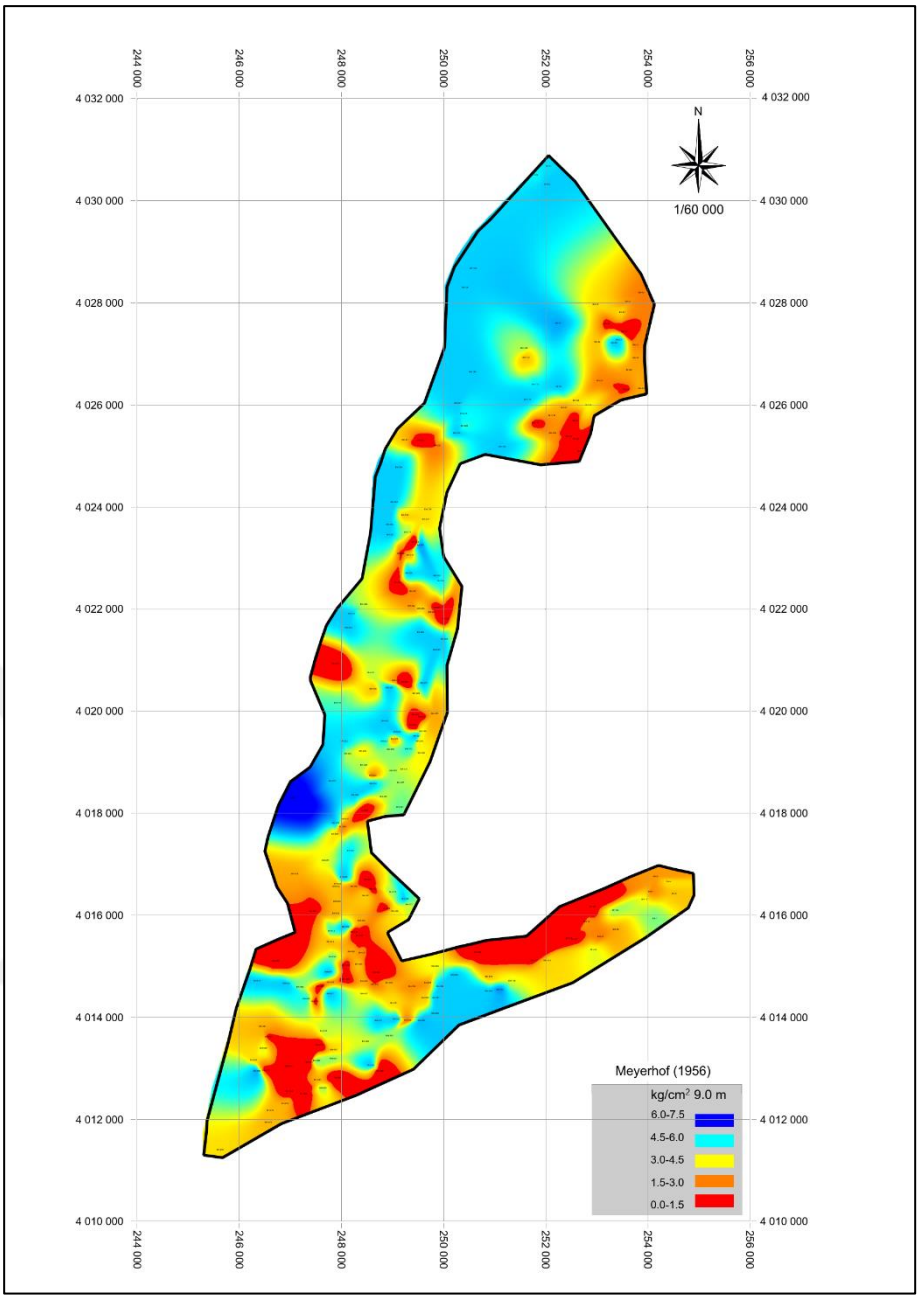

Figure 4.3. Bearing capacity map according to Meyerhof for 9.0 m depth.

4.4. Analysis of Groundwater Level and Water Content Maps

Groundwater is a critical aspect since it causes a range of issues such as clay swelling and liquefaction, corrosion of structural components because of the groundwater levels, and the collapse of water-soluble or soluble rocks due to the formation of melting voids under the influence of water. Hence, it is crucial to determine the groundwater level to mitigate the problems arising from it. Therefore Figure 4.11 depicts the groundwater depth map generated for the study area.

After analyzing the values extracted from 221 boreholes within the study area, it is found that the water level commences at 2 meters when the depth is 15 meters from the surface. It ranges between 2 meters to 8 meters since some areas, such as Güzelburç, Huzurlu neighborhood, and Narlıca in the south, are close to the Asi River. In addition, upon examining the whole study area, regions parallel to the Asi River exhibit high groundwater tables. The proximity of groundwater levels to the surface increases the liquefaction hazard if they are within 10 meters. However, if the groundwater levels lie deeper than 20 meters, and the soil has a dense, non-loose structure, the potential for liquefaction is minimum, resulting in decreased liquefaction hazards (Youd, 1984). This is valuable information in assessing the prospective risks in regions close to the Asi River, and it can guide the implementation of necessary precautions.

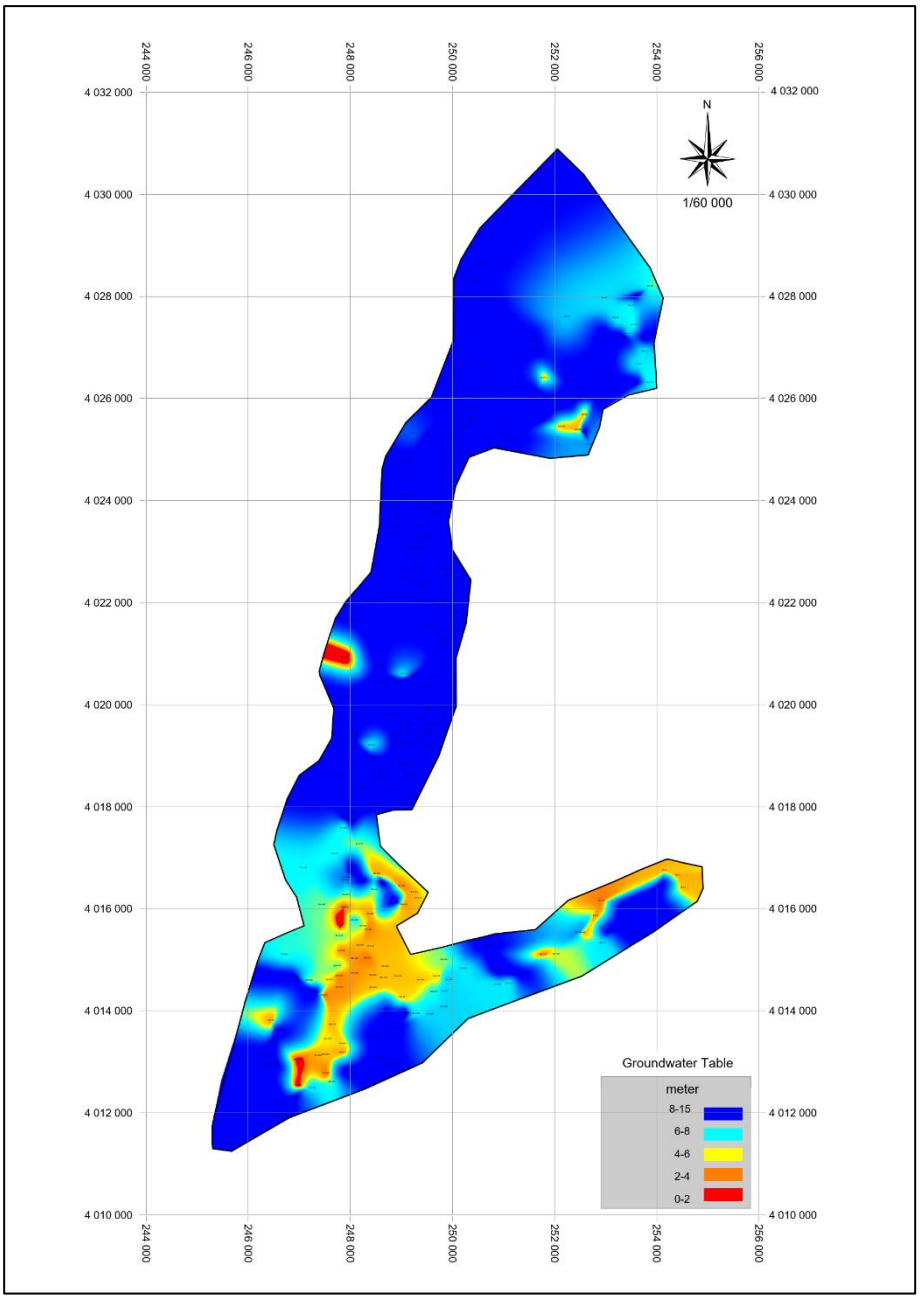

Figure 4.11. Map showing the groundwater level of the study area.

Soil water content refers to the amount of water present in the pore spaces between soil particles relative to the dry mass of the soil. This is typically determined by calculating the ratio of the weight of water remaining in the soil (after subtracting the dry weight) to the total weight of the soil. In simpler terms, it is the weight of the water in the soil pores divided by the dry weight of the soil.

Analyzing the data collected from 221 borehole logs across the study area, the distribution of water content values was observed. Across half of the boreholes didn't

show any water or the water was deeper than 15 meter. On average, the water content value for the entire study area ranges from 20% to 30%.

To visually depict this distribution, Figure 4.12 presents a map displaying the water content values within the study area.

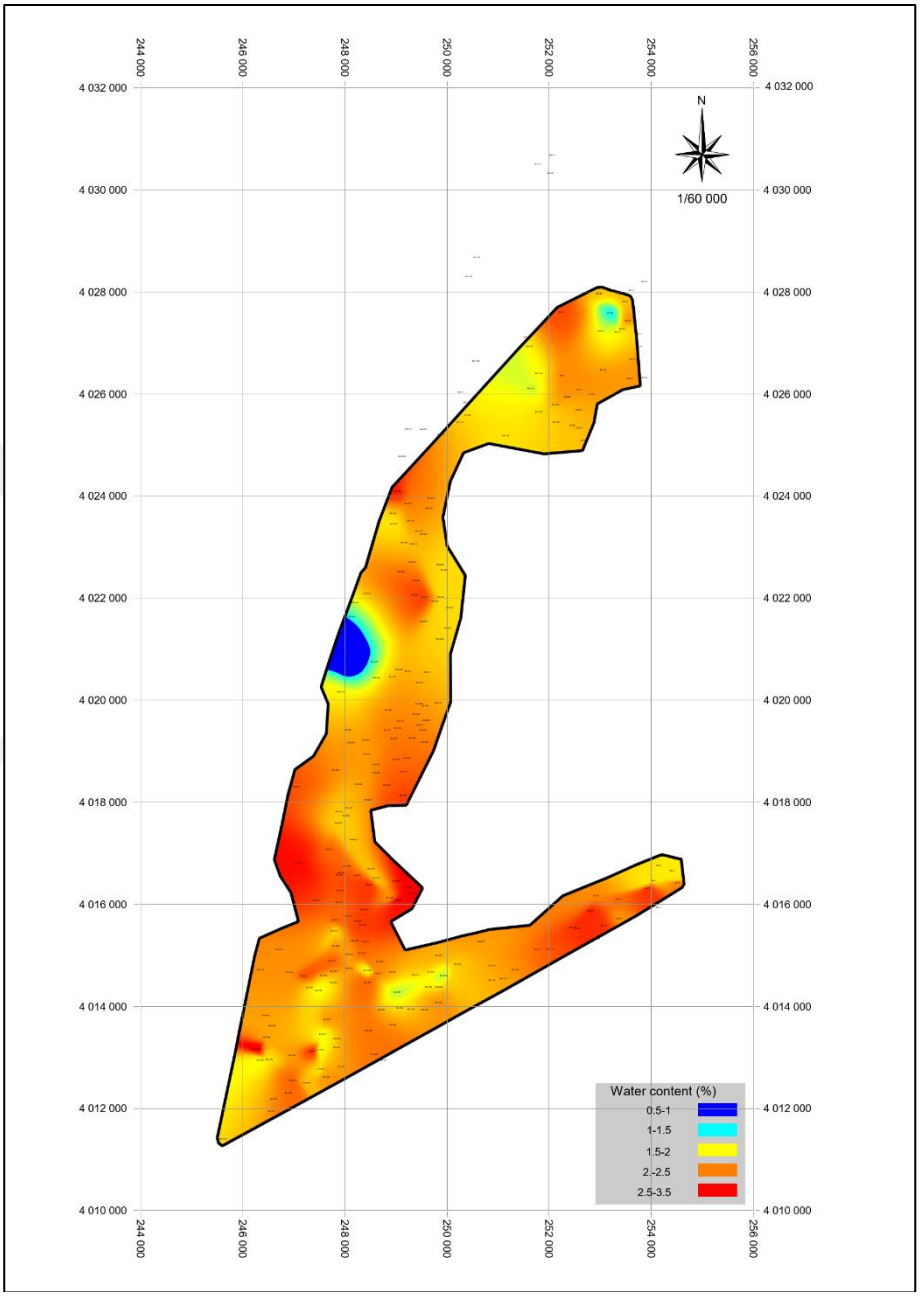

Figure 4.4. Map of laboratory water content values

4.5. Grain-Size Distribution

To determine the distribution of grain sizes in soil, a set of sieves with hole sizes of varying diameter is utilized. The soil is subjected to this process, and the weight

percentage of soil grains passing through each sieve is measured. This information helps in analyzing the grain-size distribution of soil.

For this particular research study, data from 221 boreholes were gathered to generate sieve analysis maps. These maps were utilized to investigate various engineering properties of the soil.

Figure 4.13 illustrates the gravel, sand, silt, and clay sizes as defined by international and national standards based on the grain-size distribution present in the studied soil. Based on the data obtained from the 221 boreholes located across the study area, the amount of soil remaining on the #4 (4.75 mm) sieve is depicted in Figure 4.14, and the amount of soil passing through the #200 (0.075 mm) sieve is represented in Figure 4.15.

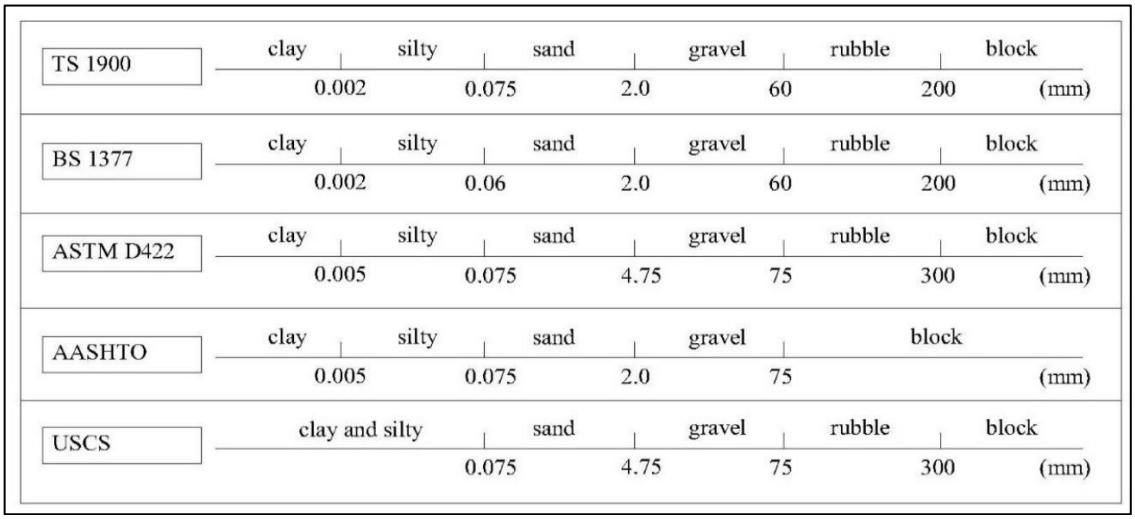

Figure 4.13. Sieve openings of gravel, sand, silt and clay described in some international and national standards (Orhan, 2022b).

Based on the standards defined by TS 1900, ASTM D422, and AASHTO (as shown in Figure 4.13), the soil that accumulates above the #4 sieve can be categorized as "gravel and coarser grained soil." Soil that falls between the #4 and #200 sieves is considered "sand," while soil that passes through the #200 (0.075mm) sieve is labeled as "clay and silt." The distribution of soil classification resulting from the sieve analysis conducted in the study area is presented in Figure 4.14 and Figure 4.15.

Figure 4.15, based on TS 1900, ASTM D422, and AASHTO standards, indicates that approximately 90% of the soil passes through the #200 (0.075mm) sieve. Therefore, it can be inferred that this soil is predominantly composed of "clay and silt." Additionally, Figure 4.14 shows that only around 10 to 20% of the soil remains on the #4 (4.75 mm) sieve, further supporting the classification of the soil in these areas as "clay and silt."

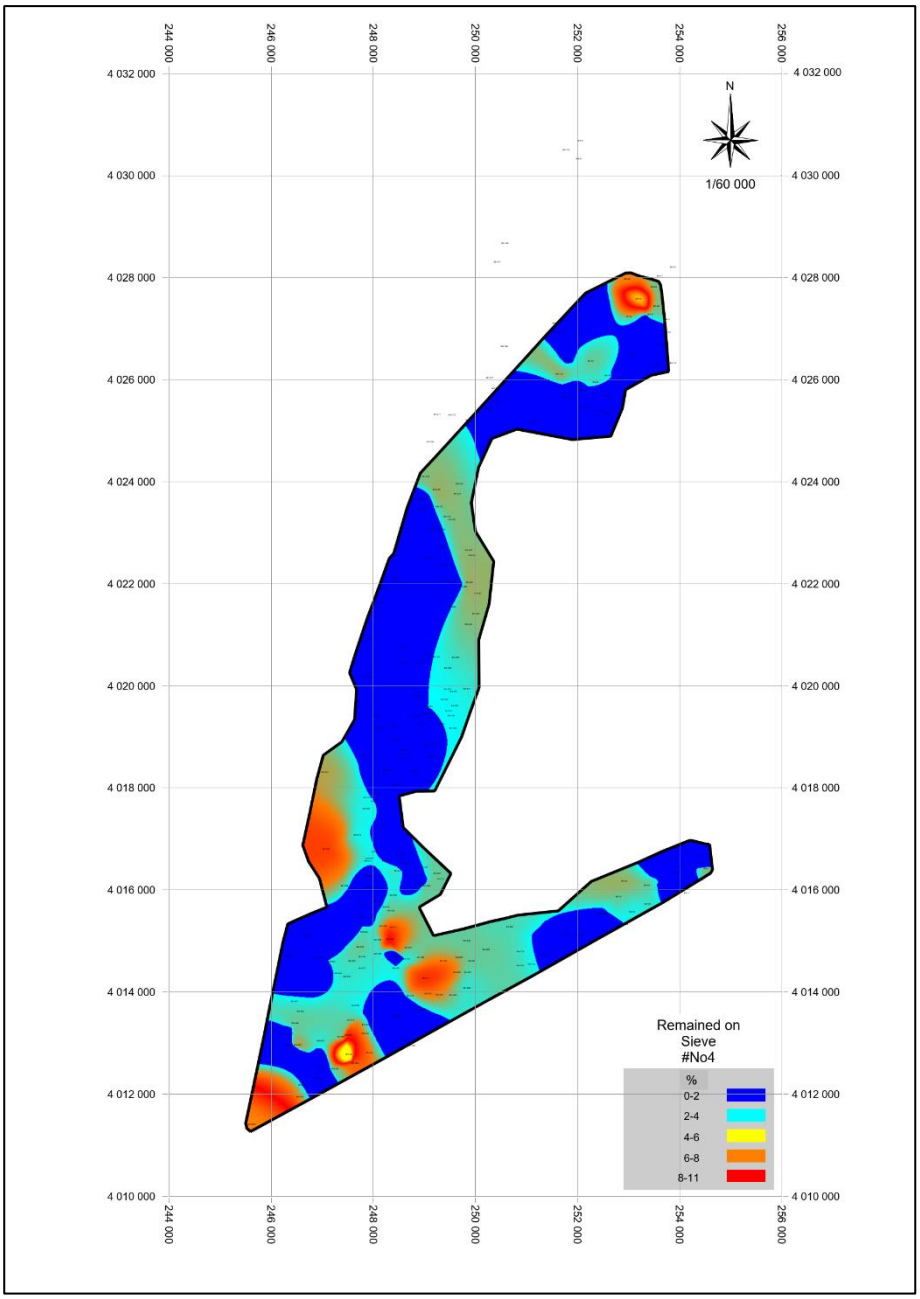

Figure 4.14. Map of remained material on sieve #4 (4.75 mm).

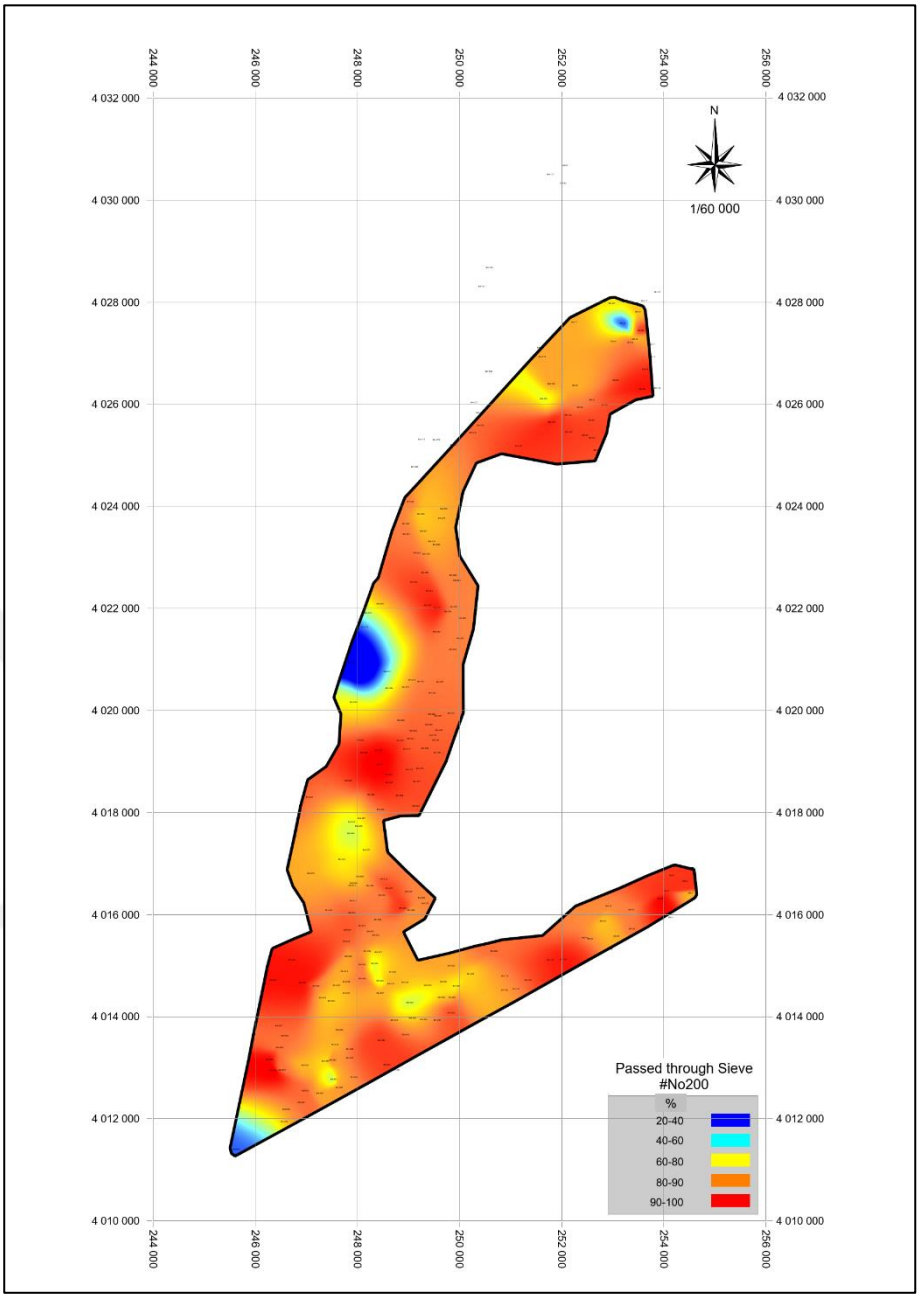

Figure 4.15. Map showing the amount passing the #200 sieve (0.075 mm).

4.6. Analysis of Consistency Limits

The soil consistency limits, including Liquid Limit (LL), Plastic Limit (PL), and Plasticity Index (PI), were determined using data obtained from the 221 boreholes within the study area. The study focused on analyzing the consistency limits of the soil.

Within the fine-grained soils (>50% passing through a 200 mesh sieve) in the study area, there was notable variation in the consistency indices. The Liquid Limit (LL) values ranged from 70 to 85, with an average value of 72%. Similarly, the Plasticity Index

(PI) values ranged from 10 to 35, with an average value of 25%. Based on these values, the average position on the plasticity map was found to be above the A line and to the right of the LL=50 limit line. This suggests that the soil in the study area exhibits high plasticity clay-silt characteristics. None of the soil samples were found to be organic. The distribution map of the LL values across all depths in the study area can be observed in Figure 4.16, the PL distribution map is represented in Figure 4.17, and the PI map is displayed in Figure 4.18.

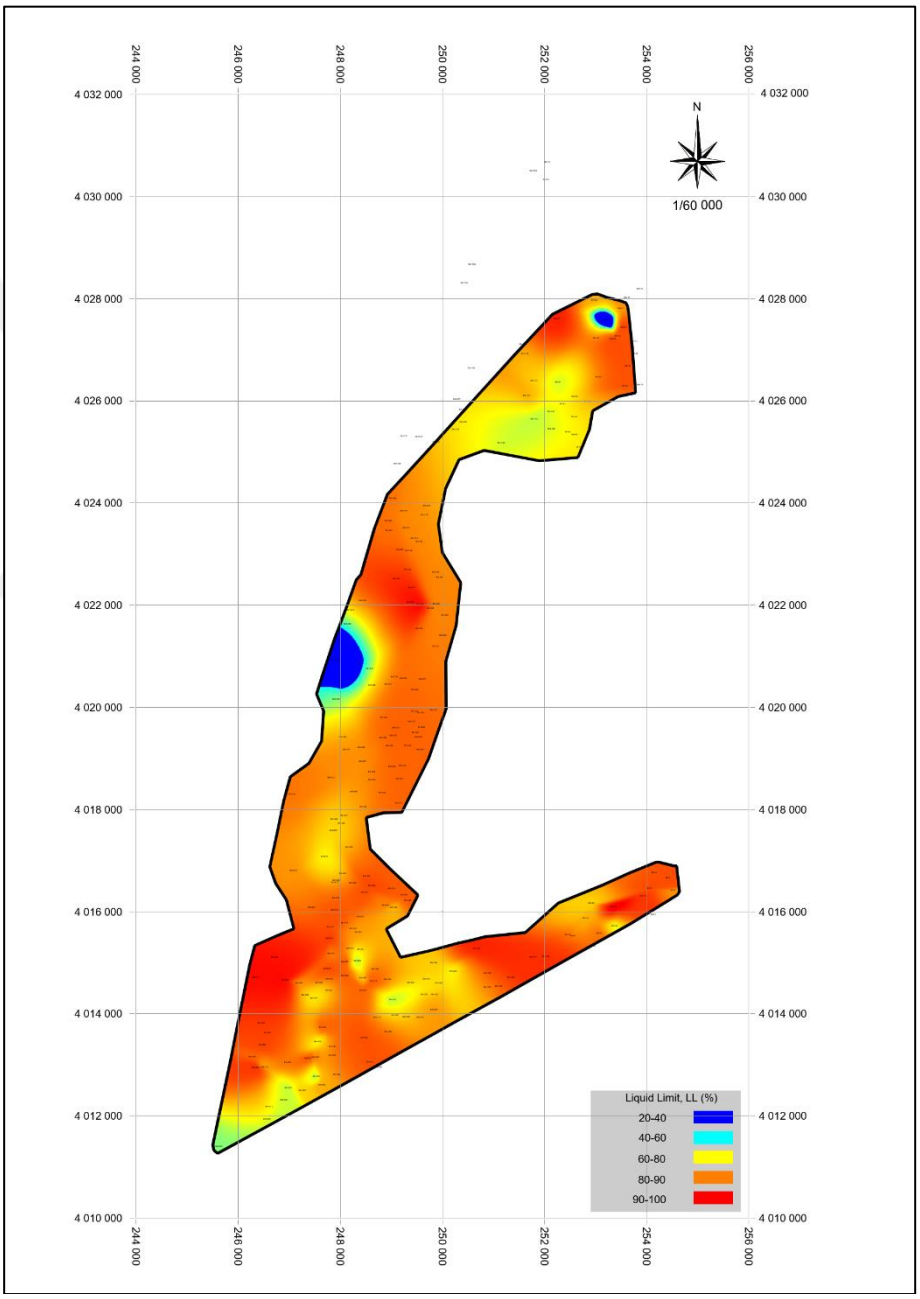

Figure 4.16. Map of liquid limit values.

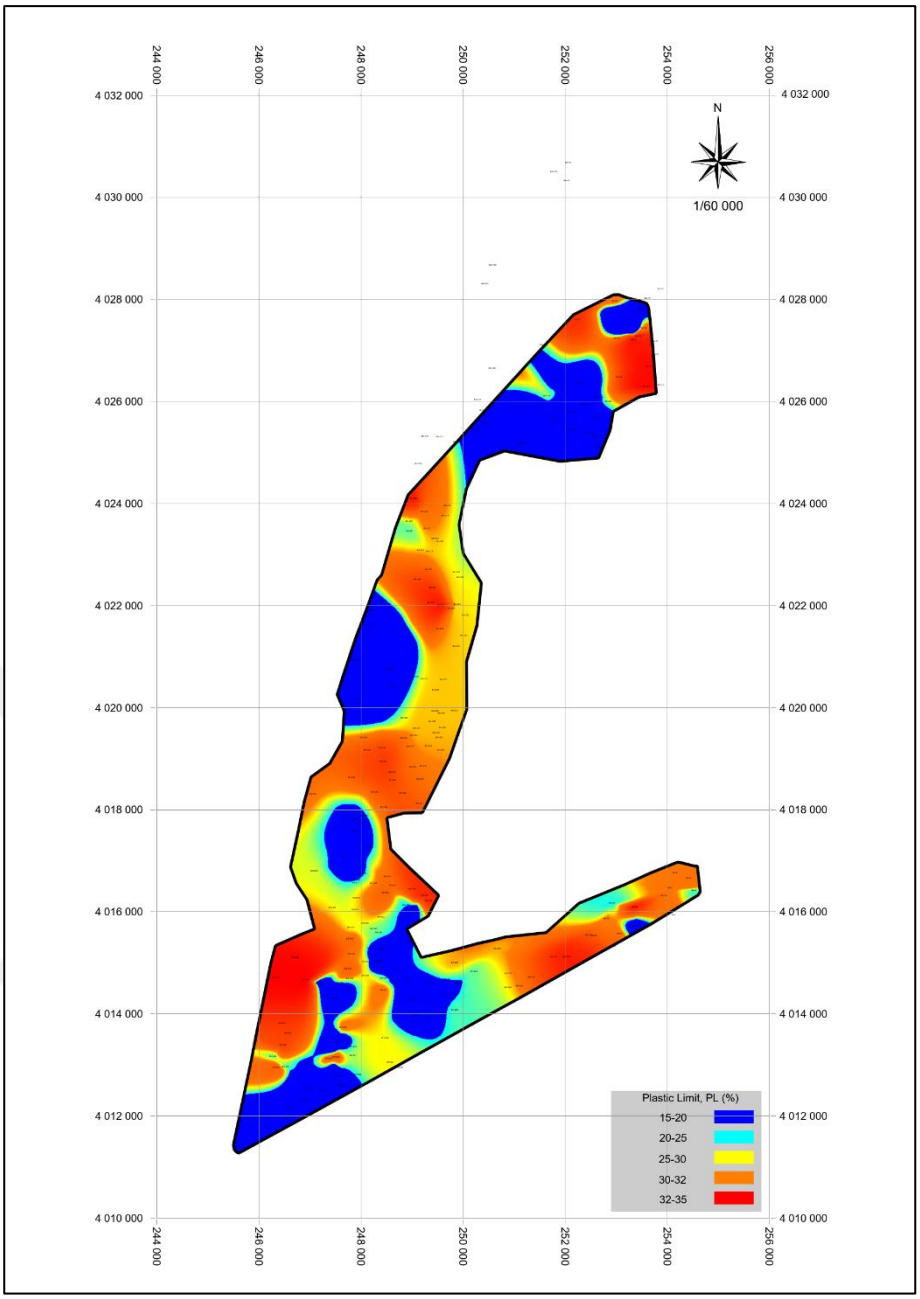

Figure 4.17. Map of plastic limit values.

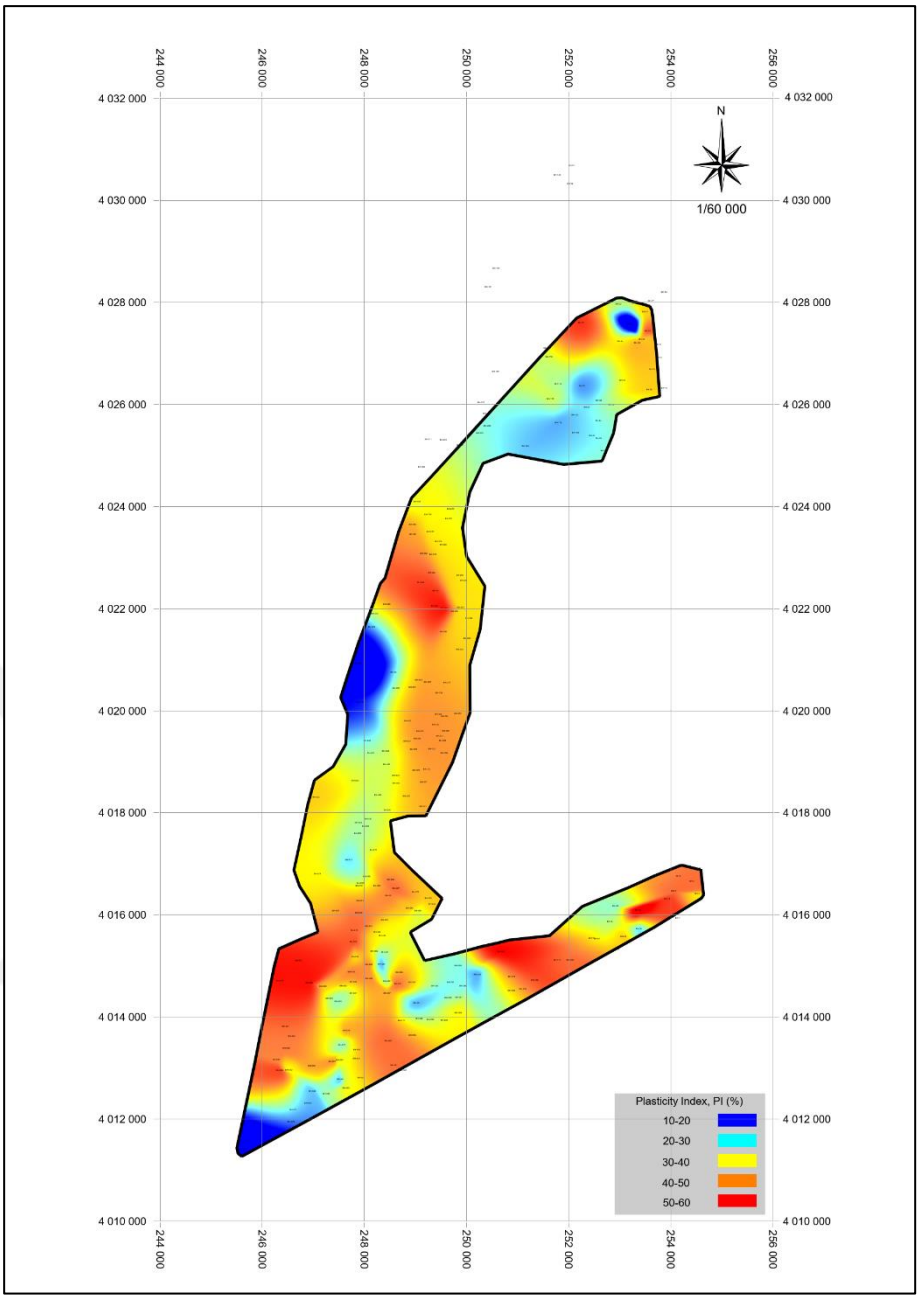

Figure 4.18. Map of plasticity index values.

4.7. Analysis of Shear Wave Velocity Maps

As part of the research, field measurements of seismic activity were conducted using the Seismic Refraction (SR) method. Seismic refraction studies provide insights into the internal structure of the ground by analyzing the velocity and reflections of sound waves. By analyzing the seismic test results, data on shear wave velocity (VS30) were obtained. These velocity measurements contain valuable physical information about the voids, density, and stress state of the soil. To analyze the data spatially, a map was created using the Geographic Information System (GIS) analysis. The ArcGIS program was

employed to generate this map, utilizing the Inverse Distance Weighting (IDW) method to estimate shear wave velocity values at 10-meter square intervals. The resulting map is displayed in Figure 4.19.

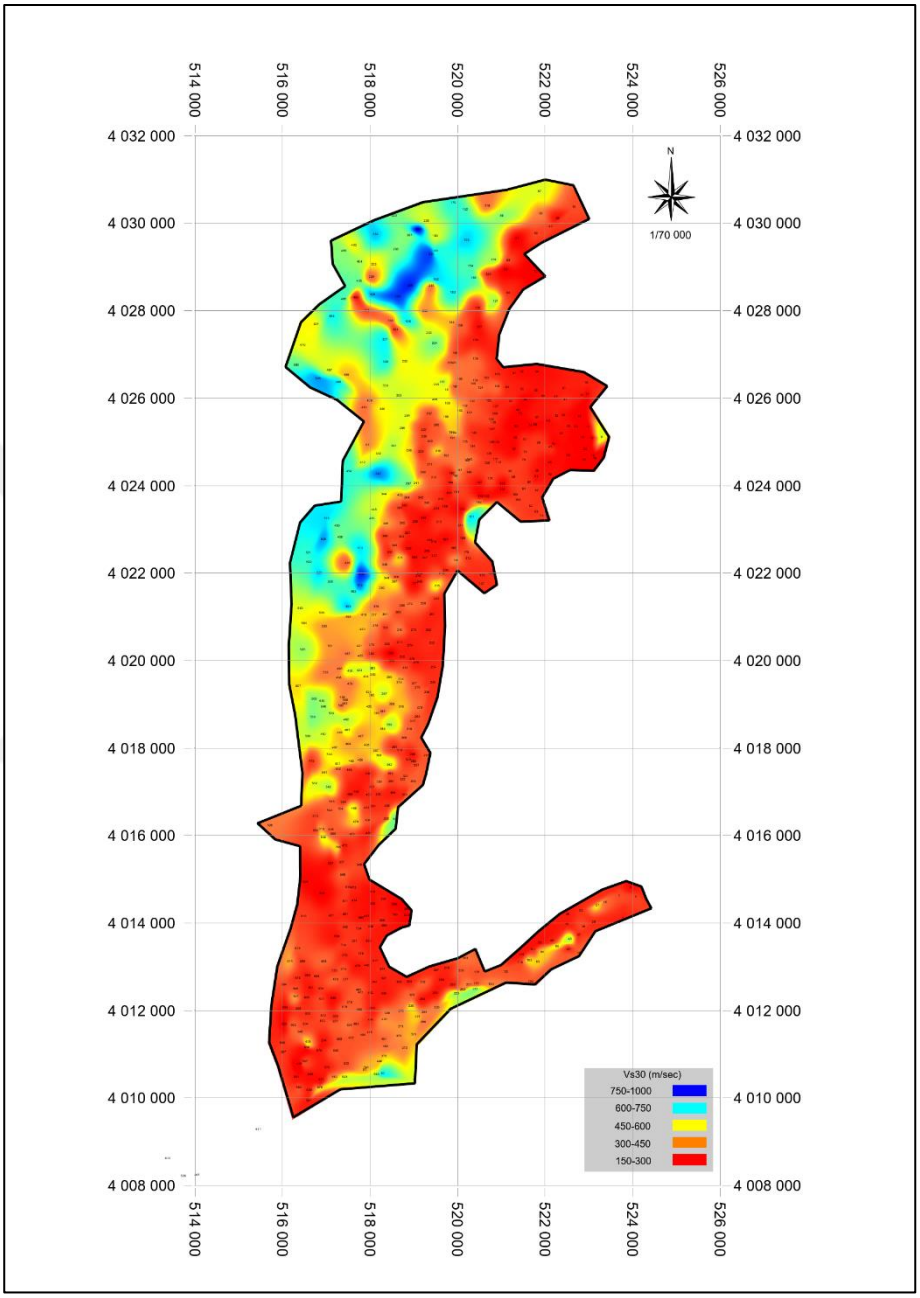

Figure 4.19. Map of shear wave velocity according to 30 m depth.

The shear wave velocity maps demonstrate a similar pattern to the SPT (Standard Penetration Test) maps, although there are variations in certain areas due to uneven distribution of boreholes and seismic data. These inconsistencies can be attributed to multiple factors, such as variations in soil engineering properties at different depths and

localized differences in soil composition. Analysis of the SPT maps revealed a linear correlation between SPT and VS30 in areas classified as "dense, very dense, or bedrock." This correlation is particularly noticeable in the northern and northeastern regions of the study area, which include the Atatürk, Akıncılar, Alahan, University, Akhisar, Anayazı, and Üçgedik neighborhoods, where SPT-N values are high.

Through seismic refraction studies conducted within the study area, researchers were able to determine the distribution of shear wave velocities at different depths. The lowest shear wave velocities were observed in the central and southern parts of the study area, ranging between 130 and 300 m/s. In contrast, the northern and northeastern parts, as well as a limited area in the center encompassing the Alahan and Karali Dikmece neighborhoods, exhibited shear wave velocity values ranging from 400 to 700 m/sec. Overall, based on the shear wave velocity distribution map, the study area demonstrates shear wave velocities ranging from 130 to 850 m/sec.

4.8. Soil Classification Analysis based on the NEHRP Earthquake Regulations

Various classification criteria have been established using shear wave velocity values obtained from geophysical measurements in order to determine soil class during field investigations. One such criterion is the NEHRP soil classification system.

The NEHRP soil classification system divides soils into six groups, designated as A, B, C, D, E, and F, based on their shear wave velocity (V_{S30}) values. The hardest soils fall under Type A, which includes those with a (V_{S30}) value equal to or greater than 1500 m/s. Type E represents the softest soils, with a (V_{S30}) value equal to or less than 180 m/s. Additionally, soils with a depth exceeding 36 meters and a (V_{S30})) value less than 180 m/s are classified as Class F soils.

To conduct GIS analysis, a map displaying the NEHRP soil classification values was produced using the shear wave velocity (V_{S30}) data acquired from field measurements. The maps were generated using the ArcGIS software, employing the Inverse Distance Weighting (IDW) method on a 10-meter square grid. These maps can be found in Figure 4.20.

As per the NEHRP classification, the prevailing soil classes in a significant portion of the study area are C and D, indicating dense soil and soft rock. However, in the northern regions of the study area, specifically in the neighborhoods of Serinyol and Ovakent, soil class B is observed. This soil class signifies firm and resistant-to-hard-rock

soil. To sum up, the study area's soil is categorized as predominantly class D and C according to the NEHRP seismic regulations, with certain areas classified as class B soil.

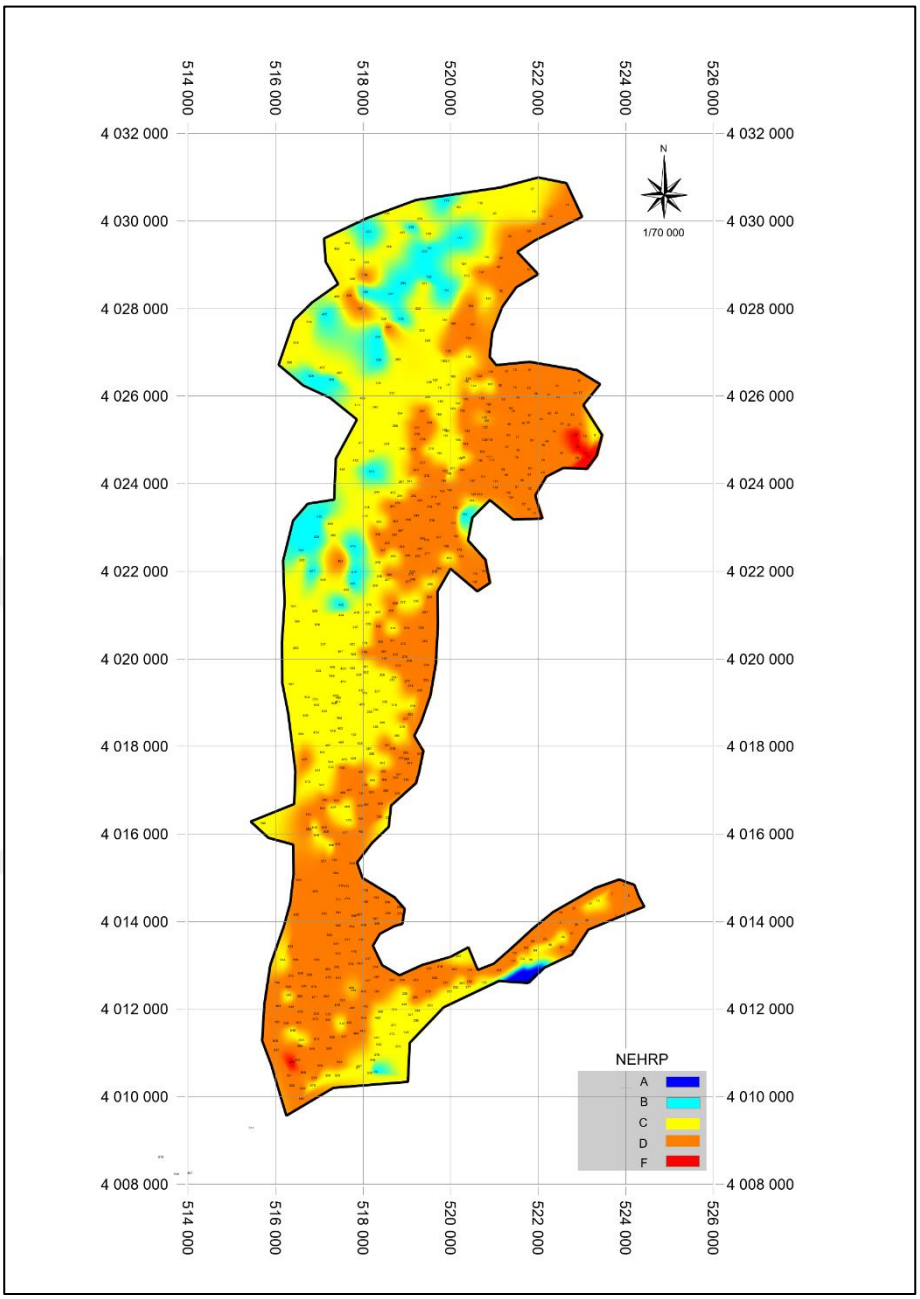

Figure 4.20. Map of soil classification according to NEHRP.

4.9. Soil Classification Analysis based on EUROCODE-8

The European design codes, known as the EUROCODE series, include EUROCODE-8, which specifically outlines the seismic design requirements for buildings. EUROCODE-8 was approved by the European Committee for Standardisation (CEN) in 2004 and provides guidelines for designing earthquake-resistant buildings.

Within EUROCODE-8, soil types relevant to seismic design are categorized into five basic categories (A, B, C, D) and two special categories (S1, S2). These soil classifications, which are based on soil strength and behavior, are presented in Table 3.5 from the previous chapter. As the soil class progresses from A to D, the strength and bearing capacity of the soil decrease. Class A represents hard and firm soils with the highest strength, whereas Class D refers to loose and weak soils with the lowest strength.

These soil classes are crucial for considering soil effects during the design process and ensuring the seismic resistance of structures. Design parameters and methods differ for each soil class.

To assist in seismic design and the selection of appropriate design methods based on soil classes, EUROCODE-8 provides guidelines for determining soil classes. This helps design structures in accordance with local soil conditions and seismic hazards, ultimately enhancing safety.

A map of EUROCODE-8 soil classification values was created for GIS analysis using shear wave velocity (VS30) data obtained from field measurements. The map, generated using the IDW method on a 10m square grid with ArcGIS software, is shown in Figure 4.21.

According to EUROCODE-8, the predominant soil types in most of the study area are C and B, with a smaller portion consisting of soil type A. This observation is also evident in the northeastern parts of the study area, specifically the neighborhoods of Atatürk, Akıncılar, Alahan, Üniversity, Akhisar, Anayazı, and Üçgedik. In summary, the study area is primarily classified as soil types C and B according to EUROCODE-8, with some areas falling under soil class A.

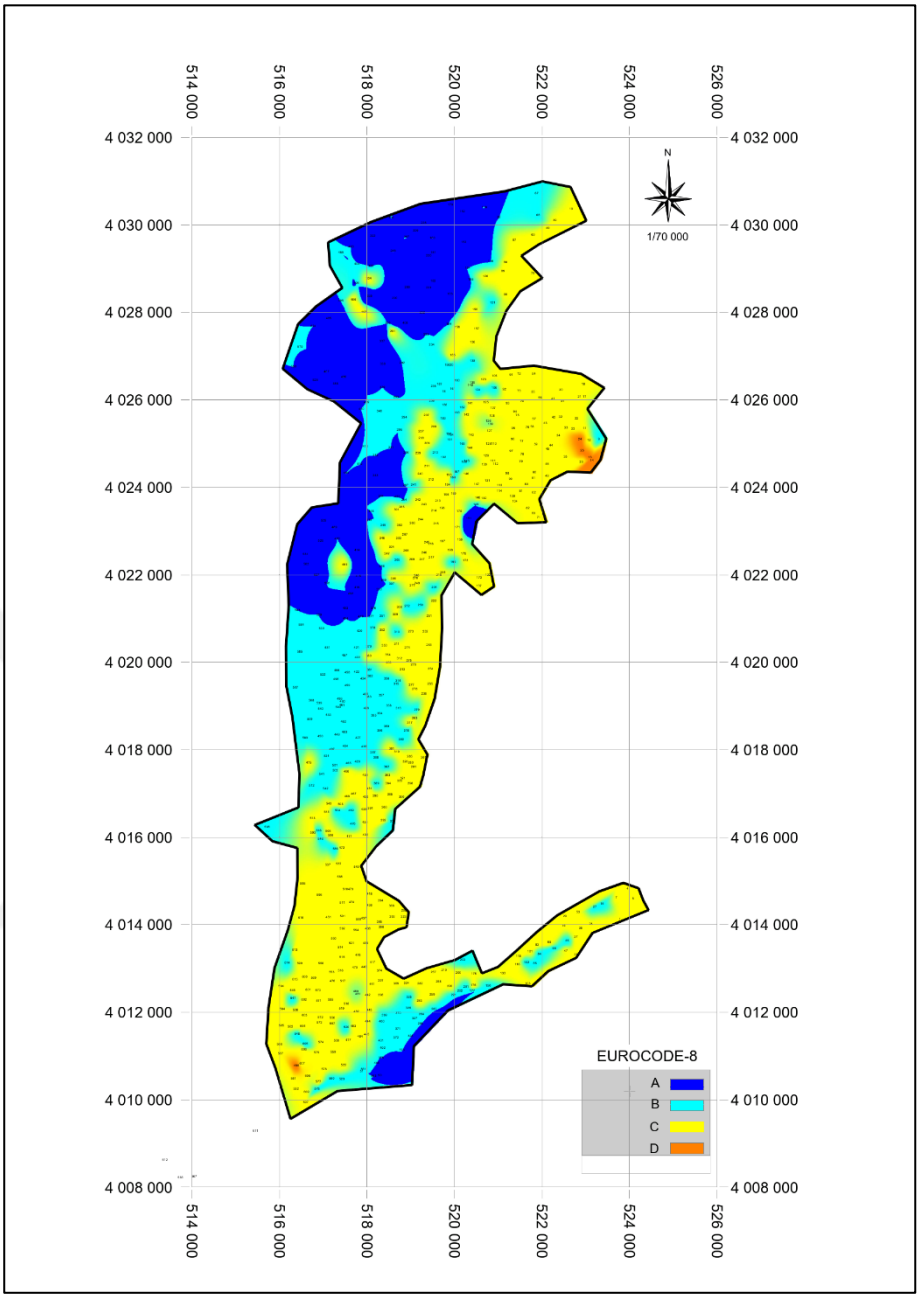

Figure 4.21. Map of soil classification according to EUROCODE-8.

4.10. Soil Classification Analysis based on TBDY 2018

Based on the shear wave velocity (V_{S30}) data determined by field measurements, a map of the TBDY 2018 soil classification values was generated for GIS analysis. These maps were produced by the IDW method on a 10 m square grid using ArcGIS software and are represented on the map shown in Figure 4.. The soil classification carried out using TBDY criteria is consistent with the one performed using NEHRP, which is the US earthquake code. Hence, there is no need to provide a separate assessment. This suggests

that the soil classification between the two codes is comparable, and the same classification standards can be employed. Consequently, the soil classification maps constructed utilizing NEHRP are in accordance with TBDY, and it is unnecessary to conduct an independent assessment. In conclusion, the TBDY seismic regulations classify the soil in the study area primarily as class Z_D and Z_C, with specific regions designated as class Z_B soil.

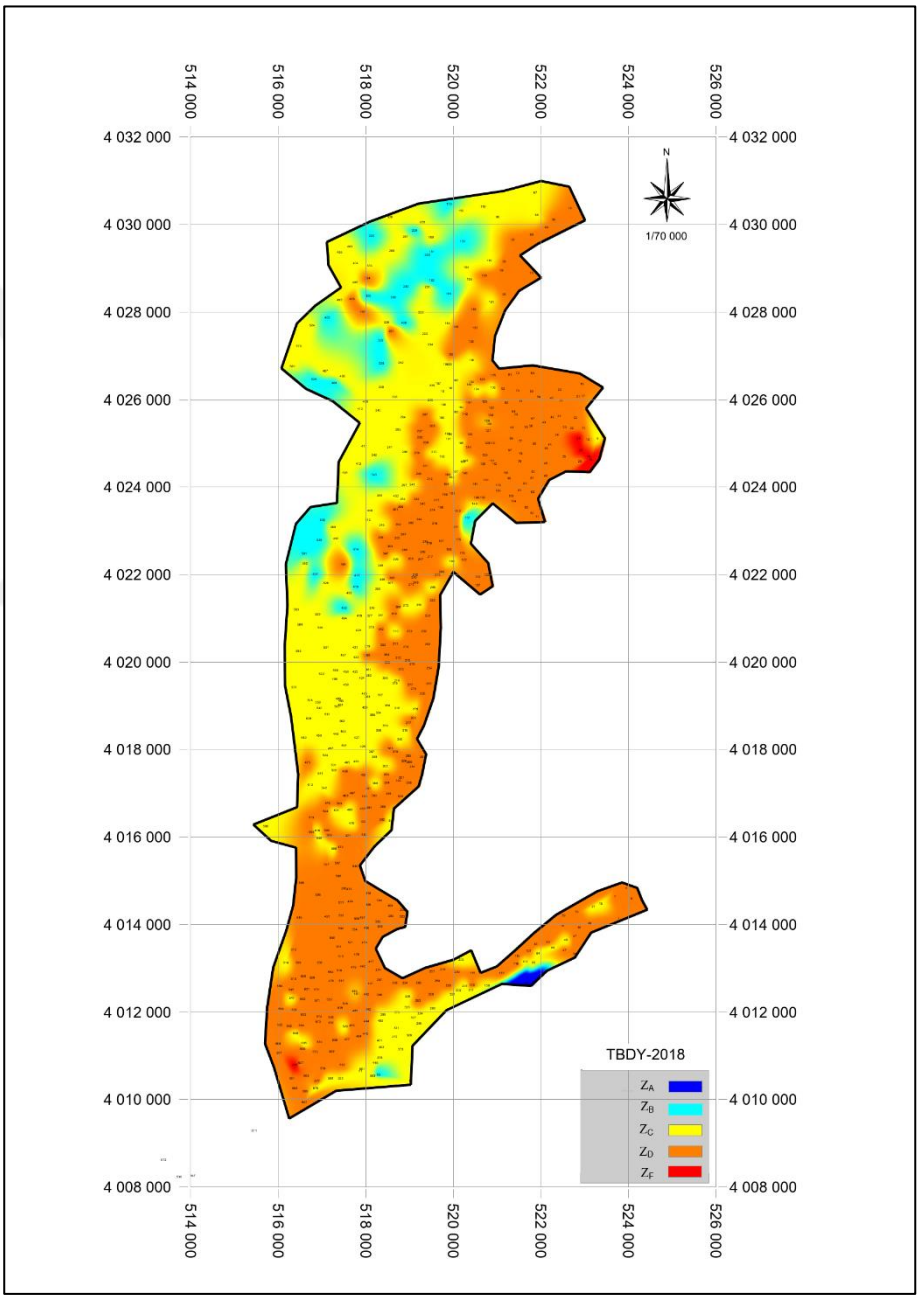

Figure 4.22. Map of soil classification according to TBDY 2018

5. CONCLUSIONS AND RECOMMENDATIONS

In this study, a database was created using the data obtained from the soil investigation reports, field and laboratory test results from the archives of the Provincial Directorate of Environment and Urbanisation of Antakya were utilized. In an area of approximately 110 km² within the of Antakya Province, geological, geophysical, and geotechnical data from 221 borehole logs were analyzed using the GIS Inverse Distance Weighting (IDW) method. Engineering properties of the soils were examined at various depths (1.5, 3.0, 6.0, 7.5, and 9.0) within the study area. The analyses conducted included the standard penetration test, bearing capacity, groundwater level, consistency limits (LL, PL and PI), shear wave velocity, and soil classification based on NEHRP, EUROCODE-8, and TDBY2018 earthquake regulations.

The primary objective of the analyses conducted was to generate maps that would make the geotechnical data for the study area more efficient and useful. The maps offer a clear and concise illustration of essential factors such as soil properties, seismic hazards, and bearing capacity. This tool is crucial in improving decision-making processes and facilitating effective planning and design studies. Below are the summarized outcomes of the study:

a) In the study area, the SPT-N values exhibit a consistent linear increase with depth. This pattern is reflected in the maps, where an increase in depth corresponds to a greater prevalence of the blue color and a decrease in the red color.
b) Within the first 3 meters of depth, the northern region of the study area, encompassing the neighborhoods of Serinyol, Ovakent, Atatürk, University, Bahçelievler, and Kuzeytepe, demonstrates higher SPT-N values.
c) Based on the values depicted on the maps generated from the aforementioned SPT-N analyses, it becomes evident that the soil in various sections of the study area exhibits distinct properties. For instance, the northern portion generally consists of dense soil, while the southern and central regions consist of loose soil.
d) The shear wave velocity maps exhibit a similar pattern to the SPT maps, but there are some deviations in certain areas due to an uneven distribution of boreholes and seismic data. These inconsistencies can be attributed to several factors, such as variations in the engineering properties of the soil at different depths and localized discrepancies in its composition.
e) During the analysis of the SPT maps, it is observed that there is a linear correlation between SPT and VS_{30} in the areas categorized as "dense, very dense, or bedrock."

This correlation is particularly evident in the northern and northeastern regions of the study area, encompassing the neighborhoods of Atatürk, Akıncılar, Alahan, University, Akhisar, Anayazı, and Üçgedik, where the SPT-N values are high.

f) Upon analyzing the maps illustrating the spatial distribution of bearing capacity based on Meyerhof's criteria, it is observed that the bearing capacity tends to increase with depth. The 1.5-meter depth map indicates a range of bearing capacity between 0.3 kg/cm^2 and 6.3 kg/cm^2. As the depth increases to 9 meters, the bearing capacity also increases, ranging from 0.6 kg/cm^2 to 7.5 kg/cm^2.

g) In the southern region of the study area, the groundwater levels range from 2 to 4 meters, gradually increasing towards the north. This variation is believed to be influenced by the presence of the Asi River. Near the river, the groundwater level rises to about 3 meters deep. As a result, the combination of high groundwater levels and the presence of silty-sandy soil classes in the study area increases the potential for liquefaction during earthquakes. When the groundwater level is within 10 meters of the surface, the likelihood of liquefaction hazard becomes higher. However, if the water table is lower and the soil is less dense and compact, the risk of liquefaction decreases. Therefore, based on the findings of this study, it can be concluded that the proximity of the Asi River increases the vulnerability to liquefaction. This information is crucial for evaluating the seismic risks in the study area and can help in implementing necessary precautions. Moreover, upon initial examination, the study area is characterized by a relatively limited groundwater resource.

h) LL ranges from 60% to 90% with an average of 70%. PL ranges from 10% to 30% with an average of 20%. PI ranges from 10% to 50% with an average of 30%.

i) During the borehole logging process within the study area, a total of 1680 soil samples were collected from the boreholes where SPT was conducted. These samples were subjected to sieve analysis and consistency limit tests, and the Unified Soil Classification system was used to classify the soil. The classification results were used to generate soil class distribution maps, which illustrate the spatial variability of soil class values at depths ranging from 1.5 m to 3.0, 6.0, 7.5, and 9.0 m within the study area.

j) The study area has been categorized into five distinct soil classes based on the Unified Soil Classification system. These classes, labeled as CH, CL, MH, SC, and SM, show that clayey soil samples make up the majority, accounting for 91%

of the study area. Overall, the distribution of soil classes in the study area varies with depth. A significant observation is the prevalence of clayey units throughout the study area, indicating that clayey soils form a significant portion of the composition in the study area.

k) When examining how soil classes vary with depth, the presence of clay content was identified as a significant factor. The soil classes of high plasticity inorganic clay (CH) and low plasticity inorganic clay (CL) were found to be prevalent, especially on the surface and at various depths in the study area. These soil classes dominate both near the surface and at other depths, reflecting the overall soil characteristics of the study area.

l) Soil classification in the study area was performed using shear wave velocity (Vs_{30}) data collected at a depth of 30 meters below the surface. The NEHRP, EUROCODE-8, and TBDY 2018 standards were used to determine the soil classes based on this data. According to the NEHRP and TBDY 2018 standards, the dominant soil classes in a large portion of the study area are C and D, indicating dense soil and soft rock. However, in the northeastern regions of Serinyol and Ovakent neighborhoods, located in the northern part of the study area, soil class B, which represents firm and resistant-to-hard-rock soil, is observed. According to EUROCODE 8, soil types C and B are predominant in most of the study area, with a limited portion being composed of soil type A. This observation is also evident in the northeastern parts of Atatürk, Akıncılar, Alahan, Üniversity, Akhisar, Anayazı, and Üçgedik neighborhoods in the northern region of the study area. In summary, the NEHRP seismic regulations classify the study area as having soil classes D and C, while according to EUROCODE 8, soil types C and B are identified. These soil classifications are crucial for evaluating the seismic properties of the study area.

m) The soil classification carried out using TBDY criteria is consistent with the one performed using NEHRP, which is the US earthquake code. Hence, there is no need to provide a separate assessment. This suggests that the soil classification between the two codes is comparable, and the same classification standards can be employed. Consequently, the soil classification maps constructed utilizing NEHRP are in accordance with TBDY, and it is unnecessary to conduct an independent assessment.

n) By conducting seismic refraction studies in the study area, researchers were able to determine the distribution of shear wave velocities with respect to depth. It was found that the lowest shear wave velocities were observed in the central and southern parts of the study area, with values ranging between 130 and 300 m/s. Conversely, in the northern and northeastern parts, as well as a limited area in the center of the province encompassing the Alahan and Karali Dikmece neighborhoods, shear wave velocity values were in the range of 400 to 700 m/s. Overall, based on the shear wave velocity distribution map, the study area exhibits shear wave velocities ranging from 130 to 850 m/s.

o) The destructive earthquake that occurred on February 6, 2023 in Kahramanmaras highlighted the necessity for Türkiye to undertake preventative measures against natural disasters, implement suitable construction standards, and enhance disaster management strategies that acknowledge the seismic reality. In order to minimize the impact of disasters and identify secure settlement areas, it is crucial to evaluate the soil characteristics of residential regions. Geographic Information System (GIS) analysis can be employed as a means to visualize this data on maps and conduct comprehensive analyses.

p) The National Seismic Strategy and Action Plan 2012-2023 calls for the promotion of investigations for microzonation maps, earthquake hazard maps, and liquefaction potential maps of settlement areas. Collaboration between relevant institutions and local authorities is necessary for the implementation of these studies. Making the findings of these investigations widely known can encourage further research in earthquake-prone areas and engaging with local administrations is critical for accurately determining earthquake risks and safeguarding residential areas. These studies offer insight into the specific soil characteristics of a region, help update seismic risk maps, and facilitate the adoption of appropriate safeguards. As such, supported studies play a pivotal role in comprehending seismic hazards and mitigating disaster damage.

q) Through the analysis of collected data, this study aims to present insights into soil properties. Furthermore, the resulting maps serve to enhance the accuracy of interpretations in other studies conducted within the same region. These maps, along with their visual representation of soil properties, are valuable in facilitating a better understanding of the region's soil conditions and can serve as inspiration for future research endeavors. It is anticipated that they will provide planners and

practitioners with valuable insights during the planning phase. While the databases and microzonation maps generated in this study offer a broad assessment of the region, it is necessary to conduct more detailed and comprehensive investigations, taking into account the variations in geological units and the effects of anisotropy, in order to obtain more precise information about the soil properties.

6. REFERENCES

AFAD. (2023). AFAD Deprem Kataloğu. https://deprem.afad.gov.tr/event-catalog

Akdeniz, E. (2015). Eskişehir Zemini İçin Kayma Dalgası Hızı (Vs) ile Standart Penetrasyon (SPT) Sayısı Arasındaki İlişkinin Modellenmesi. Anadolu University (Turkey).

Akdeniz, E. (2015). Eskişehir Zemini İçin Kayma Dalgası Hızı (Vs) ile Standart Penetrasyon (SPT) Sayısı Arasındaki İlişkinin Modellenmesi. Anadolu University (Turkey).

Ateş, Ş., Keçer, M., Osmançelebioğlu, R., & Kahraman, S. (2004). Antakya (Hatay) İl Merkezi ve Çevresinin Yerbilim Verileri. MTA Genel Müdürlüğü Jeoloji Etütleri Dairesi Başkanlığı, Ankara.

Avin, Ö. (2011). Balıkesir İli İmar Planındaki Mahallelerin 7.Emin-Jeoteknik Değerlerinin ArcGis Programı Kullanılarak Haritalandırılması [Yüksek Lisans Tezi]. Balıkesir Üniversitesi Fen Bilimleri Enstitüsü, Jeoloji Mühendisliği Anabilim Dalı.

Ayday, Altan, Nefeslioglu, Canıgür, Yerel, & Tün. (2001). Eskişehir yerleşim yerinin yerleşim amaçlı jeoloji ve jeoteknik etüt raporu. Anadolu Üniversitesi, Uydu ve Uzay Bilimleri Araştırma Enstitüsü, Eskişehir.

Baştürk, F. (2003). Avcılar İlçesi'nin coğrafi bilgi sistemleri ile sismik mikrobölgelemesi [Yüksek Lisans Tezi]. Yıldız Teknik Üniversitesi Fen Bilimleri Enstitüsü.

Bouchier, E. S. (1921). A short history of Antioch: 300 B.C. - A.D. 1268. Oxford: Basil Blackwell.

Bowles, J. E. (1996). Foundation Analysis & Design 5th Edition McGraw-Hill Companies. Inc.

Bowles, J.E. (1988) Foundation Analysis and Design. 4th Edition, McGraw Hill.

Çabalar, A. F., Canbolat, A., Akbulut, N., Tercan, S. H., & Isik, H. (2019). Soil liquefaction potential in Kahramanmaras, Turkey. Geomatics, Natural Hazards and Risk, 10(1), 1822–1838.

Çekmecelioğlu, E. (2016). Antakya Kentindeki Geleneksel Ticaret Mekânlarının Değişimi. İstanbul: Yıldız Teknik Üniversitesi, Fen Bilimleri Enstitüsü, Mimarlık Anabilim Dalı, Mimari Tasarım Programı, Yüksek Lisans Tezi.

Çelik, M. A. (2012). Antakya-Kahramanmaraş Grabeninde Bitki Örtüsü İle Yağış Koşulları Arasındaki İlişkilerin Modıs Verileri (2000-2010) Kullanılarak İncelenmesi. Kahramanmaraş: Kahramanmaraş Sütçü İmam Üniversitesi, Sosyal Bilimler Enstitüsü, Coğrafya Anabilim Dalı, Yüksek Lisans Tezi.

Clayton, C. R. (1995). The standard penetration test (SPT): Methods and use. Construction Industry Research and Information Association.

Coppock, J. T., & Rhind, D. W. (1991). The history of GIS. Geographical Information Systems: Principles and Applications, 1(1), 21–43.

Çabuk, K. M., & Çabuk, A. (2015). Coğrafi Bilgi Sistemlerine Giriş: Vol. no. 2058 (1. baskı.). Anadolu Üniversitesi Açıköğretim Fakültesi.

Çinicioğlu, S. F. (2005). Zeminlerde statik ve dinamik yükler altında taşıma gücü anlayışı ve hesabı. Seminer, IMO İstanbul Şubesi.

ÇSB. (2017). Sanliurfa İli 2017 Yılı Çevre Durum Raporu. Çed ve İzin Şube Müdürlüğü,Sanliurfa Valiliği.

Dai, F. C., & Lee, C. F. (2001). Terrain-based mapping of landslide susceptibility using a geographical information system: A case study. Canadian Geotechnical Journal, 38(5), 911–923.

Danışman, E. (2022). Şanlıurfa Taş Ocaklarından Elde Edilen Agregaların Beton Üretiminde Kullanılabilirliğinin Araştırılması [Yüksek Lisans Tezi]. Antalya Bilim Üniversitesi.

Deere D.U., 1964. Technical description of rock cores for engineering purposes. Felsmechanik und Ingenieurgeologie, 1, 16-22.

Demir, A. (1996). Çağlar İçinde Antakya. İstanbul: Akbank Yayınları.

Demir, G. (2013). Gürsu (Bursa) Yerleşim Alanındaki Temel Zeminin Jeo-Mühendislik Özelliklerinin Coğrafi Bilgi Sistemleri (CBS) Kullanılarak Hazırlanması [Yüksek Lisans Tezi]. Balıkesir Üniversitesi Fen Bilimleri Enstitüsü, Jeoloji Mühendisliği Anabilim Dalı.

Demirtaş, O. (2022). Mapping geotechnical data by GIS: a case study of Elazığ city, Turkey [M.Sc. Thesis in Civil Engineering]. Hasan Kalyoncu University, Graduate Education Institute.

ERCAN A., 2001. Yer Araştırma Yöntemleri; Bilgiler Kurallar TMMOB Jeofizik Müh. Odası Yayını, 339 sayfa.

Genç, D. (2008). Zemin Mekaniği ve Temeller. TMMOB Jeoloji Mühendisleri Odası Yayınları.

Genç, D. (2008). Zemin Mekaniği ve Temeller. TMMOB Jeoloji Mühendisleri Odası Yayınları.

Göksular, F. (2022). Mapping geotechnical properties using geographical information system: A case study of Siirt city [M.Sc. Thesis in Civil Engineering]. Hasan Kalyoncu University, Graduate Education Institute.

Gümüşçü M., Özcan N., Kaya N. (2004). "Şanlıurfa'da Betonarme Yapıların Mevcut Durumu", TMH -Türkiye Mühendislik Haberleri Sayı 434 - 2004/6 ss. 41-48

GÜRPINAR, O., YALÇIN, N., TUĞRUL, A. ve DALGIÇ, S., 2004. Birecik(Şanlıurfa) Yöresinin Temel Jeolojik Özellikleri ve Jeolojik Miras Envanteri. TÜBA Kültür Envanteri Dergisi, 158-159..

GÜZEL , A., 2005. Şanlıurfa İli Yerleşmeleri. Ankara, 34-35.

GÜZEL , A., 2020. Şanlıurfa İli Doğal Coğrafya Özellikleri. Uluslararası Sosyal Araştırmalar Dergisi, 203-204.

GÜZEL , A., 2020. Şanlıurfa İli Doğal Coğrafya Özellikleri. Uluslararası Sosyal Araştırmalar Dergisi, 197-198.

Haşimoğlu, A., & Murat, Ü. (2004). Zemin Etüt Bilgi Sisteminin Oluşturulmasının Önemi: Yoncalı (Kütahya) Örneği. Kütahya İmar İşleri Müdürlüğü Planlama Servisi.

Holtz, R. D., Kovacs, W. D., & Sheahan, T. C. (1981). An introduction to geotechnical engineering (Vol. 733). Prentice-Hall Englewood Cliffs.

IMO. (2016). Soil Investigation,TMMOB Chamber of Civil Engineers.

IMO. (2016). Soil Investigation,TMMOB Chamber of Civil Engineers.

Isik, M., Aktuğ, Ö., & Yücel, E. (2014). Active tectonics of Turkey and its surroundings. Tectonophysics, 617, 1-22.

İmamoğlu, M. Ş., & Çetin, E. (2007). GÜNEYDOĞU ANADOLU BÖLGESİ ve YAKIN YÖRESİNİN DEPREMSELLİĞİ. Dicle Üniversitesi Ziya Gökalp Eğitim Fakültesi Dergisi, 9, 93–103.

İyisan, R. (1994). Geoteknik özelliklerin belirlenmesinde sismik ve penetrasyon deneylerinin karşılaştırılması [Doctoral Thesis]. İstanbul Teknik Üniversitesi Fen Bilimleri Enstitüsü.

Kalinski, M. E. (2011). Soil mechanics: Lab manual. (Issue Ed. 2). John Wiley & Sons.

Kanai, K. (1983). Engineering Seismology. IIESEE Lecture Note.

Karabaş, B. (2019). Use Of Geographic Information System For Evaluating The Some Geotechnical Properties In Malatya, Turkey [M.Sc. Thesis in Civil Engineering]. Hasan Kalyoncu University, Graduate Education Institute.

Karaca, Ö. (2007). Fethiye Yerleşim Alanı Zeminlerin Mühendislik Özelliklerinin Belirlenmesi ve Jeoteknik Haritalarının Coğrafi Bilgi Sistemleri (CBS) Kullanılarak Hazırlanması [Doctoral Thesis]. Süleyman Demirel Üniversitesi, Fen Bilimleri Enstitüsi, Jeoloji Mühendisliği Anabilim Dalı.

Keçeli, A. (1990). Sismik Yöntemlerle Müsaade Edilebilir Dinamik Zemin Taşıma Kapasitesi ve Oturmasının Saptanması. Jeofizik, 4(2), 83-92.

KGM. (2023). İller Arası Mesafe Sorgulama. https://www.kgm.gov.tr/Sayfalar/KGM/SiteTr/Uzakliklar/illerArasiMesafe.aspx

Koçman, A. (1993). Türkiye İklimi. Ege Üniversitesi Edebiyat Fakültesi Yayınları: 72.

Kolat, Ç. (2010). Developing A Geotechnical Microzonation Model For Yenişehir (Bursa) Settlement Area [Doctoral Thesis]. Geological Engineering Department, Middle East Technical University.

KRDAE, 2021 http://www.koeri.boun.edu.tr/new/

Kunapo, J., Dasari, G. R., Phoon, K.-K., & Tan, T.-S. (2005). Development of a Web-GIS based geotechnical information system. Journal of Computing in Civil Engineering, 19(3), 323–327.

Kurnaz, T. F. (2011). İstanbul Esenler zeminlerinin coğrafi bilgi sistemleri (CSB) tabanlı geoteknik mikrobölgelemesi [Doctoral Thesis, Sakarya Üniversitesi]. https://acikerisim.sakarya.edu.tr/handle/20.500.12619/76440

Küpçü, S., Çabuk, A., & Uyguçgil, H. (2015). Coğrafi Bilgi Sistemleri: Vol. no. 2057 (1. baskı.). Anadolu Üniversitesi Açıköğretim Fakültesi. https://go.exlibris.link/4kx76xVh

Mayne, P. W., Christopher, B. R., & DeJong, J. (2002). Subsurface Investigations—Geotechnical Site Characterization: Reference Manual. United States. Federal Highway Administration.

Midorikawa, S. (1987). Prediction of isoseismal map in the Kanto plain due to hypothetical earthquake. Journal of Structural Engineering, 33, 43–48.

Okman, C. (1998). Zemin Mekaniği. Ankara Üniversitesi Ziraat Fakültesi Yayın No: 1502.

Orhan, A. (2005). Eskişehir İl Merkezi Güney Bölümü Temel Zemin Birimlerinin Jeo-Mühendislik Özellikleri ve Coğrafi Bilgi Sisteminin Uygulanması [Doctoral Thesis]. Eskişehir Osmangazi Üniversitesi Fen Bilimleri Enstitüsü Jeoloji Mühendisliği Anabilim Dalı.

Orhan. (2022a). Geoteknik Mühendisliği ve Temel İnşaatı—Cilt 1. Ankara: Gazi Yayın Dağıtım.

Orhan. (2022b). Geoteknik Mühendisliği ve Temel İnşaatı—Cilt 2. Ankara: Gazi Yayın Dağıtım.

Orhan. (2022b). Geoteknik Mühendisliği ve Temel İnşaatı—Cilt 2. Ankara: Gazi Yayın Dağıtım.

Över, S., Ünlügenç, U. C., & Özden, S. (2001). Hatay bolgesinde etkin gerilme durumlari. Hacettepe Universitesi Yerbilimleri Uygulama ve Arastırma Merkezi Bulteni, Yerbilimleri, 23, 1-14.

Özaydın, K. (2015). Zemin Mekaniği. Birsen Yayınevi.

Özcan, A. (2012). Selçuklu (Konya) Civarındaki Zeminlerin Jeoteknik Değerlendirilmesi [Yüksek Lisans Tezi]. Aksaray Üniversitesi Fen Bilimleri Enstitüsü Jeoloji Mühendisliği Anabilim Dalı.

Özcan, C., Yılmaz, E., Lafcı, B., Küçükpehlivan, T., Aksoy, T., Ağaçsapan, B., & Sarı, S. (2021). Coğrafi Bilgi Sistemlerinin Türkiye'deki Tarihsel Gelişimi Ve Mevcut Durumu. GSI Journals Serie C: Advancements in Information Sciences and Technologies, 4(1), Article 1.

Özşahin, E. (2010). Antakya'da Hatay Yer Seçiminin Jeomorfolojik Özellikler Ve Doğal Risk Açısından Değerlendirilmesi. Balıkesir Üniversitesi Sosyal Bilimler Enstitüsü Dergisi, 13(23), 1-16.

Özşahin, Emre, Kaymaz, Çağlar K. "Rüzgâr Enerji Santrallerinin (RES) Yapım Yeri Seçimi Üzerine Bir CBS Analizi: Hatay Örneği", TÜBAV Bilim Dergisi, C. VI, Sayı 2, 2013, s. 14.

Öztürk, M. Z., Çetinkaya, G., & Aydın, S. (2017). Köppen-Geiger İklim Sınıflandırmasına Göre Türkiye'nin İklim Tipleri. Coğrafya Dergisi, 17-27.

Poisson Oranı. Maden Mühendisliği Bülteni. Cilt 17, Sayı 3, 2023.

Poisson Oranının Kayaçların Özelliklerine Etkisi. Jeoloji Mühendisliği Dergisi. Cilt 25, Sayı 1, 2022.

Poisson's Ratio. Wikipedia, the Free Encyclopedia. Wikimedia Foundation, Inc. https://en.wikipedia.org/wiki/Poisson%27s_ratio

Rifaioğlu, M. N. (2012). An Enquiry into The Definition of Property Rights in Urban Conservation: Antakya (Antıoch) From 1929 Title Deeds and Cadastral Plans. Ankara: Middle East Technical University, The Department of Architecture, PhD.

Schaefer, V., Stevens, L., Ceylan, H., & White, D. (2008). *Design Guide for Subgrades and Subbases*.

SEGAL, J. B., 2002. Edessa Kutsal Şehir Urfa. (A. Aslan, Çev.) İstanbul: İletişim Yayınları, 34-35.

Sekercioglu, E. (1993). Yapilarin Projelendirilmesinde Mühendislik Jeolojisi. TMMOB. Jeoloji Mühendisleri Odasi Yayini, 28, 216.

Selçuk, H. (1985). Kızıldağ-Keldağ-Hatay dolayının jeolojisi ve jeodinamik evrimi. MTA Rapor, (7787).

Shaik, A. W. (2007). Towards more reliable site investigation information. Proceedings of the 16th South-East Asian Geotechnical Conference, 8–11.

Singh, V. P., & Fiorentino, M. (2013). Geographical information systems in hydrology (Vol. 26). Springer Science & Business Media.

SÖZER, A. N., 1984. Güneydoğu Anadolu'nun Doğal Çevre Şartlarına Coğrafi Bir Bakış . Ege Coğrafya Dergisi 2, 30-42

Şengör, A. (1980). Türkiye'nin Neotektoniğinin Esasları. Türkiye Jeoloji Kurumu.

Şişman, E. (2006). Fethiye Yerleşim Alanındaki Zeminlerin SPT ve Kayma Dalga Hızı Verileriyle Sıvılaşma Potansiyelinin Değerlendirilmesi [Yüksek Lisans Tezi]. Gazi Üniversitesi Fen Bilimleri Enstitüsü İnşaat Mühendisliği Anabilim Dalı.

T. S. Turkish Standards Institute, TS 3530 EN 933-1/Nisan 1999, Agregaların Geometrik Özellikleri için Deneyler Bölüm 1:Tane Büyüklüğü Dağılımı Tayini-Eleme Metodu.

T.C. Meteoroloji Genel Müdürlüğü. (2022, 04 07). T.C. Çevre ve Şehircilik Bakanlığı, Meteoroloji Genel Müdürlüğü. T.C. Çevre ve Şehircilik Bakanlığı, Meteoroloji Genel Müdürlüğü: https://www.mgm.gov.tr/veridegerlendirme/il-ve-ilceleristatistik.aspx?k=A adresinden alındı

TDBY. (2018). Türkiye Deprem Bölgelerinde Yapılacak Binalar Hakkında Yönetmelik. Afet ve Acil Durum Yönetim Başkanlığı.

Thitimakorn, T. (2003). Determination of Shear-wave Velocity Profiles from Surface (Rayleigh) Seismic Waves: Wahite Ditch and St. Francis River Bridge Sites, Southeast Missouri.

https://transportation.mst.edu/media/research/transportation/documents/072-cr.pdf
Topaloğlu, A. A. (2021). Peyzaj Tasarım Kriterleri İle Vandalizm İlişkisinin Kent Parkları Örneğinde İncelenmesi, Yüksek Lisans Tezi. Ankara: Ankara Üniversitesi, Fen Bilimleri Enstitüsü.
Töreyen, G., Özdemir, İ., & Tekinalp, K. (2010). ArcGIS 10 Desktop Uygulama Dokümanı (Ekim 2010). İşlem Coğrafi Bilgi Sistemleri Mühendislik ve Eğitim Ltd. Şti.
Tüzen, M. (2019). Zemin Su Muhtevası ile Elektrik Direnci İlişkisi [M.Sc. Thesis in Civil Engineering]. Gümüşhane Üniversitesi.
URL-1 https://en-us.topographic-map.com/map-fdflkl/%C5%9Eanl%C4%B1urfa/
URL-2 https://mgm.gov.tr/,2020
URL-3 http://www.exploratorium.edu/faultline/earthquakescience/eqscience4.html
Uyan, A. (2018). Coğrafi Bilgi Sistemleri Kullanılarak Ayşebacı ndeki (Karesi/Balıkesir) Zeminlerin Jeo-Mühendislik Özelliklerinin Değerlendirilmesi [M.Sc. Thesis in Civil Engineering]. Balıkesir Üniversitesi / Fen Bilimleri Enstitüsü / Jeoloji Mühendisliği Ana Bilim Dalı.
Uyanık, O. (2015). Deprem ağır hasar alanlarının önceden belirlenmesi ve şehir planlaması için makro ve mikro bölgelendirmelerin önemi. Süleyman Demirel Üniversitesi Fen Bilimleri Enstitüsü Dergisi, 19(2), 24–38.
Uyanık, O. (2015). Deprem ağır hasar alanlarının önceden belirlenmesi ve şehir planlaması için makro ve mikro bölgelendirmelerin önemi. *Süleyman Demirel Üniversitesi Fen Bilimleri Enstitüsü Dergisi*, *19*(2), 24–38.
Uyguçgil, H. (2011). Coğrafi bilgi sistemlerinin tarihçesi. İçinde Çabuk, A. Coğrafi Bilgi Sistemlerine Giriş, 134–136.
Uzuner, B. A. (2007). Çözümlü Problemlerle Temel Zemin Mekaniği. 7. Derya Kitapevi.
Uzuner, B. A. (2016). Çözümlü Problemlerle Temel Zemin Mekaniği. 10.
Wan-Mohamad, W. N. S., & Abdul-Ghani, A. N. (2011). The use of geographic information system (GIS) for geotechnical data processing and presentation. Procedia Engineering, 20, 397–406.
Whyte, I. L. (1982). Soil plasticity and strength—A new approach using extrusion. Ground Engineering, 15(1).
Yalçinkaya, E. (2002). Zemin özelliklerinin deprem hareketine etkisi: 1 Ekim 1995 Dinar ve 27 Haziran 1998 Adana-Ceyhan depremi örnekleri [Doctoral Thesis]. İstanbul Üniversitesi Fen Bilimleri Enstitüsü Jeofizik Mühendisligi Anabilim Dalı.
Yomralıoğlu, T. (2000). Coğrafi Bilgi Sistemleri Temel Kavramlar ve Uygulamalar. Akademi Kitabevi, 2. Baskı, 479 sayfa.
Yurddaş M. (2022) Industrial geography of Şanlıurfa province [Master Thesis]. Kahramanmaraş Sütçü Imam Üniversitesi Sosyal Bilimler Enstitüsü Coğrafya Ana Bilim Dali. 22-30.